NOTICE

The quality of this microform is heavily dependent upon the quality of the original thesis submitted for microfilming. Every effort has been made to ensure the highest quality of reproduction possible.

If pages are missing, contact the university which granted the degree.

Some pages may have indistinct print especially if the original pages were typed with a poor typewriter ribbon or if the university sent us an inferior photocopy.

Reproduction in full or in part of this microform is governed by the Canadian Copyright Act, R.S.C. 1970, c. C-30, and subsequent amendments.

AVIS

La qualité de cette microforme dépend grandement de la qualité de la thèse soumise au microfilmage. Nous avons tout fait pour assurer une qualité supérieure de reproduction.

S'il manque des pages, veuillez communiquer avec l'université qui a conféré le grade.

La qualité d'impression de certaines pages peut laisser à désirer, surtout si les pages originales ont été dactylographiées à l'aide d'un ruban usé ou si l'université nous a fait parvenir une photocopie de qualité inférieure.

La reproduction, même partielle, de cette microforme est soumise à la Loi canadienne sur le droit d'auteur, SRC 1970, c. C-30, et ses amendements subséquents.

ISBN 0-315-53265-3

The Effect of Process Variables on Mixer-Settler Performance

By
Wayne Foster Luinstra
Ottawa, Ontario. December 1988

A THESIS
PRESENTED TO THE SCHOOL OF GRADUATE STUDIES
AT THE UNIVERSITY OF OTTAWA
IN PARTIAL FULFILLMENT OF THE
THESIS REQUIREMENT FOR THE DEGREE OF
MASTER OF APPLIED SCIENCE
IN
CHEMICAL ENGINEERING

References

The operation of a gravity settler for the water-uranyl sulphate -kerosene system was studied. The effect of process variables, which include flowrate, agitation intensity, phase ratio and air entrainment, on the dispersion band height-area relationship in a gravity settler was investigated. Using synthetic solutions a model was developed for the prediction of dispersion band heights for the following mixer geometries: 1) square mixer, 2) cylindrical mixer, 3) closed mixer (no air entrainment).

The model was tested using an actual leach liquor solution from Key Lake. The predicted band heights were found to be generally higher than experimental values, indicating that conservative designs would arise from the use of synthetic solutions in the absence of 'crud'. The absence of air entrainment required more power for the prevention of phase inversion. The investigation also showed definite advantages by operating the system with a continuous organic phase.

Acknowledgement

I would like to thank Dr. J.A. Golding and Mr. Gordon Ritcey (CANMET) for their guidance and financial support without which this project would not have been possible.

A hearty thanks to Dr. D.D. McLean for his patience and guidance in helping with the mathematical modelling. Special thanks goes to J. Gasperetti, D. Lefebvre and A. Bonaldo whose excellent craftsmanship was displayed throughout the project.

I would also like to thank my colleagues at the University of Ottawa for their help, patience and communication, which made the rough spots alot smoother.

Finally, I would like to dedicate this to my parents Wietze and Japje Luinstra whose love and support will never be forgotten.

Nomenclature

Symbols in the text, unless otherwise stated, have the following meaning:

a	parameter
A	settler area, cm^2
b	parameter
C	general constant
d	drop diameter
h	film thickness
H	dispersion band height, cm
j	general constant
K	general constant
N	impeller speed (rotations per minute)
PR	dispersed phase ratio
Q	volumetric flowrate, mL/min.
RPM	impeller speed (rotations per minute)
SSR	sum of squares of residuals
t	time
T	parameter
V	volumetric flowrate, mL/min.
w	general constant
y	general constant

ϕ	dispersed phase ratio
ρ	density, g/cm^3
μ	viscosity, cp
γ	interfacial tension, dynes/cm
β	initial parameter estimates

Subscripts

c	continuous phase
d	dispersed phase
o	initial properties
Ac	actual
fd	feed

Contents

List of Tables

List of Figures

Chapter 1

Introduction

In the production of uranium yellow cake, required for the production of nuclear fuels, the following operations are involved. The uranium ore is first mined, ground to 80% minus 200 mesh and then leached. Sulphuric acid is used to leach the ore and solubilize the uranium. The uranium in solution can occur in several different forms [1]:

$$UO_3 + 2H^+ \longleftrightarrow UO_2^{+2} + H_2O$$

$$UO_2^{+2} + SO_4^{-2} \longleftrightarrow UO_2SO_4$$

$$UO_2SO_4 + SO_4^{-2} \longleftrightarrow (UO_2(SO_4)_2)^{-2}$$

$$(UO_2(SO_4)_2)^{-2} + SO_4^{-2} \longleftrightarrow (UO_2(SO_4)_3)^{-4}$$

Uranium is recovered from the leach solution using either ion exchange or liquid-liquid extraction. Solvent extraction transfers the uranium from the aqueous leach liquor to an organic solution by contacting the two immiscible phases. When the

uranium has been concentrated in the organic solvent it is stripped into a second aqueous phase, from which uranium is then recovered by precipitation.

Solvent extraction employs selective amine extractants such as Alamine 336, Amberlite LA-1 and Primene JMT. One of the most commonly used for the extraction of uranium is the tertiary amine Adogen 364 [2]. Accordingly, in the extraction stage, the uranium is transferred from the aqueous to the organic phase in the following manner:

$$\overline{(R_3NH)_2SO_4} + (UO_2(SO_4)_2)^{-2} \longleftrightarrow \overline{(R_3NH)_2UO_2(SO_4)_2} + SO_4^{-2}$$

$$\overline{2(R_3NH)_2SO_4} + UO_2(SO_4)_3^{-4} \longleftrightarrow \overline{(R_3NH)_4UO_2(SO_4)_2} + 2SO_4^{-2}$$

The overbar indicates the organic phase.

Uranium is recovered from the loaded organic phase by stripping with an ammonium sulphate solution. The stripping stage transfers the metal back into an aqueous phase. Finally, uranium is precipitated from the strip liquor as yellow cake by using ammonium hydroxide or hydrogen peroxide [3]. The tertiary amine is recycled and conditioned with sulphuric acid to change the amine to the sulphate form. A scrub stage may be included in the process by contacting the loaded organic with water to remove impurities from the organic.

The equipment traditionally used in the uranium processing industry is the mixer-settler. This involves mixing of the two phases in the mixer, where mass transfer takes place, and then letting the phases separate in a gravity settler. Mixer-settlers are capable of large throughputs and good mass transfer. However, the separation of the two phases has many uncertainties which has led to overdesign of the gravity-settler. This results in:

- High capital cost.
- Large solvent inventory.
- Excessive evaporation losses.

- Control difficulties.
- Large space requirements.

In a gravity settler a dispersion band forms at the interface of the two phases. The relationship between the depth of the settler, dispersion band height and area of the settler can be considered as design variables with two degrees of freedom. In other words, if two variables are set the other becomes fixed. Since the limitations for depth and area of the settler are physical, they can be selected arbitrarily, resulting in the overdesign of gravity-settlers. Thus, accurate prediction of dispersion band height with respect to area can be used to optimize settler dimensions.

The process variables which can effect dispersion band height are throughput (Q), agitation intensity in the mixer (RPM) and the dispersed phase ratio in the feed (PR). Having a mathematical model to predict the dispersion band height with respect to these variables would be of benefit for mixer-settler design.

The initial equation developed by Ryon, Daley and Lowrie [4] related the dispersion band height (H) to the throughput (Q) per unit area of the settler (A). This was confirmed theoretically by Barnea and Mizrahi [5]. The equation,

$$H = C(Q/A)^y \tag{1}$$

does not clearly identify the influence of the process variables agitation intensity (RPM) and phase ratio (PR) since C and y were experimentally determined constants.

Gondo and Kusunoki [6] were able to expand the equation developed by Ryon et al. [4] to include the process variables (RPM and PR) of a water in kerosene system. However, their equation contradicts the accepted coalescence mechanism of dispersions.

A dimensional analysis approach was attempted by Smith and Davies [7]. The assumed dependence of band height on some physical properties (e.g. viscosity and interfacial tension) was found to be negligible. As well, a direct relationship between process variables and the physical properties of the system is still required for prediction of the dispersion band height.

Allak and Jeffries [8] pursued an iterative droplet-layer-height approach but which required knowledge of a critical film thickness which could only be obtained from experimental data.

Golob and Modic [9], Vieler et al. [10], and Jeelani and Hartland [11], all approached the problem of dispersion band height prediction with a similar premise. They attempted to predict dispersion band height for a continuously operated gravity-settler from batch dispersion tests. None of these authors attempted to directly relate the dispersion band height and the process variables (i.e. agitation intensity and phase ratio).

The necessity for an equation which relates the process variables to dispersion band height becomes evident. Such an equation would be of benefit in the design of mixer-settlers, since by imposing any physical limitations, say area, the equation could then be used to optimize the remaining physical dimension, depth.

Atkinson [1] attempted to develop a predictive dispersion band height equation for the uranyl-sulphate-Adogen 364 system. Using aqueous continuous operation, the focus of the investigation was to determine the effect of the process variables such as agitation intensity (RPM), dispersed phase ratio (PR), throughput (Q) on the settler area (A)-dispersion band height (H) relationship. A mathematical model was developed for a square mixer. Inconsistent data resulted in a poor model for a closed cylindrical mixer.

In the present study, organic phase continuous operation was used to determine the effect of agitation intensity (RPM), dispersed phase ratio (PR) and throughput (Q), on the dispersion band height-settler area relationship.

The objective was to develop mathematical models, relating dispersion band height and process variables, for different mixer configurations (i.e. square and cylindrical) and to determine the mixer type effect, on dispersion band heights. A closed mixer was used to examine the effect of air entrainment on mixer-settler operation. These studies of mixer configuration and air entrainment effects can be expected to aid equipment selection for mixer-settler processes.

The final objective was to test the mathematical models obtained with aqueous/organic continuous phase operation by substituting the synthetic leach solution

with Key Lake leach liquor and comparing the data with that predicted by the model.

It was hoped that the effect of these variables on the dispersion band height could be modelled and a feasible design equation for predicting band heights developed.

Chapter 2

Background and Literature Review

2.1 Coalescence

The following factors are of concern in mixer settlers: 1) mass transfer 2) droplet size distribution and the rate of phase disengagement or coalescence. It is this rate of phase disengagement which is of prime importance as it directly affects dispersion band heights and hence settler size.

A dispersion occurs when two immiscible phases are vigorously mixed, such that the droplets of one phase (the dispersed phase) are dispersed in the second phase (the continuous phase). The phases will separate over time, by the coalescence of droplets in each phase. In a continuously operated system (e.g. a mixer-settler), a dispersion band is formed between the two immiscible phases. This is shown in Figure 1. The height of the dispersion band is represented by H. The dispersion band height, along with settler depth and area determine the capacity of the settler for operation in the process.

It has been proposed that coalescence between dispersed phase droplets and the interface occur in five consecutive stages [5]. The stages though are not necessarily independent and can be summarized as follows; 1) the approach of a drop towards the interface, which causes both drop and interface deformation; 2) the damped

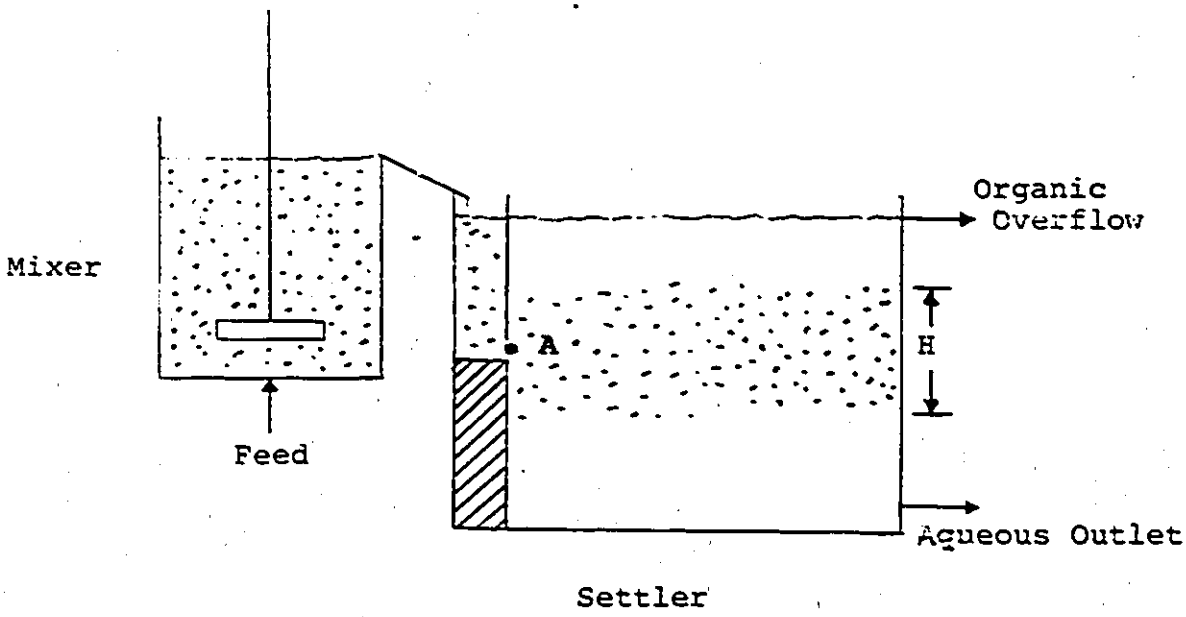

Figure No. 1 : Dispersion Band in a Gravity Settler.

oscillation of the drop near the interface; 3) the formation of a film of continuous phase between the drop and its bulk (dispersed) phase; 4) the drainage, rupture and removal of the film; and 5) the transfer of the contents of the drop into its bulk phase. Coalescence also occurs between the individual drops. In drop-interface coalescence, gravity holds the drop at the interface until the film drains and ruptures. In drop-drop coalescence the effect of gravity is much less, consequently adjacent drops may not remain in sufficiently close proximity long enough for film drainage and rupture to occur.

The exact mechanism of settling and coalescence in solvent extraction is not clearly understood. The time required for a droplet to coalesce into its bulk phase is referred to as the coalescence rate. The faster the coalescence rate, the quicker separation of the two phases occurs and thus a smaller dispersion band height is predicted.

The relationship between the coalescence rate and dispersion band height can be determined by examination of the dispersion band structure.

2.2 Dispersion Band Structure

It has been suggested by different investigators that the structure of the dispersion band is made up of two or three zones. Allak and Jeffreys [8] proposed three distinct zones, a coalescing zone, a packing zone and a flocculating zone. This is illustrated in Figure 2. This figure represents an aqueous continuous system. (Note: Since the organic phase is dispersed the droplets rise, however, for the system investigated in this study the aqueous phase was dispersed and the droplets fall. This diagram is used as an illustration of the different zones in a dispersion, the fact that droplets rise or fall does not change the concept.) In the flocculating zone, when the drops enter the bed they are jostled about with the result that, although they remain spherical, they arrange themselves in the most compact way and trap the continuous phase in the interstices. In the packing zone, the drops pass into the band and are squeezed together extruding the continuous phase. In the coalescing zone, which is only one or two drops thick, the droplets tend to coalesce with the interface more than with

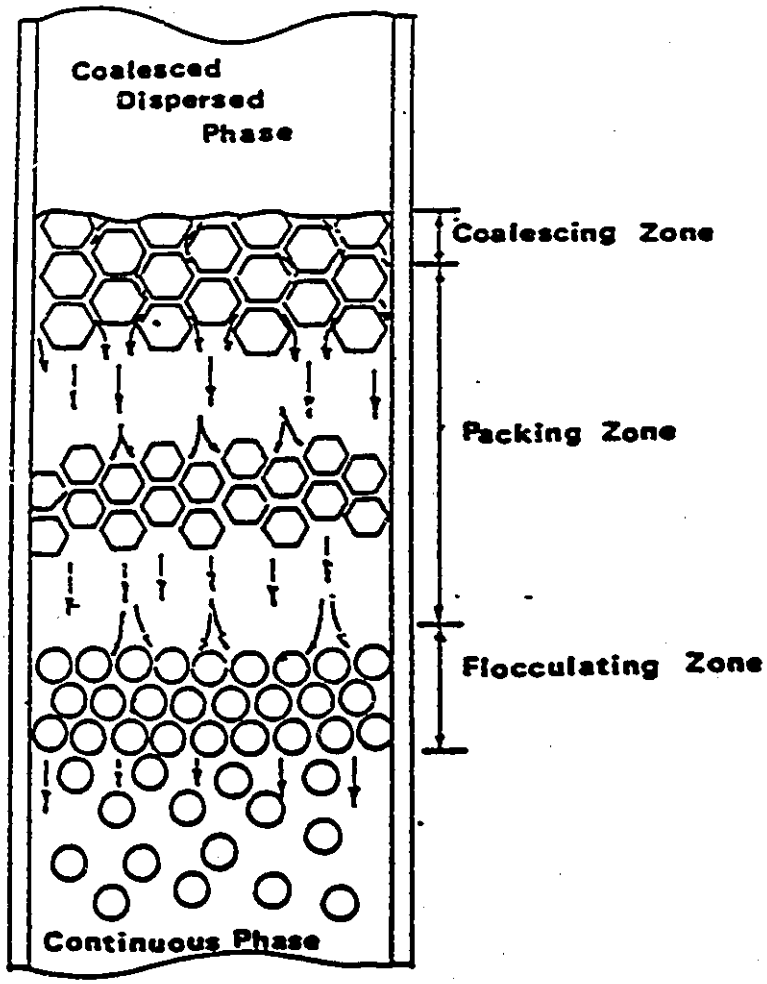

Figure No. 2 : Allak and Jeffreys Dispersion Band Structure.

each other.

Barnea and Mizrahi [5] suggested that two zones existed. The first being referred to as the 'dense' layer, which can be found in the vicinity of the coalescence front. It is equivalent to Allak and Jeffries [8] coalescing zone and occupies 10 to 20% of the total volume of the dispersion band. The second zone is referred to as the 'even' concentration layer which constitutes the majority of the volume of the dispersion band.

According to Barnea and Mizrahi, the role of the 'dense' sub-layer is to expand the effective area of the interface available for precoalescence so that bigger drops reach the coalescing front. The role of the 'even' concentration layer is to provide for the conditions and residence times necessary so that drop to drop coalesence can take place. The total thickness of the 'even' concentration layer adjusts itself to provide sufficient residence time for all droplets, which were originally too small to rise or fall, to grow by coalescence. When the appropriate size is reached, the droplets approach the coalescing front (dense sub-layer) to become part of their bulk phase.

For settlers then, it is apparent that their capacity depends more on the mechanism of hindered settling of drop populations and drop-drop coalescence than on the droplet coalescence rate at the coalescence front.

The coalescence rate is affected by the throughput (Q) and the dispersed phase ratio (PR), which determine the residence time in the 'even' concentration sub-layer of the band. The agitation intensity (RPM) determines the droplet size which will in turn affect the coalescence rate. Thus, by manipulating these process variables, their effect on the coalescence rate can be measured with dispersion band heights.

Before investigation of the effect of process variables on the dispersion band height, it is necessary to review the equations developed by other authors to understand the different approaches utilized.

2.3 Dispersion Band Equation Development

The equations developed for prediction of dispersion band heights are presented in two main groups. The first group can be classified as 'direct', in that they attempt to relate dispersion band height to process variables directly from continuously operated gravity-settler data. The second group attempts to predict dispersion band heights from batch settling data, their objective being to eliminate extensive pilot plant work. This group can be classified as 'indirect', since they attempt to predict dispersion band heights for steady-state gravity settlers indirectly.

Ryon, Daley and Lowrie initiated the direct methods of predicting dispersion band heights when they first reported an equation based on experimental data collected from the Amex system [4]. The authors concluded that, dispersion band height as a function of flowrate per unit cross-sectional area was virtually independent of settler size, and that the specific flowrate (Q/A) could be used as a reliable basis for design of larger scale equipment. The equation developed was:

$$H = C(Q/A)^y \tag{2}$$

Where H was the dispersion band height, Q the total throughput and A the area of the settler. C and y were experimentally determined constants. The equation does not indicate how dispersed phase ratios (PR) and agitation intensity (RPM) in the mixer influence the experimental constants, C and y. Expansion of these experimental constants to include dispersed phase ratio (PR) and agitation intensity (RPM) is necessary to optimize settler design.

Barnea and Mizrahi [5] confirmed the equation developed by Ryon et al. [4] by studying the effect of 'dense' and 'even' concentration layers on dispersion band heights. The study was restricted to settlers with dispersion band heights greater than 15 centimeters. Their dispersion band height equation, is developed below. At steady state the volume of continuous phase entering the dispersion band is equal to the volume leaving the band. Therefore, the average draining velocity over the whole area is;

$$\frac{Q(1-\phi_0)}{A} \tag{3}$$

where ϕ_0 is the dispersed phase fraction. Barnea and Mizrahi denote U_ϕ, the relative velocity between two phases, as the average vertical velocity of the continuous phase divided by the average fraction of horizontal area occupied by the continuous phase.

$$U_\phi = \frac{Q(1-\phi_0)}{A} * \frac{1}{1-\phi} \tag{4}$$

where ϕ is the local concentration of the dispersed phase in the 'even' concentration layer. Therefore,

$$U_\phi \propto Q/A \tag{5}$$

Also, the relative velocity between the phases is proportional to the i'th power of the average drop diameter,

$$U_\phi \propto d^i \tag{6}$$

where

$$2 \geq i = f(Re_\phi) \geq 0.5 \tag{7}$$

and the average drop diameter is a function of the residence time in the 'even' concentration layer,

$$d \propto t^{1/j} \tag{8}$$

with j>3 and where 1/j is a function of the rate of growth of the drops due to coalescence in the 'even' concentration layer. Combining equations (5) and (6) for relative velocity gives;

$$Q/A \propto d^i \tag{9}$$

The average residence time in the 'even' concentration layer, t, is given by

$$t = V'/Q * \phi_0/\phi \tag{10}$$

where V' is the volume of the even concentration layer. Also, $t \propto V'/Q$ since ϕ_0/ϕ are constants at steady state.

If the 'even' concentration layer is considered to be a constant proportion of the total thickness of the dispersion band, V, then combining equations (8) and (10) gives,

$$d \propto t^{1/j} \propto (V/Q)^{1/j} \tag{11}$$

or since V = H*A

$$d \propto (H * A/Q)^{1/j} \propto (H/(Q/A))^{1/j} \tag{12}$$

Rearranging equation (12) yields

$$d^j \propto H/(Q/A) \tag{13}$$

or

$$H \propto d^j(Q/A) \tag{14}$$

Equating equations (9) and (13) gives,

$$(Q/A)^{1/i} \propto (H/(Q/A))^{1/j} \tag{15}$$

and isolating H yields,

$$H \propto (Q/A)^{j/i+j} \tag{16}$$

or

$$H \propto (Q/A)^y \tag{17}$$

where $y = j/i + 1$. If $j>3$ and $2.0 \geq i \geq 0.5$, then $y \geq 2.5$.

Although this development has imposed a lower limit on the experimentally determined constant y, the effect of dispersed phase ratio (PR) and agitation intensity (RPM) is not clear. Again, expanding the constants C and y to include the effect of PR and RPM is necessary.

Gondo and Kusunoki[6] using a 'direct' method, published their experiments on the separation of a water in kerosene dispersion in a vertical glass settler. The height of the dispersion band (H) was correlated with the feed throughput (Q), the dispersed phase ratio (ϕ) and the speed (N) of the mixer impeller. The following empirical correlation resulted:

$$\Delta H = \phi^{4.9} N^{2.8} (Q/A)^{3.1} \tag{18}$$

Although this equation agrees with the results of Barnea and Mizrahi, there is one significant difference. The equation indicates that ΔH should decrease if the continuous phase throughput was increased, all other variables held constant. This

contradicts the concepts of coalescence and dispersion separation which indicate that, increasing the the continuous phase throughput (or decreasing the dispersed phase ratio) should decrease the coalescence rate, thereby increasing the dispersion band height. A closer look also indicates that the constant 3.1 must be expanded to include the effect of RPM (or N) and PR (or ϕ).

Smith and Davies[7] attempted to directly predict dispersion band heights , and developed an equation using dimensional analysis. By studying eight different systems, the following equation was obtained:

$$\frac{H}{d_0} = 3499 \left(\frac{V_d \mu_c}{\gamma}\right)^{0.846} \left(\frac{d_0^2 \Delta\rho g}{\gamma}\right)^{-0.878} \left(\frac{\mu_d}{\mu_c}\right)^{0.770} \tag{19}$$

where V_d is the volumetric flowrate of the dispersed phase, d_0 the dispersed phase droplet size, $\Delta\rho$ the density difference between the phases and g, μ, and γ the gravitational constant, viscosity and interfacial tension respectively. The subscripts c and d represent properties of the continuous and dispersed phase.

Close study of this equation indicates that there is little effect of continuous phase viscosity and interfacial tension. This is unlikely when the mechanisms of coalescence are considered, as it is the continuous phase which must drain between the dispersed droplets before their coalescence. Therefore, a large dependence on continuous phase viscosity would be expected. Dimensional analysis also assumes knowledge of the relationships between the process variables and the physical properties of the system. This may be difficult to obtain and by modelling the system directly with the process variables this problem may be overcome.

Allak and Jeffreys[8] developed a mathematical model, based on film rupture thickness to predict dispersion band height as a function of inlet drop size, flowrate, and the physical properties of the system.

The iterative procedure developed, estimates the dispersion band height as follows. As the dispersion band forms from drops of initial diameter d_0, continuous phase is trapped in the amount expressed by

$$Q_u = \left(\frac{1-\phi}{\phi}\right) * V \tag{20}$$

where Q_u represents the upward flow of the continuous phase, V the superficial velocity and ϕ the dispersed phase ratio in the feed.

The initial film thickness between drops, h, is estimated from equation (21).

$$h = \left(\frac{1-\phi}{3.32\phi}\right) d \tag{21}$$

The drops pass into the band and continuous film drains until the critical film thickness h_c is reached. Time taken for draining to occur is estimated by

$$t = \frac{55}{981}\left(\frac{V\mu^5 d^9}{\rho g \gamma^4 \phi^2 h_c^7}\right)^{1/4} \tag{22}$$

Since V is known, the thickness of the first increment of the band is $H_1 = V * t$. Upon coalescence of a pair of drops, d:ϕ:V change and are recalculated for the next increment. These steps are repeated until the initial Q_u is reduced to zero. The total band thickness is $\sum H_i$.

Several questions arise from this method. What is the critical film thickness? Upon coalescence, what do d:ϕ:V become? Can an increment of dispersion band height be determined by the coalescence of a single pair of droplets? This final assumption does not lend credibility to the procedure since droplets coalesce at different rates within the band itself.

The next group of equations have been classified as 'indirect'. The hypothesis that continuous dispersion heights can be calculated indirectly from batch settling data is noteworthy, however, the objective of eliminating pilot plant work is not practical from a process design viewpoint. This, coupled with the fact that, the effect of process variables on dispersion band height have not been investigated, are the inherent weaknesses of these equations for use in mixer-settler design.

Golob and Modic[9] studied the relationship between batch and continuous settling rates as a method of determining the dispersion band height. Their results show that at equal dispersion thicknesses, the batch coalescence rate and the continuous systems' dispersed phase throughput per unit settler area are equal, allowing batch results to be used for the design of continuous settlers. Observations in the Amex[4] extraction process were used to formulate the equation,

$$H = 1.45\nu_d^{3.1} = 1.45(Q_d/A)^{3.1} \tag{23}$$

where the coalescence rate ν_d is equivalent to the dispersed phase throughput Q_d per unit area (A).

This equation indicates that the continuous phase throughput has no effect on the dispersion band height. This would contradict the mechanisms proposed for the coalescence of a dispersion. The effect of agitation intensity in the mixer (RPM), dispersed phase ratio (PR) and total throughput (Q) are not clear. The effect of these variables become important in process and equipment design.

Vieler, Glasser and Bryson[10] derived an internal age-distribution model to relate a batch settler with a continuous steady-state settler. They proposed that, if the internal phase disengagement rate is a function of age, as well as other properties, there exists a non-uniqueness in going from batch to continuous experiments. They explained their hypothesis in the following manner.

Suppose that in a dispersion one defines $\Psi(t)dt$ as the volume of the dispersion in the settler of age, between t and t+dt, where age is defined as the time since the volume element entered the system. Associated with this volume element, one defines a phase-disengagement rate g(x,t) which is the fraction of the volume disengaging per unit time when the age is t and the properties of the system are x. Examples of such properties might be the phase ratio and the total dispersion band thickness. In terms of these two quantities a material balance over a differential age interval leads to the equation,

$$\frac{d\Psi(t)}{dt} = -g(x,t)\Psi(t) \tag{24}$$

The major assumptions in the derivation of this equation, is that one can define a property of the system as g. The validity of the assumption that one can relate g from the batch and continuous experiments has not been confirmed.

However, the authors propose that the continuous results can be summarized in the equation

$$\frac{V}{Q} = aH + b \tag{25}$$

where V is the volume of the dispersion, Q the total throughput and H the dispersion band height. Both constants a and b should be positive as V/Q represents a coalescence time and must increase with increasing dispersion band height.

Again, this equation fails to show the effect of process variables such as agitation intensity in the mixer (RPM) and phase ratio (PR), necessary for process design.

The prediction of dispersion band height from batch settling data was also developed by Jeelani and Hartland[11]. They were able to develop an equation which related the total band height (H) to dispersed phase throughput (Q_d) per unit area (A) of the settler.

$$H = K(Q/A)^w \tag{26}$$

The constant K was found to be dependent upon the average dispersed phase hold-up fraction in the continuous settler. The constants w and K were both determined from batch settling data, thus by-passing extensive pilot plant work. However, pilot plant testing is required for scale-up.

Inspection of equation (26) shows that throughput of the continuous phase has no influence on dispersion band height. This contradicts the proposed mechanism for coalescence in dispersions which states that, increasing the continuous phase throughput would raise the dispersion band height by impeding the motion of the dispersed phase droplets to their bulk phase.

Citing the need for pilot plant work and equation weaknesses, the necessity of an equation which can predict dispersion band height with respect to process variables is warranted.

The present study is a continuation of work initiated by Atkinson[1]. Using the 'direct' method of studying a continuous steady-state settler, Atkinson[1] investigated a uranyl-sulphate-Adogen 364 system. The focus of the investigation was to determine the effect of the process variables such as agitation intensity (RPM), throughput (Q), dispersed phase ratio (Φ) and settler cross-sectional area. The effects of these variables on the dispersion band height for an open square mixer configuration were determined for an aqueous phase continuous system. He also investigated the effects of a cylindrical mixer configuration with no air entrainment (i.e. closed). A mathematical model for the square mixer was developed. A complete mathematical model could not be developed for the closed cylindrical mixer configuration.

The investigation utilized synthetic phases. The organic phase comprised 3.5%

Adogen 364, 3.5%isodecanol and 93% Shell 140 kerosene. The aqueuos phase comprised sulphuric acid in water at a pH of 1.6. The model developed for the square mixer was,

$$H = (T_1/RPM + T_2 * Q)\exp((T_3 * \Phi_d + T_4 * Q)/A) \quad (27)$$

where $T_1, T_2, T_3 \text{and} T_4$ are parameters determined by nonlinear regression analysis.

The model was not compared to data for actual leach solutions. As well, this particular system should have been operated organic phase continuous to minimize organic loss through entrainment. This was not investigated nor confirmed operationally with actual leach solutions. No equation could be developed for the closed cylindrical mixer data which indicate an influence of either air entrainment or mixer configuration.

It was hoped that, in the present study, the effect of process variables on the dispersion band height could be modelled for both mixer configurations and no air entrainment. From this a feasible design equation for predicting band heights could be developed.

Chapter 3

Experimental

In the current investigation, an extension of Atkinsons' work (1) was undertaken. It was decided to continue the development of a single stage mixer-settler using the uranyl-sulphate-Adogen system. Again, the focus of the investigation was the effect of process variables on the dispersion band height.

Using simulated phases, the study investigated an extraction stage operated with the organic phase being continuous. Organic continuous operation is desirable since organic loss due to entrainment can be eliminated when compared to aqueous continuous operation. By measuring dispersion band heights at different operating conditions, a mathematical model for predicting band height can be developed. The use of synthetic solutions to develop appropriate models is necessary since, each solvent extraction system can be ore dependent. The developed model can then be compared to dispersion band height data obtained using actual leach liquors.

The apparatus configuration used is shown in Figure 3. A plexiglass settler, 50 cm high x 50 cm long x 20 cm wide, was used to separate dispersions produced in a mixer. The square mixer, 13.6 cm x 13.6 cm x 13.6 cm, and the cylindrical mixers, 14 cm high x 15 cm diameter, had a capacity of 2500 mL. Agitation was provided to the mixers by a 6-bladed turbine impeller, 5.2 cm diameter x 1.4 cm high, which was rotated by a variable speed motor. Rotational speed was set and monitored with a calibrated strobe light. A moveable full width baffle was inserted into grooved slots in the settler side walls to provide different settling cross-sectional

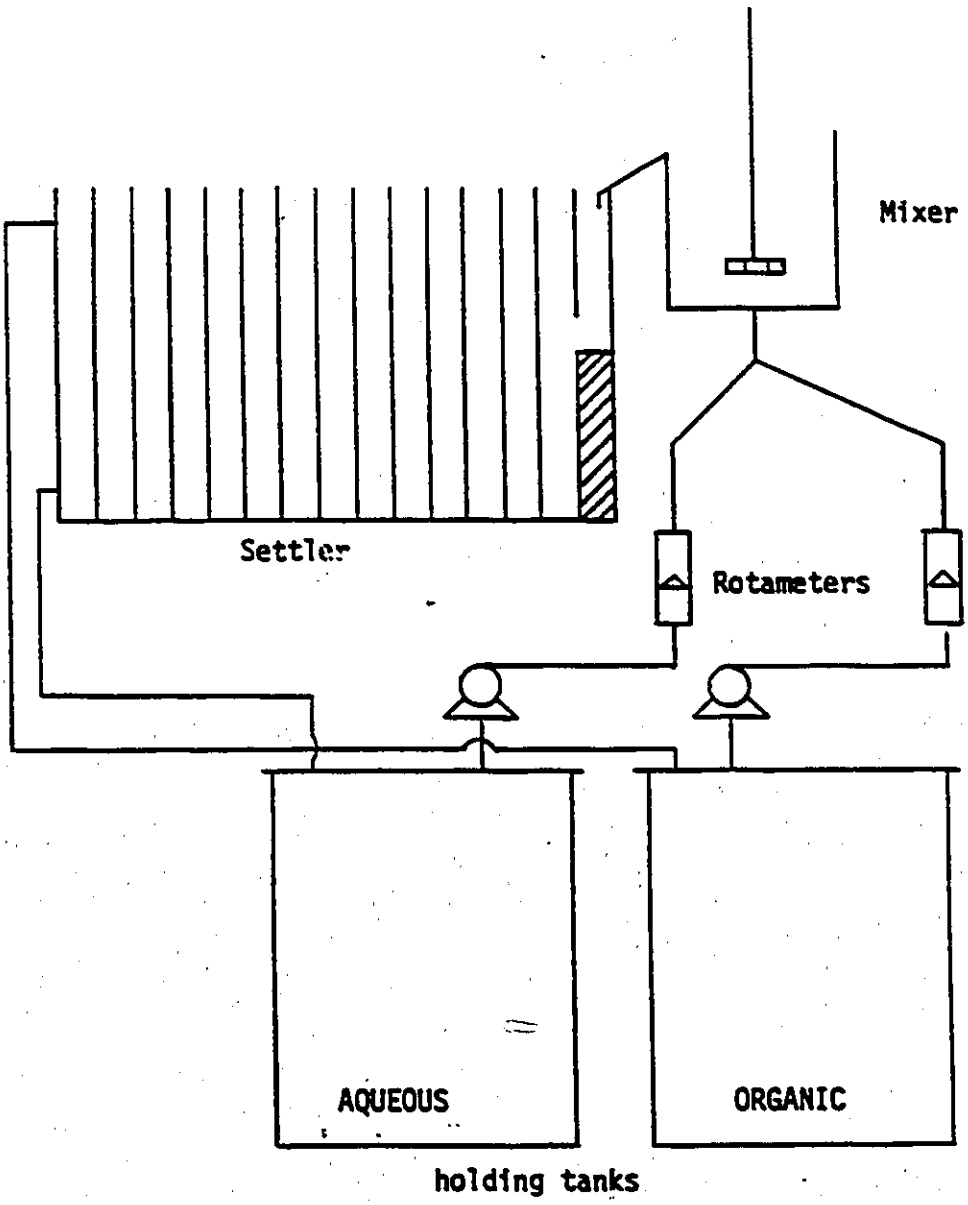

Figure No. 3 : Experimental Apparatus.

areas ranging from 134 cm^2 to 787 cm^2 (See Appendix D for intermediate areas).

The aqueous and organic phases were pumped from their respective holding tanks to the mixer with Masterflex peristaltic pumps. The flowrates were monitored using inline glass rotameters (TRI-FLAT, Fischer and Porter Co.) which were calibrated for each of the experimental solutions used. The phases were introduced into the bottom of the mixer at a Y-joint placed at the mixer inlet. After mixing, the dispersion overflowed by gravity into the settler. The dispersion entered the settler through a full width slit 5 cm high at point A in Figure 1. The phases left the settler through cylindrical ports and flowed by gravity to the holding tanks. A flow restrictor was placed on the aqueous return line to allow for adjustment of the aqueous phase level (and subsequent dispersion band position) in the settler. The organic and aqueous phases were recycled from the settler to their respective holding tanks which were situated below settler level.

City of Ottawa tap water acidified to pH = 1.6 with concentrated sulphuric acid was used as the aqueous phase. The organic phase comprised of 93% Shell 140, 3.5% isodecanol and 3.5% Adogen 364 by volume. Sixty litres of each phase was prepared. The organic phase was conditioned by contacting with 5% sulphuric acid in water to obtain the sulphate form of the tertiary amine. The aqueous and organic phases were then contacted by mixing to eliminate any mass transfer effects. The settled phases were allowed to remain in contact for four days. After settling, the pH of the aqueous phase was adjusted to 1.6 with the addition of a few drops of sulphuric acid.

Start up commenced with rinsing the settler with tap water and shaking dry. Continuous phase (organic) was pumped into the mixer and the flowrate was adjusted. When liquid began to enter the settler the impeller was started and the speed set. The pump for the dispersed phase was then started and set. Once the height of the aqueous phase reached the dispersion inlet, the flow constrictor on the aqueous outlet was adjusted to maintain the position of the dispersion band. The apparatus was allowed to operate for one hour before the baffle was placed in the settler.

Phase flowrates and the agitation intensity were maintained for each run. The

settler baffle was moved to vary the cross-sectional area available for settling. The baffle was moved to the different positions in a random order. After positioning the baffle in a specific slot, the dispersion band height was allowed to reach steady state. The band height was not recorded until the height had remained constant for ten minutes.

The shape of the dispersion band varied from tall and narrow to flat and wide depending on the cross-sectional area available. If the band took on a wedge-like shape, an indication that the cross-sectional area was to large, band height measurements were not recorded. The surfaces of the dispersion bands were visible through the transparent sides of the settler and the upper and lower limits of the dispersion bands were well defined. Band heights were measured in centimeters.

Three mixer configurations were used. The first was a square open mixer fed from the bottom and overflowing by gravity. The second was of cylindrical shape. The third mixer was cylindrical as well, however, the top of the mixer was sealed to eliminate air entrainment. The dispersion left the mixer through a small opening around the impeller shaft and then flowed via a walled trough into the settler.

A pseudo 3-level experimental design was implemented to investigate the effects of agitation, throughput and phase ratio on the dispersion band height-cross sectional area relationship. For each run, (i.e. at a given RPM, Q and Phase Ratio)the area was varied randomly in the slotted spaces provided. Table 1 represents a 3-level factorial experimental design for the variables RPM, Q and PR. A total of thirty runs (including 3 replicate runs at the zero point conditions) were performed. The variables were coded by subtracting half the sum of the upper and lower limits from the operating value. This value was then divided by half the range. Using RPM as an example: Coded Variable = (Z-200)/50 where Z equals an operating value (i.e. 250,200 or 150).

The experimental conditions are shown in Table 2. The levels of the process parameters used were determined in the following manner. The total throughput (Q) was calculated using residence times in the mixer most common in solvent extraction processes. A residence time of one to four minutes is commonly used in the copper-LIX 64 system and it is not unusual to utilize a residence time of up to

five minutes in the Amex process [12]. Equipment restrictions made residence times greater than 2.5 minutes and less than 1.0 minute difficult. It was thought that these times would sufficiently represent the uranyl-sulphate-Adogen 364 system. Knowing the volume of the mixer, the corresponding upper and lower limits of the flowrate were 2000 mL/min and 1000 mL/min. A center point selection of 1500 mL/min completed the experimental design.

The dispersed phase ratio's (PR) employed were determined from industrial operating practice. The Amex process maintains a phase ratio of 0.5 (i.e.A/O = 1/1). However, process variations may occur. Thus, phase ratio's of 0.6 (i.e. A/O = 3/2) and 0.4 (i.e. A/O = 2/3) were taken as upper and lower limits.

Determination of agitation intensity was based on a method of maintaining constant phase ratio in the mixer, reported by Bouyatiotis and Thornton [13]. It involved varying the speed of the mixer and measuring the actual phase ratio (PR_{Ac}) entering the settler and comparing it to the phase ratio in the feed (PR_{fd}). This was done by stopping the mixer and feed pumps simultaneously, letting the phases separate, and measuring the height of the phases in the mixer. A plot of the ratio PR_{Ac}/PR_{fd} versus agitation speed yields a curve from which the agitation speeds can be determined. The lower limit chosen was in the region where PR_{Ac}/PR_{fd} is less than 0.75 without phase inversion, and the upper limit where the ratio approaches 1.0 (i.e. 0.98). This was carried out for each mixer configuration. All runs were operated with the organic phase continuous.

Table 1: Experimental design

RPM	Q	Phase Ratio (PR)
+1/-1	+1/-1	+1/-1
+1/-1	+1/-1	0
+1/-1	0	+1/-1
0	+1/-1	+1/-1
0	0	+1/-1
0	+1/-1	0
+1/-1	0	0
0	0	0

Table 2: Experimental conditions

Q mL/min	AQUEOUS mL/min	ORGANIC mL/min	RPM	PR	Level
2000	1200	800	250	0.6	+1
1500	750	750	200	0.5	0
1000	400	600	150	0.4	-1

Chapter 4

Results and Modelling

4.1 Square Mixer Results and Modelling

The equation developed by Ryon et al.[4], $H = C(Q/A)^y$, can also be written, $H = C(1/A)^y$. It was desired to expand the experimentally determined constants C and y with respect to throughput (Q), agitation intensity (RPM) and dispersed phase ratio (PR).

The experimental data for the square mixer configuration are presented in Figures 4 through 7.

The data is presented in the form: dispersion band height (H) versus the inverse of the settler area (1/A). In general, the data was consistent in showing concave upward shape for all the plots. This lends support to the equations developed by Ryon et al.[4], Barnea and Mizrahi [5], and Gondo and Kusunoki [6]. Figure 4 shows the effect of throughput (Q) on the dispersion band height-settler area relationship. Figure 5 demonstrates the effect of agitation intensity (RPM). From Figure 6, the effect of dispersed phase ratio (PR) can be seen. Replicate run data shown in Figure 7 indicates a definite time trend. Inspection of all data show the general trends of increasing dispersion band height with increased throughput, agitation intensity and dispersed phase ratio.

The model developed by Vieler et al.[10] was shown to be inadequate when plots of V/Q versus H failed to display a positive slope for the data. This is shown in

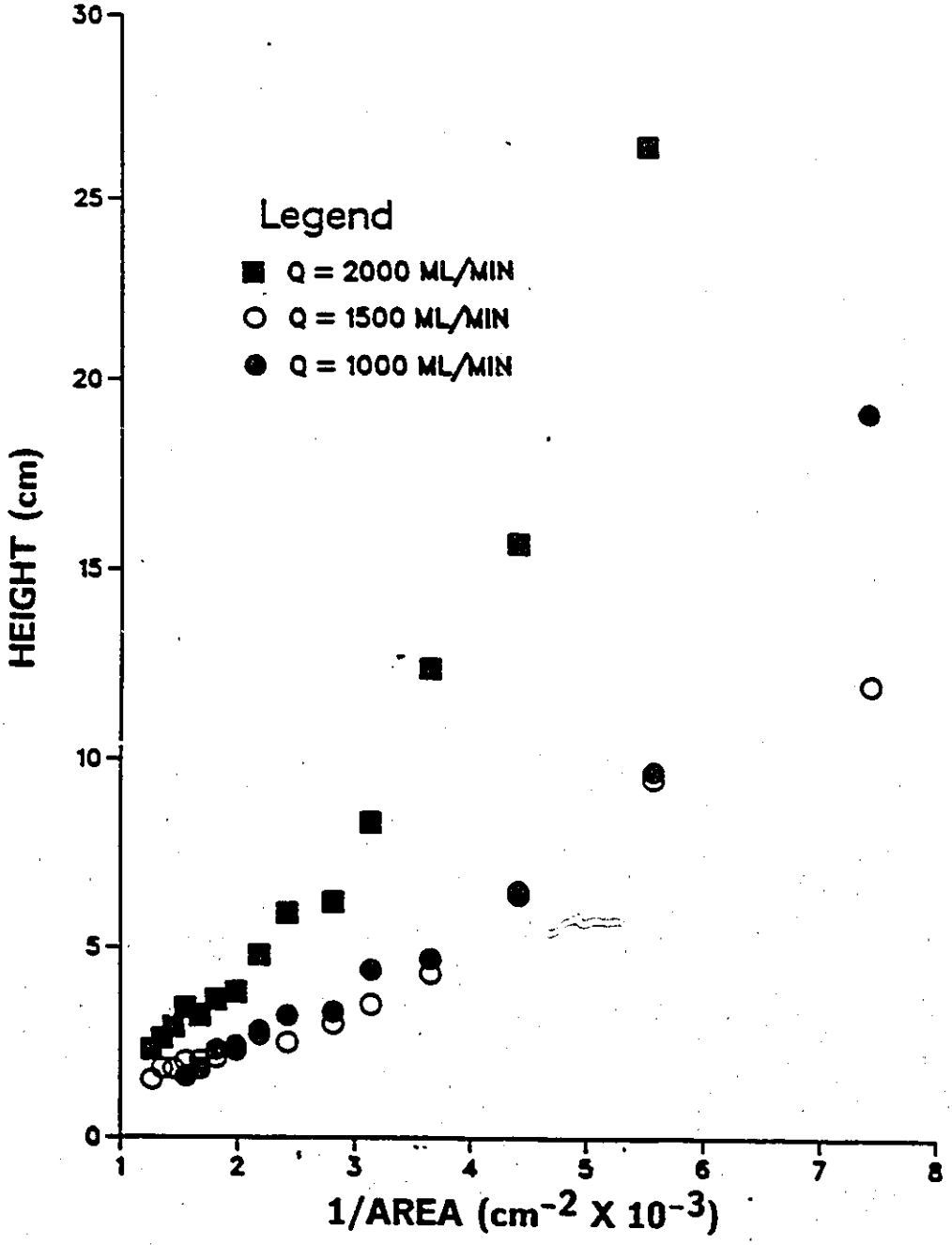

Figure No. 4 : Experimental data for the square mixer.
Dispersion band height vs. 1/area at RPM = 250 and PR = 0.6

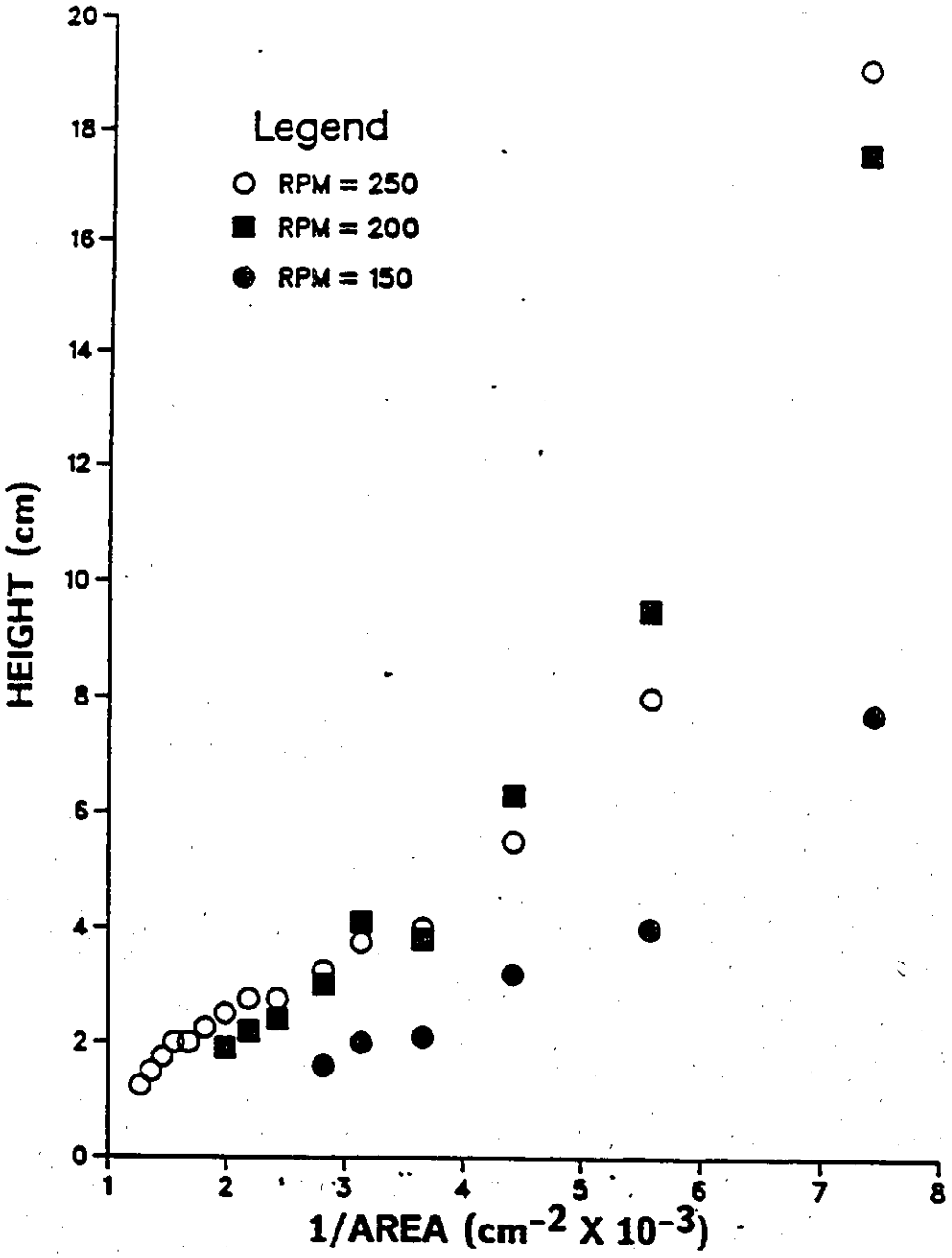

Figure No. 5: Experimental data for the square mixer. Dispersion band height vs. 1/area at Q = 1500 mL/min., and PR = 0.5

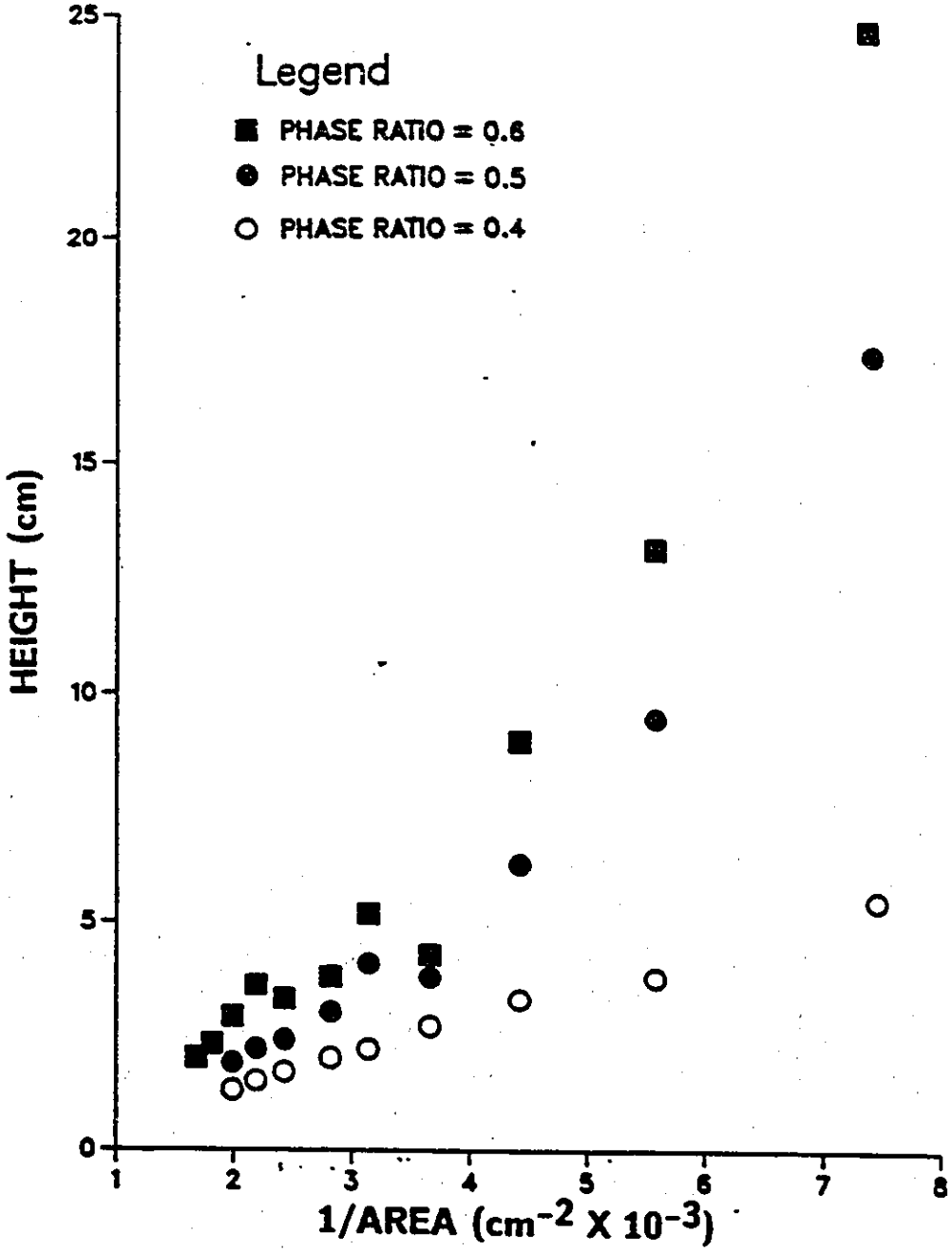

Figure No. 6: Experimental data for the square mixer. Dispersion band height vs. 1/area at Q = 1500 mL/min., and RPM= 200

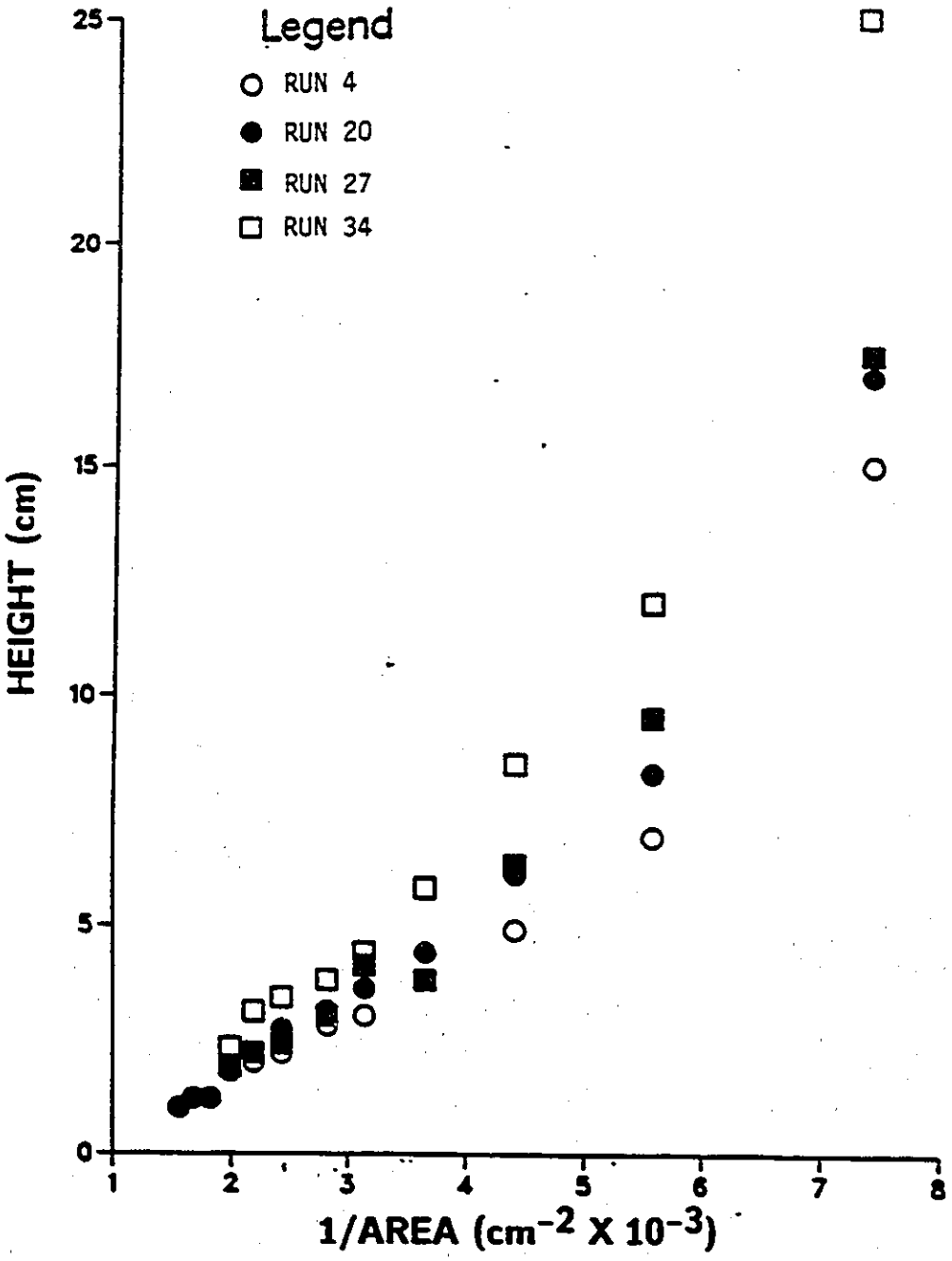

Figure No. 7: Replicate run data for the square mixer. Dispersion band height vs. 1/area at Q = 1500 mL/min, RPM = 200 and PR = 0.5

Figure 8. A positive slope is necessary since V/Q represents a residence time for coalescence, and should increase with increasing dispersion band height [10].

The experimental data (H versus 1/A) did not display straight line behaviour. A transformation was desired to continue mathematical modelling using linear regression analysis.

The transformations, ln H versus ln (1/A) and ln H versus 1/A, were both found to yield straight lines for the experimental data. In order to decide which transformation is best suited to represent the data, R^2 values for each individual run were compared. The R^2 value is a measure of how well the model represents the data. The value of R^2 can range from 0 to 1. In general, as the value of R^2 approaches one, the better the model represents the data [14]. The R^2 values for each transformation are presented in Table 3.

To determine which transformation was significantly better in representing the data, the R^2 values were 'blocked' into individual runs and the average difference between the two transformations, for all runs, calculated. From this value, a 95% confidence interval for the difference between the average R^2 values, for all runs, calculated. If the 95% confidence interval included the value of zero, the difference between the two transformations was not considered significant, and either transformation could be used for further modelling.

The 95% confidence interval for the difference in R^2 values was [0.000825 to 0.0307]. Since the value of zero did not lie within the interval, there exists, a difference between the two transformations. The mean R^2 values for the ln H versus ln (1/A) and ln H versus 1/A transformations were 0.936 and 0.952 respectively. Thus, the transformation ln H versus 1/A was chosen for further modelling.

Plotting ln H versus 1/A yielded straight lines for each individual run. The plots are presented in Figures 9 through 11, and Appendix C. From this, the model selected for the system studied was:

$$\ln H = \beta_0 + \beta_1(1/A)$$

where β_0 and β_1 are experimentally determined constants.

If such a model was found to adequately represent the data for each individual

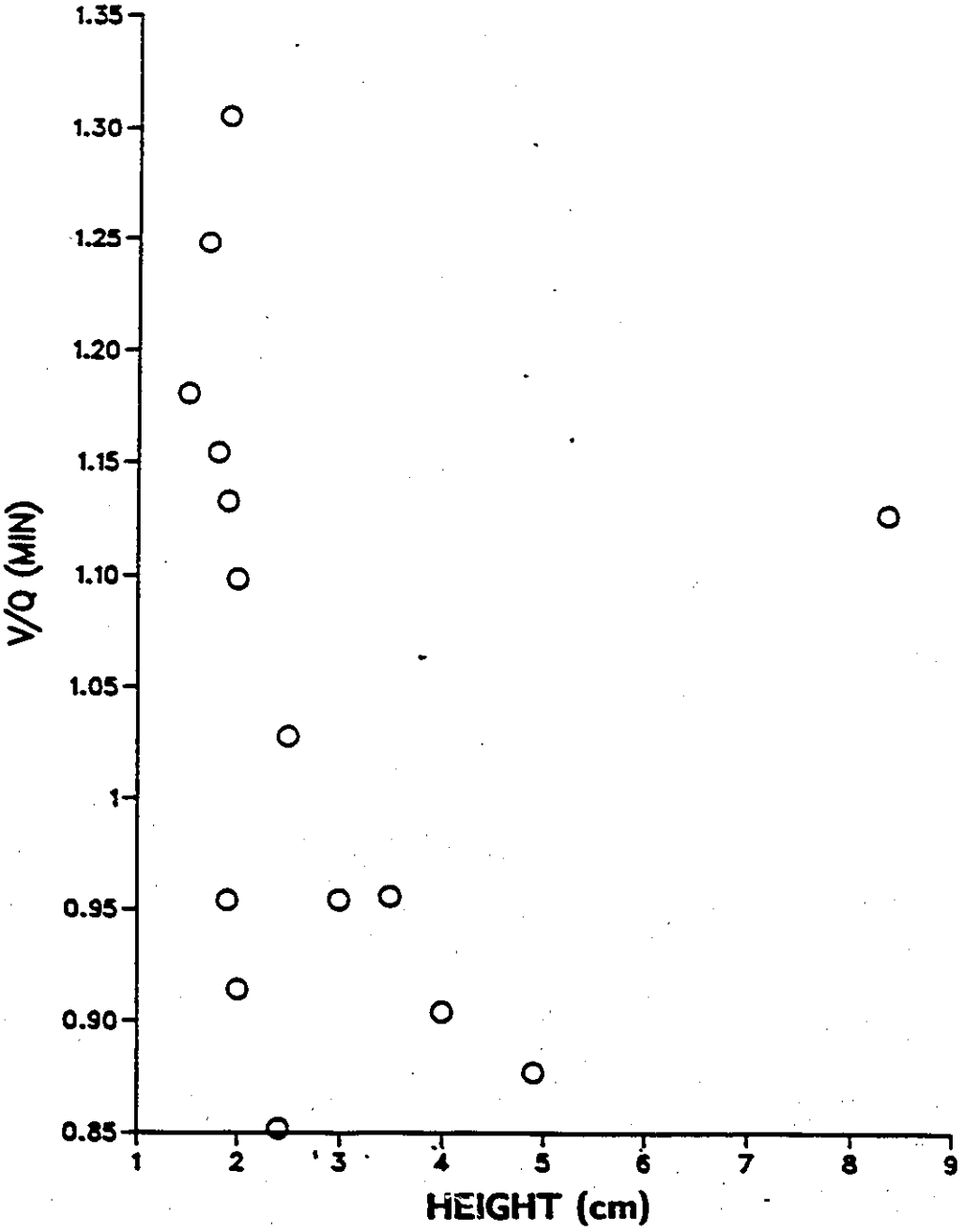

Figure No. 8: V/Q versus H plot for the square mixer data at Q = 1000 ml/min, RPM = 250 and PR = 0.5

Table 3: R^2values for the Square Mixer Data

Run No.	ln H vs. 1/A	ln H vs. ln(1/A)
1	0.9278	0.8697
4	0.9740	0.9488
7	0.9660	0.9646
8	0.9795	0.9458
9	0.9755	0.9442
10	0.9949	0.9525
11	0.9531	0.8990
12	0.9740	0.9459
13	0.9887	0.9586
14	0.9312	0.8650
15	0.9337	0.8493
16	0.9449	0.9919
17	0.9819	0.9108
18	0.9862	0.9559
19	0.8933	0.9247
20	0.9953	0.9725
21	0.9705	0.9381
22	0.8970	0.8365
23	0.7996	0.8392
24	0.9850	0.9754
25	0.9882	0.9610
26	0.8743	0.9532
27	0.9340	0.9854
28	0.9802	0.9788
29	0.9442	0.9834
30	0.9642	0.9480
31	0.9783	0.9770
32	0.8629	0.8404
33	0.9822	0.9792
34	0.9879	0.9809

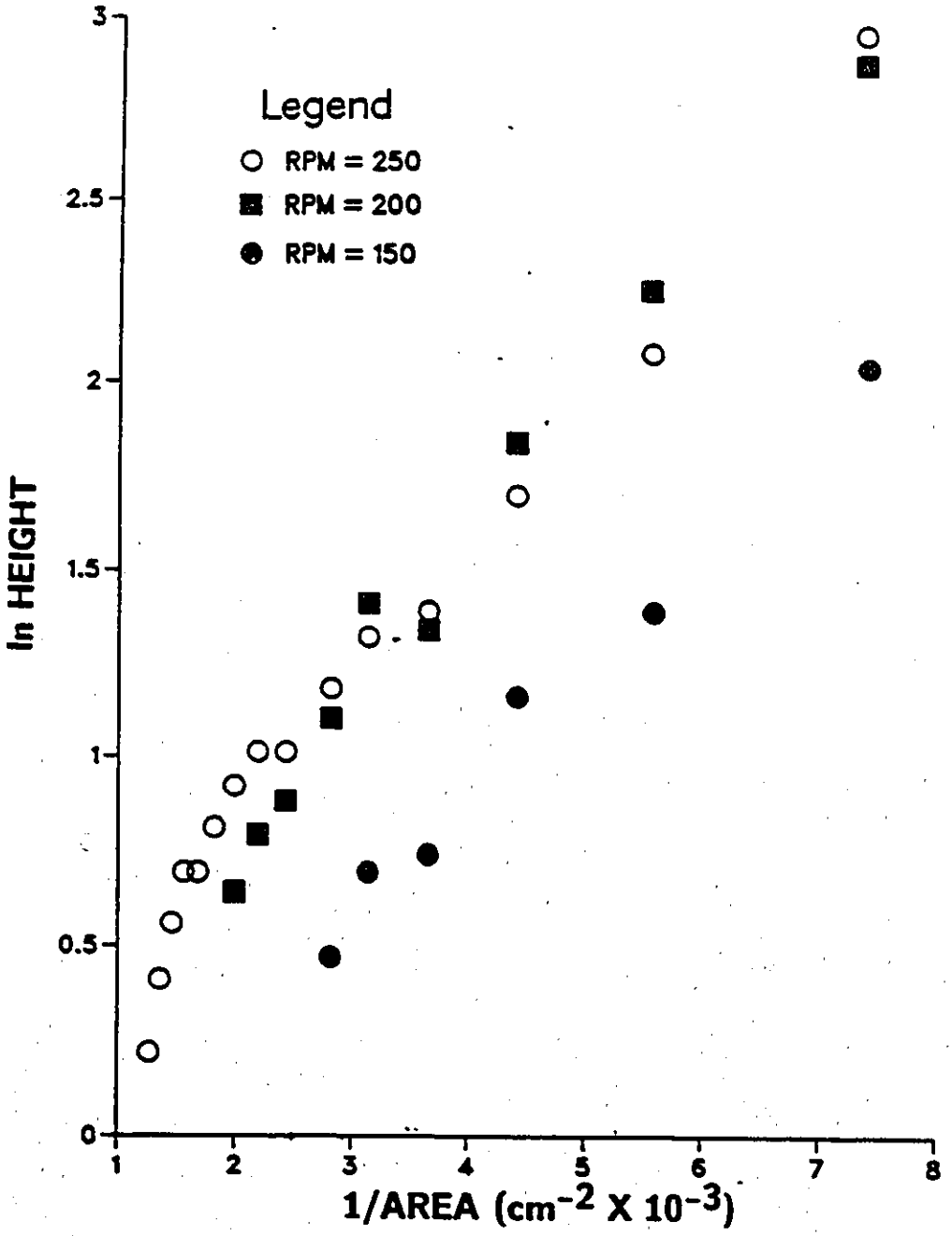

Figure No. 9: ln Height versus 1/area for the square mixer data at Q = 1500 mL/min and PR = 0.5

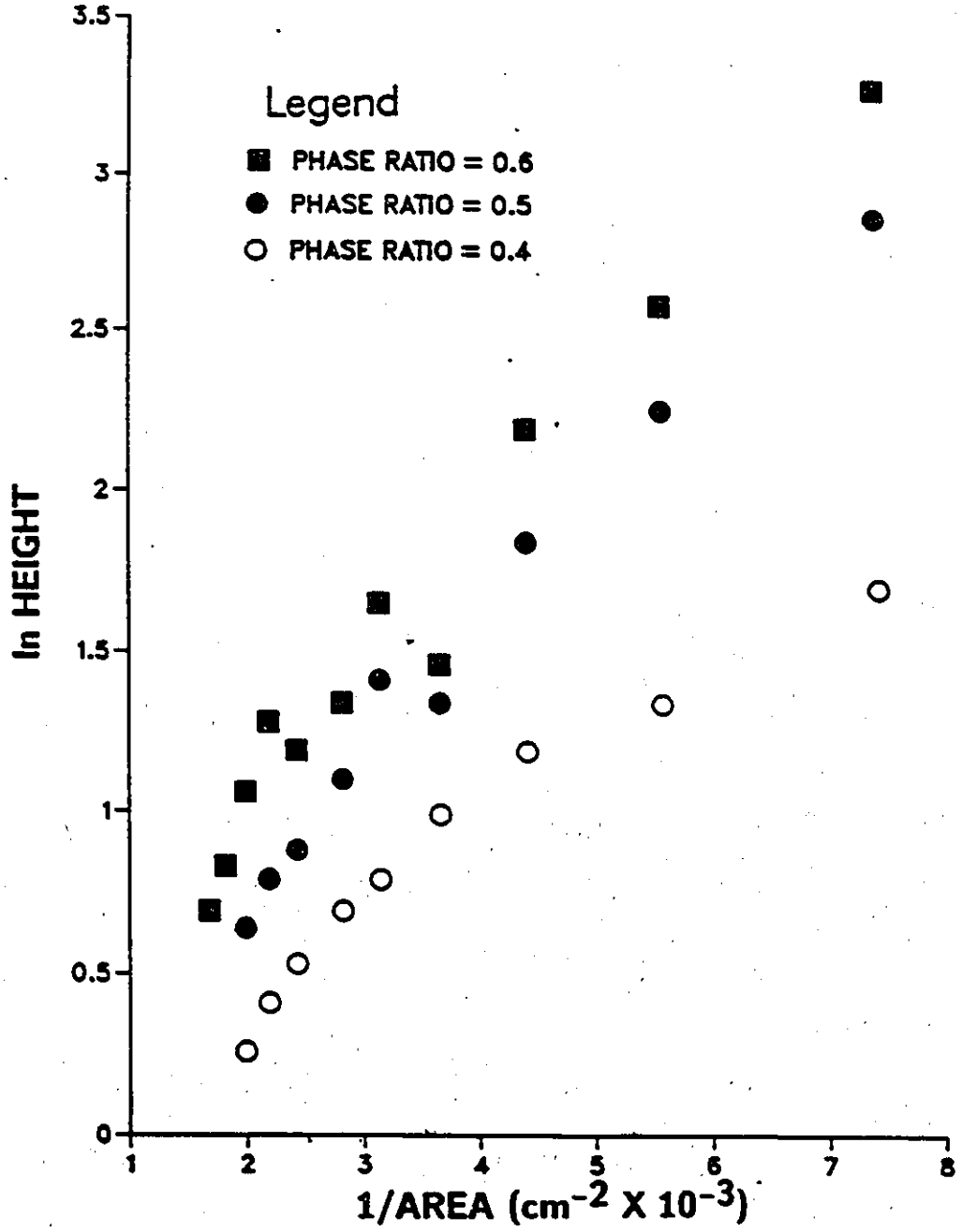

Figure No. 10: ln Height versus 1/area plot for the square mixer data at Q = 1500 mL/min and RPM = 200

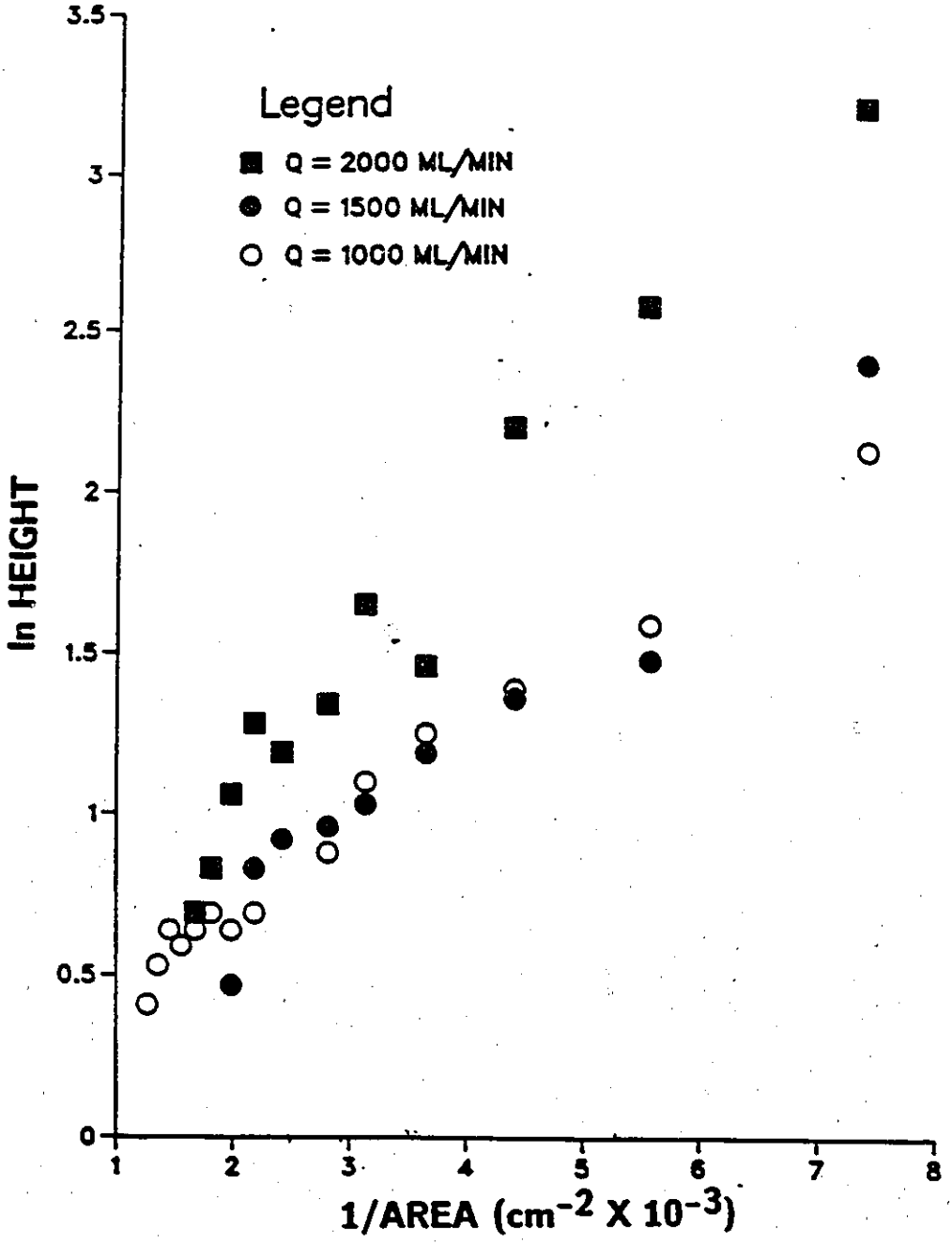

Figure No. 11: ln Height versus 1/area plot for the square mixer data at RPM = 250 and PR = 0.5

run, the parameters, β_0 and β_1, may be distinct functions of the process variables and thereby assist in the identification of those variables which have a significant effect on the dispersion band height and in the development of a model which represents the dispersion band height in terms of throughput, agitation intensity and dispersed phase ratio.

The Grid Technique is a modelling technique developed by Sylvestre and Scott [15]. It involves, the estimation of the parameters for each individual run. These parameter estimates are then plotted versus the remaining process variables (e. g. Q, RPM, PR) to observe any possible trends (i. e. a straight line or quadratic function). If trends exist, the original parameter estimates are modelled with respect to that process variable which exhibited a trend. This introduces new parameters into the model with which the algorithm may be repeated until each variable has been tested for inclusion in the model. Citing weaknesses within this technique (i. e. require an experimental design with more than three levels of the process variables to evaluate any trends), a model containing ten parameters failed to adequately represent the experimental data.

Instead, a modified version of this technique was implemented successfully. The original parameters, β_0 and β_1, were expanded into a linear quadratic polynomial:

$$\beta = a_0 + \sum_{i=1}^{3} a_i x_i + \sum_{i=1}^{3}\sum_{j=1}^{3} a_{ij} x_i x_j$$

with respect to all of the process variables (Q, RPM, PR). Using the Statistical Analysis Systems (SAS) procedure STEPWISE, estimates of the parameters were determined. The STEPWISE procedure introduces or eliminates parameter estimates based on the Q ratio. The Q ratio is:

$$Q = \frac{1}{\hat{\sigma}^2} \frac{(\text{SSRmodel1}) - (\text{SSRmodel2})}{(\text{No.ofParametersModel2}) - (\text{No.ofparametersModel1})}$$

where $\hat{\sigma}^2$ is an estimate of pure error variance. The decision at each step about whether to add a term to the existing model is made within the routine by comparing this Q ratio to an F value specified by the user. This F value remains constant throughout the sequence of fits [16]. The F value is determined from a three dimensional probability distribution function using the degrees of freedom from each

model. The degrees of freedom for a model is equal to (n-p), where n is the number of data points and p the estimated number of parameters.

The results of the STEPWISE procedure, for the expansion of β_0 and β_1, are presented in Table 4. Parameter estimates for β_0 and β_1 are represented as a and b values respectively. Parameters with standard deviations larger than the estimated value were not included in the model.

Table 4: Parameter Estimates for the Square Mixer

parameter	Estimate and Std. Deviation
a_0	0.00833 +/- 0.00010
a_2	0.08628 +/- 0.04902
a_3	0.07978 +/- 0.04902
b_0	373.95 +/- 0.35
b_1	79.83 +/- 11.95
b_2	62.77 +/- 11.95
b_3	39.37 +/- 11.95
b_{13}	32.60 +/- 14.64
b_{22}	-42.97 +/- 18.900

Coded variables were used for analysis (i. e. +1, 0, -1). The subscripts 1, 2, and 3 denote Q, RPM, and PR respectively.

Therefore, for the square mixer the original parameters become:

$$\beta_0 = a_0 + a_2(\mathrm{RPM}) + a_3(\mathrm{PR})$$

$$\beta_1 = b_0 + b_1(\mathrm{Q}) + b_2(\mathrm{RPM}) + b_3(\mathrm{PR}) + b_{13}(\mathrm{Q} * \mathrm{PR}) + b_{22}(\mathrm{RPM})^2$$

These values can then be substituted back into the original equation for the calculation of dispersion band heights. The final model was then plotted against the experimental data. This is represented in Figures 12 through 14. These plots represent the extreme and centre point data from the experimental design (i. e. -1,-1,-1 and +1,+1,+1 and 0,0,0). A residual plot is shown in Figure 15.

Figures 12 through 15 show that the model underpredicts the dispersion band heights for the square mixer configuration. The models' lack of fit has several sources, some of which are experimental or modelling technique.

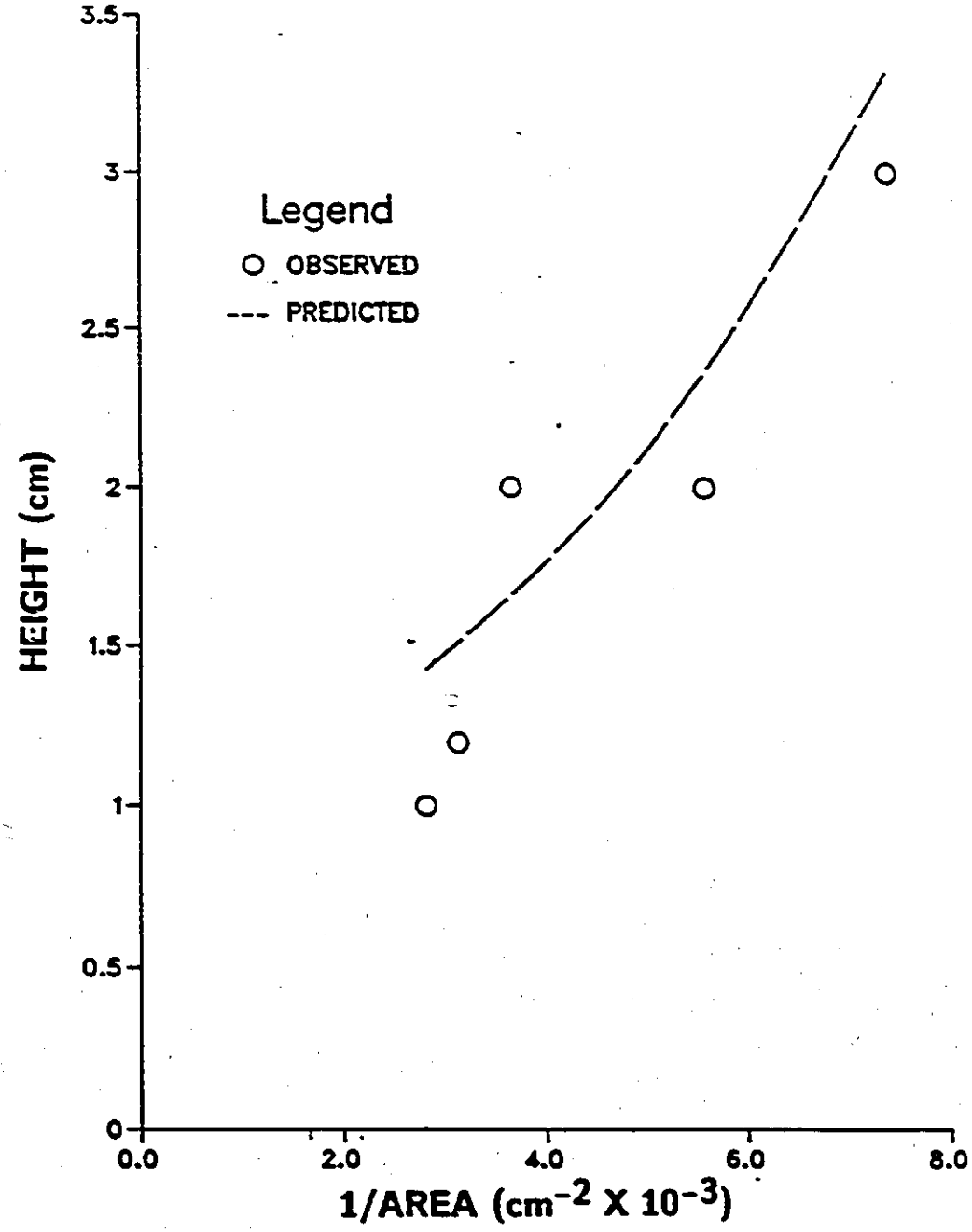

Figure No. 12: Observed and Predicted dispersion band heights versus 1/area for the square mixer. At Q = 1000 mL/min, RPM = 150 and PR = 0.4

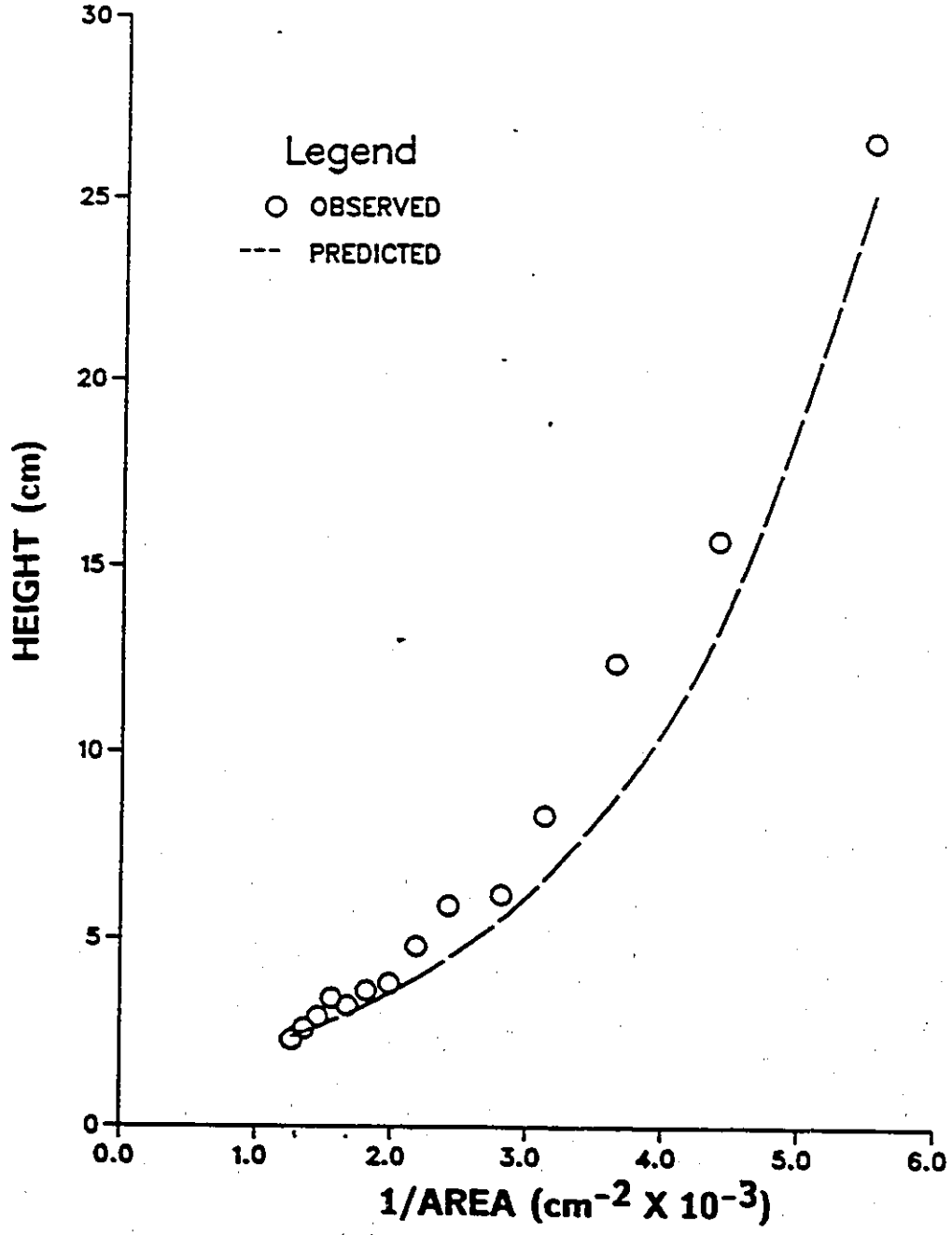

Figure No. 13: Observed and Predicted dispersion band heights versus 1/area for the square mixer. At Q = 2000 mL/min, RPM = 250 and PR = 0.6

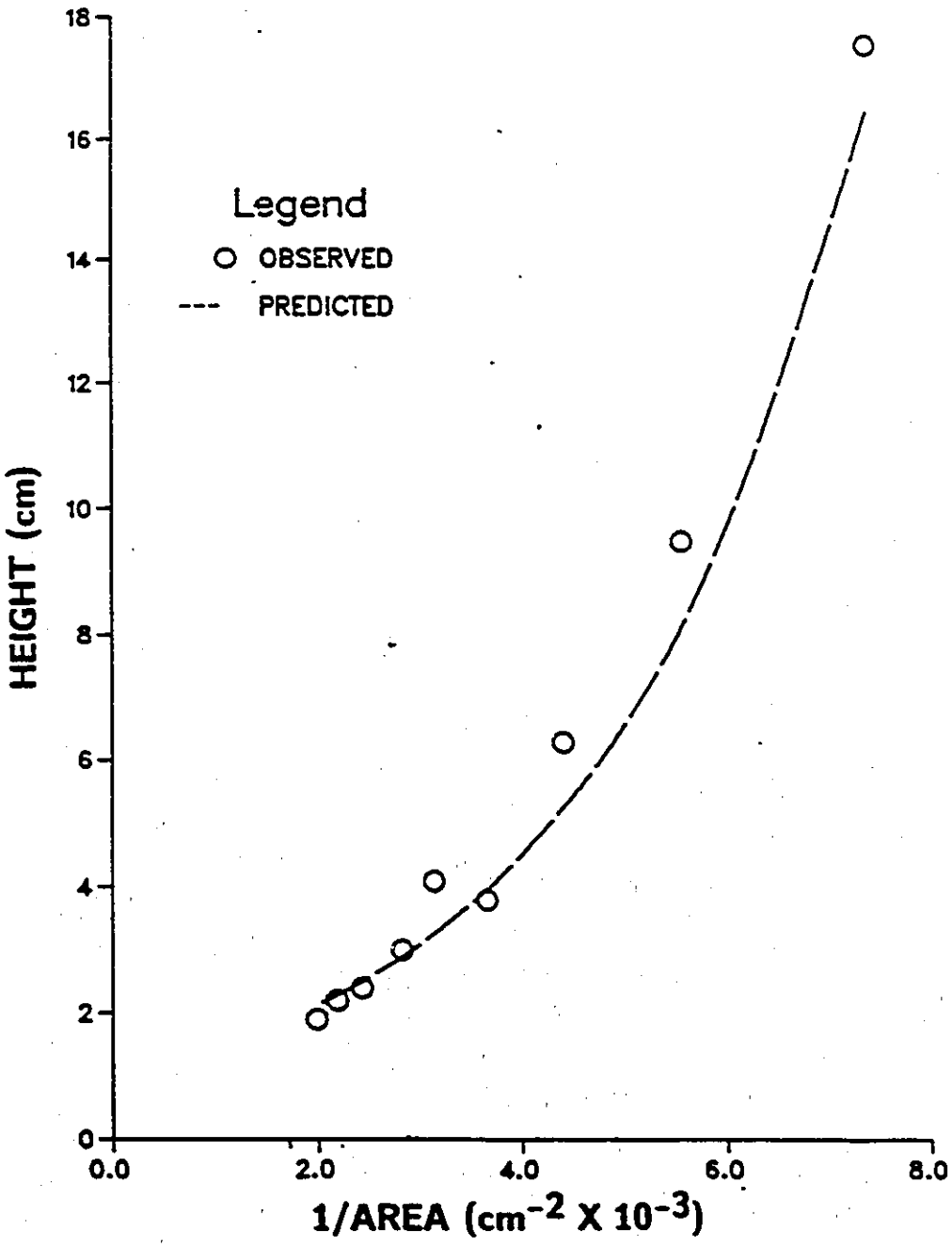

Figure No. 14: Observed and Predicted dispersion band heights versus 1/area for the square mixer. At Q = 1500 mL/min, RPM = 200 and PR = 0.5

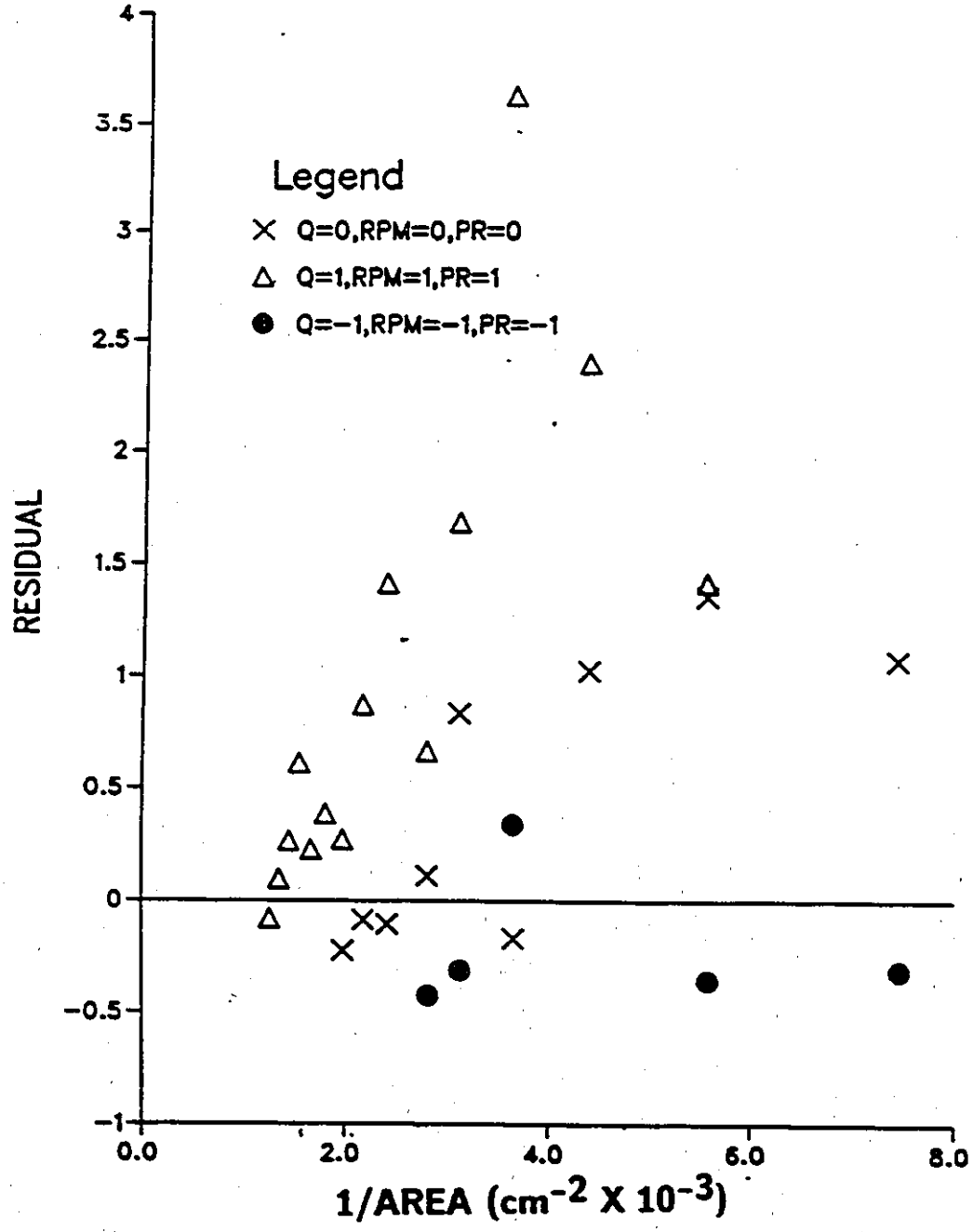

Figure No. 15: Residual plot for the square mixer model.

The time trend shown in Figure 7 probably occurs because of solvent degradation. Degradation may occur, since the experiments were performed over a one year period. To overcome this problem, periodic addition of fresh organic solvent would be required. The assumption that, moving the baffle to vary settling area while all other process variables were held constant, would not show dispersion band height correlation, was a second experimental error which may contribute to model inadequacy.

The mathematical modelling technique also contributed to model inadequacy shown in Figures 12 through 15. The decision of appropriate transformation by R^2 values is not reliable. Modelling with the alternative transformation may improve model fit of the data. The use of other quantitative/qualitative methods for decision of appropriate transformation, may also improve model fit.

The use of stepwise regression does not necessarily produce the fitted model with the fewest terms nor even the combination of a specified number of terms that provides the best fit to the data. One must bear this in mind when using stepwise regression [16].

Considering the many sources for model inadequacy, a model has been developed for the square mixer configuration. The number of parameters is prohibitive (9), however, the model can be used for comparison with other models developed for different mixer configurations.

Atkinsons' [1] model contained only four parameters. This model was developed for an aqueous continuous mixer operation. As well, the use of nonlinear regression analysis was implemented. Both of these approaches would contribute to differences between Atkinsons' model and the model developed in the present study.

The square mixer model, developed in the present study, shows dependence on all of the process variables tested. This model then, agrees with the mechanism of dispersion coalescence proposed by Barnea and Mizrahi [5].

4.2 Cylindrical Mixer Results and Modelling

Using an open baffled cylindrical mixer yielded similar data as the square mixer. The experimental data for the cylindrical mixer is presented in Figures 16 through 19 and Appendix B. The data is presented in the form: dispersion band height (H) versus the inverse of the area (1/A). In general, the data shows concave upward shape. The plots reveal an increase in dispersion band height with increasing throughput (Figure 16) and phase ratio (Figure 17). The effect of agitation intensity (Figure 18) shows an inconsistent trend, that is, dispersion band heights are greater for the impeller speed of 200 RPM as opposed to 250 RPM. Usually, higher agitation intensities would produce smaller droplets, which would in turn increase dispersion band heights, according to the proposed mechanism of dispersion coalescence. This discrepancy was not reported in the literature. Figure 19 indicates that a time trend exists, as was reported earlier for the square mixer data.

Selecting an appropriate transformation was necessary for modelling the effects of process variables on dispersion band height. As was done with the square mixer data, the cylindrical mixer data was plotted as ln H versus 1/A and ln H versus ln (1/A). The R^2 values were used to determine the transformation which best represented the data. The R^2 values are presented in Table 5. The mean R^2 values for the ln H versus 1/A and ln H versus ln (1/A) transformations were 0.8754 and 0.9081 respectively. The 95% confidence interval calculated for the difference between the mean R^2 values for each transformation was [0.0109 to 0.0556]. Since the value of zero did not lie within the interval, the two transformations were considered significantly different. The selection process indicates the transformation ln H versus ln (1/A) best represents the data as a straight line.

The transformed data is presented in Figures 20 to 22 and Appendix C. The selected model

$$\ln H = \beta_0 + \beta_1 * \ln(1/A)$$

with experimentally determined parameters, β_0 and β_1, serves as the starting point for further mathematical modelling.

The previously utilized version of the Grid Technique[15] was again implemented

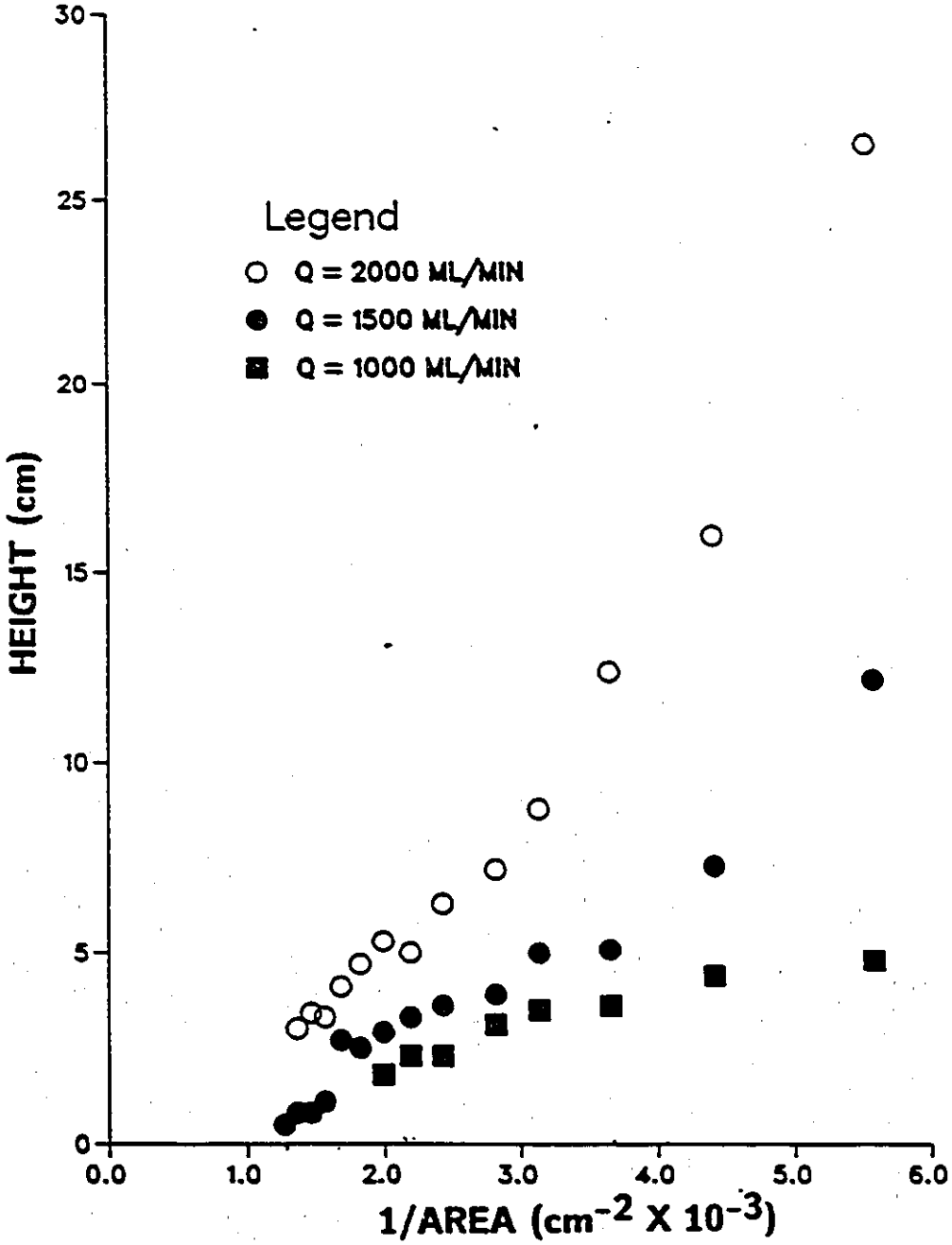

Figure No. 16: Experimental data for the cylindrical mixer data. Dispersion band height vs. 1/area ar RPM = 250 and PR = 0.6

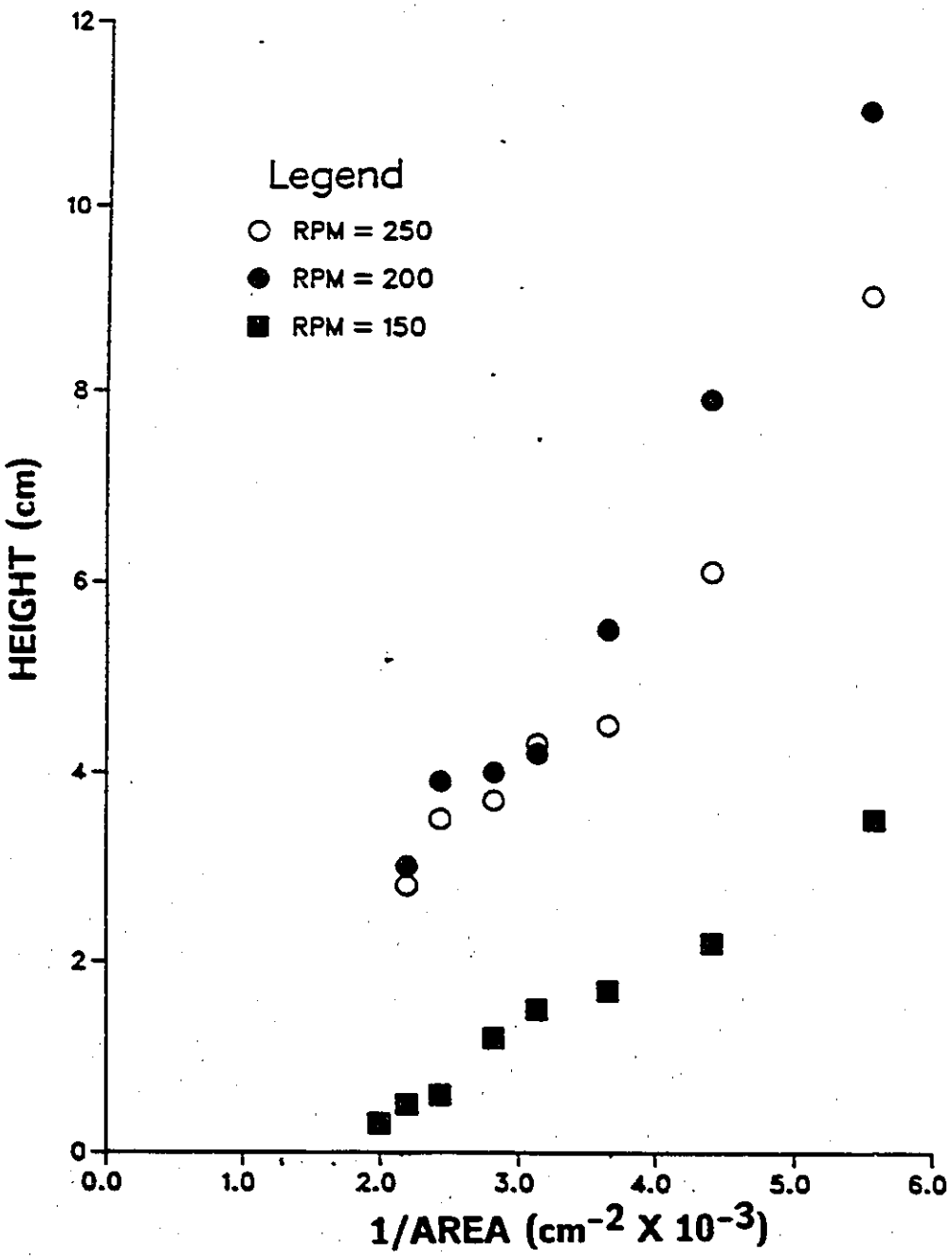

Figure No. 17: Experimental data for the cylindrical mixer data. Dispersion band height vs. 1/area at Q = 1500 mL/min and PR = 0.5.

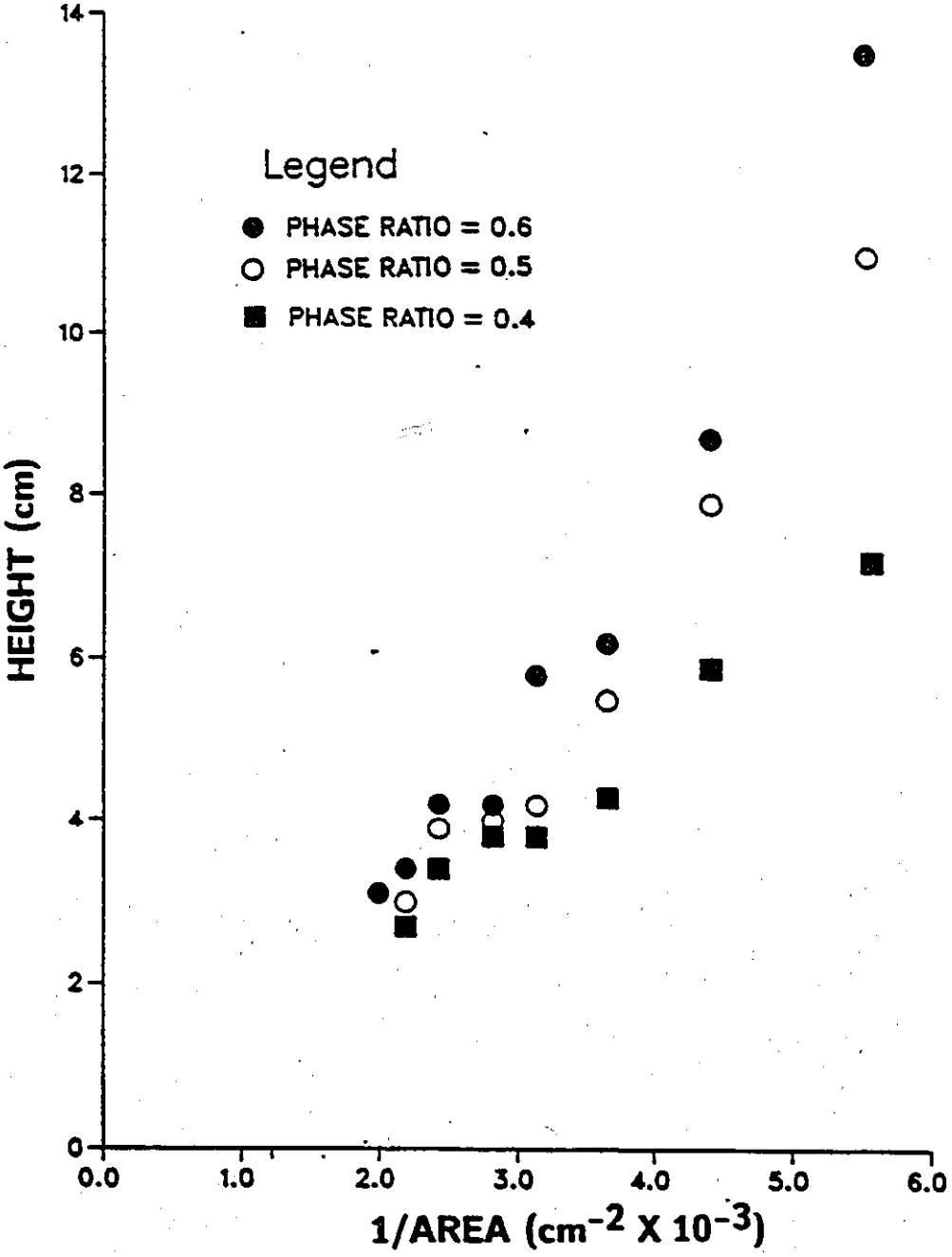

Figure No. 18: Experimental data for the cylindrical mixer data. Dispersion band height vs. 1/area at Q = 1500 mL/min and RPM = 200

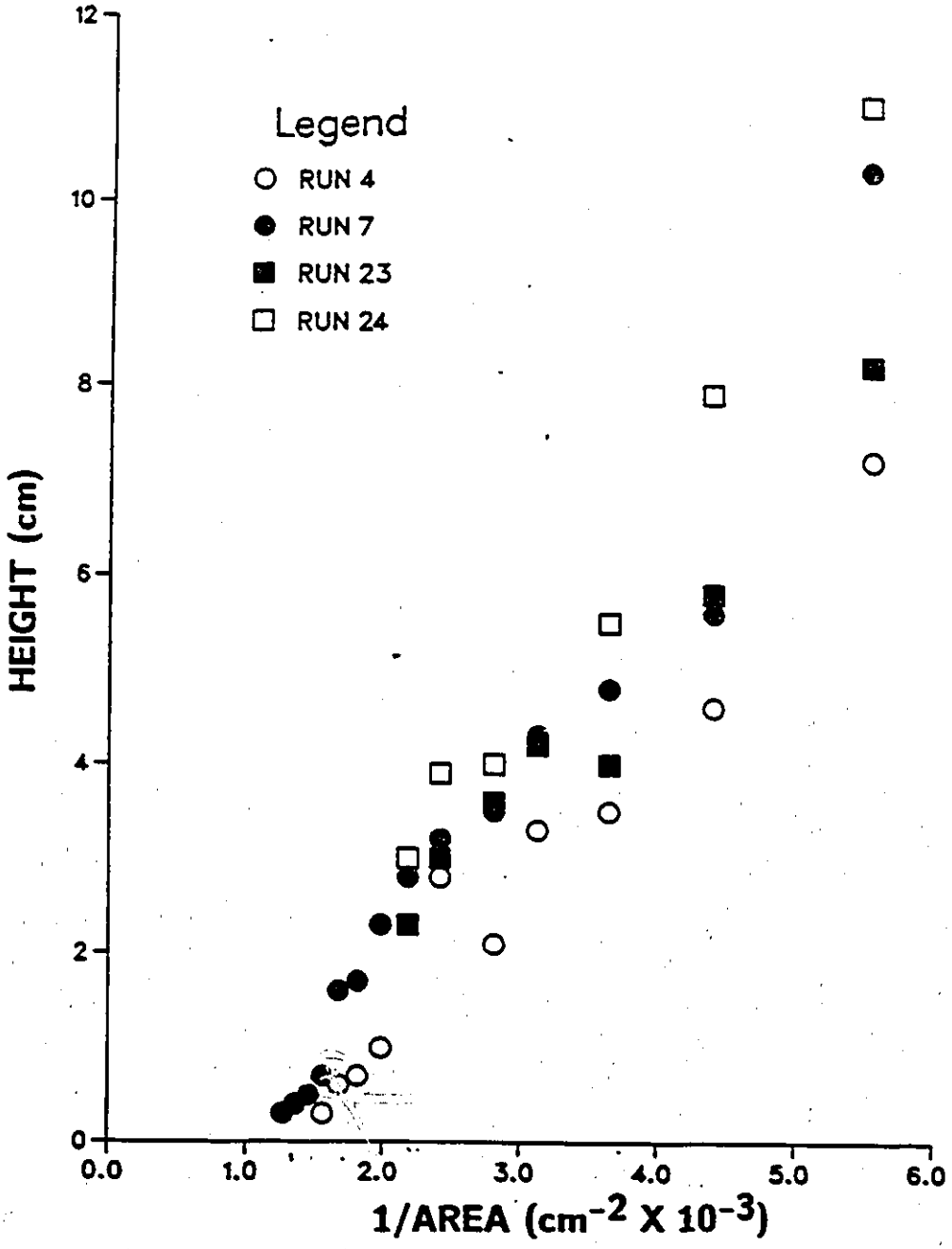

Figure No. 19: Replicate run data for the cylindrical mixer data. Dispersion band height vs. 1/area at Q = 1500 mL/min, RPM = 200 and PR = 0.5

Table 5: R^2 values for Cylindrical Mixer Data

Run no.	ln H vs. 1/A	ln H vs ln(1/A)
1	0.8532	0.9410
2	0.7538	0.8707
3	0.6813	0.8257
4	0.7707	0.8786
5	0.8583	0.9356
6	0.7631	0.8726
7	0.7409	0.8726
8	0.8365	0.9112
9	0.8531	0.9070
10	0.8713	0.7851
11	0.8827	0.8128
12	0.9474	0.9676
13	0.7925	0.8495
14	0.9158	0.9357
15	0.8340	0.8668
16	0.8525	0.8918
17	0.9918	0.9695
18	0.8548	0.9333
19	0.7745	0.8234
20	0.9931	0.9799
21	0.9157	0.8348
22	0.9799	0.9632
23	0.9451	0.9562
24	0.9768	0.9615
25	0.9655	0.9934
26	0.7800	0.8277
27	0.9566	0.9586
28	0.9828	0.9737
29	0.9580	0.9638
30	0.9824	0.9807

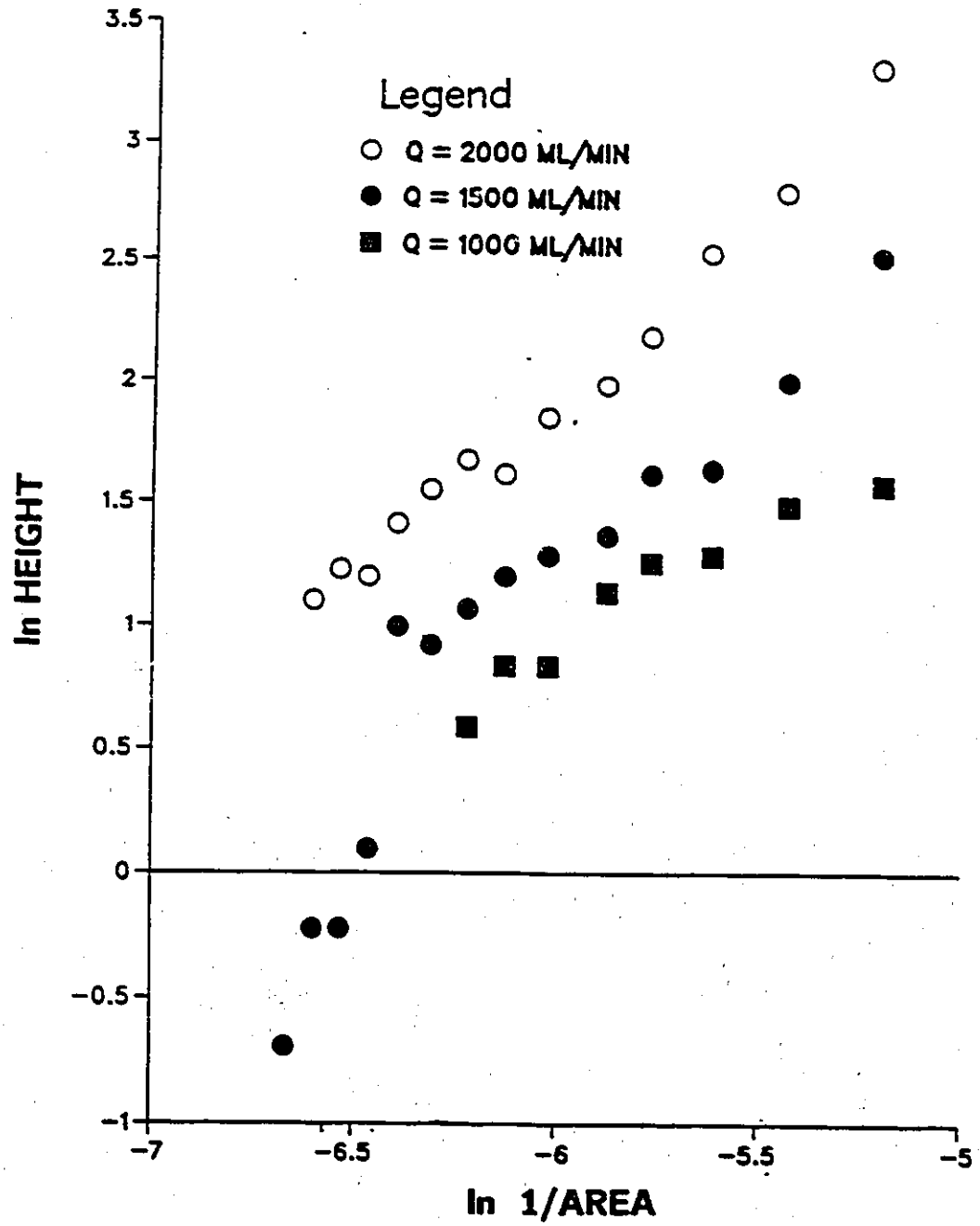

Figure No. 20: ln Height versus ln 1/area plot
for the cylindrical mixer data at RPM = 250 and PR = 0.6

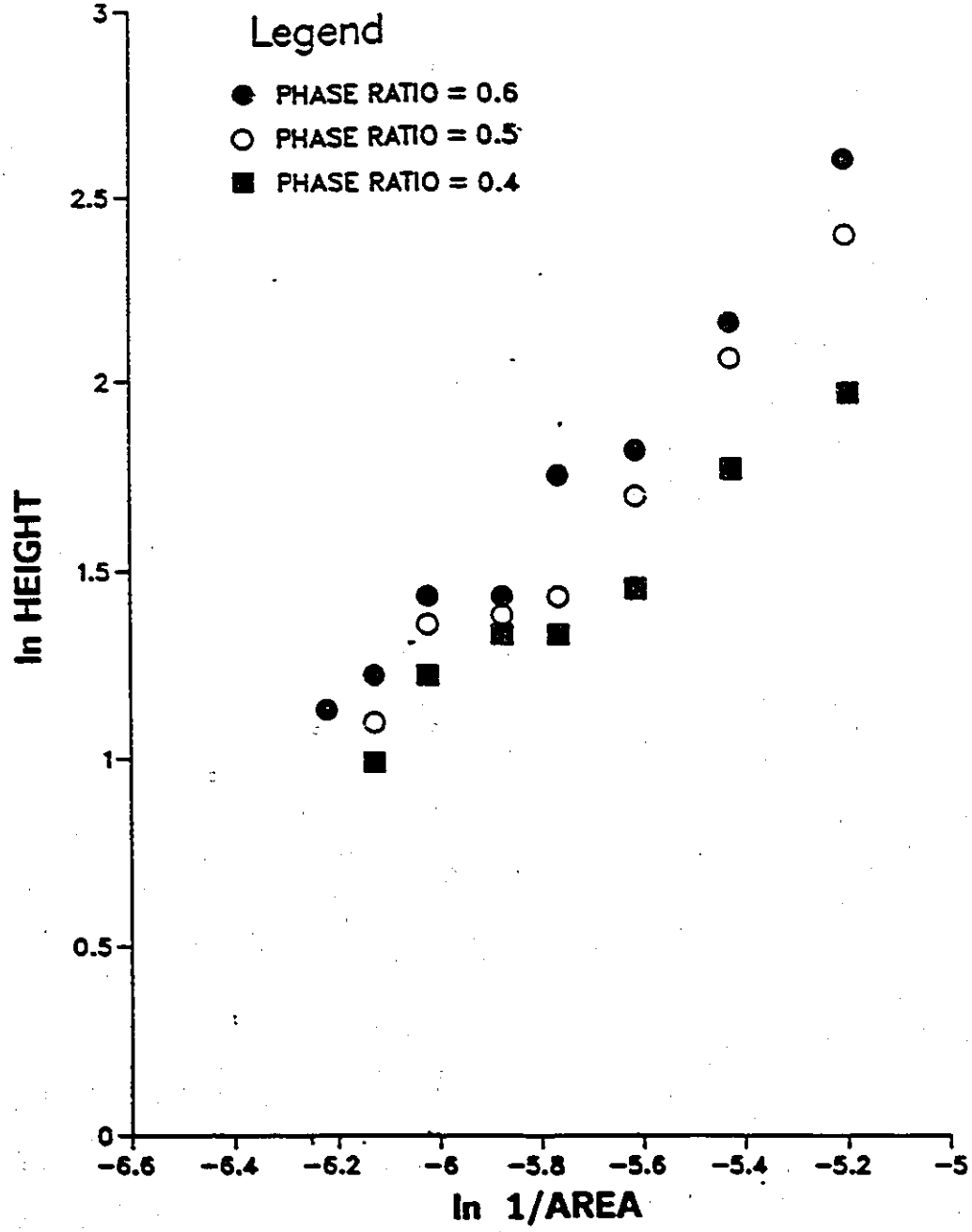

Figure No. 21: ln Height versus ln 1/area plot for the cylindrical mixer data at Q = 1500 mL/min and RPM = 200

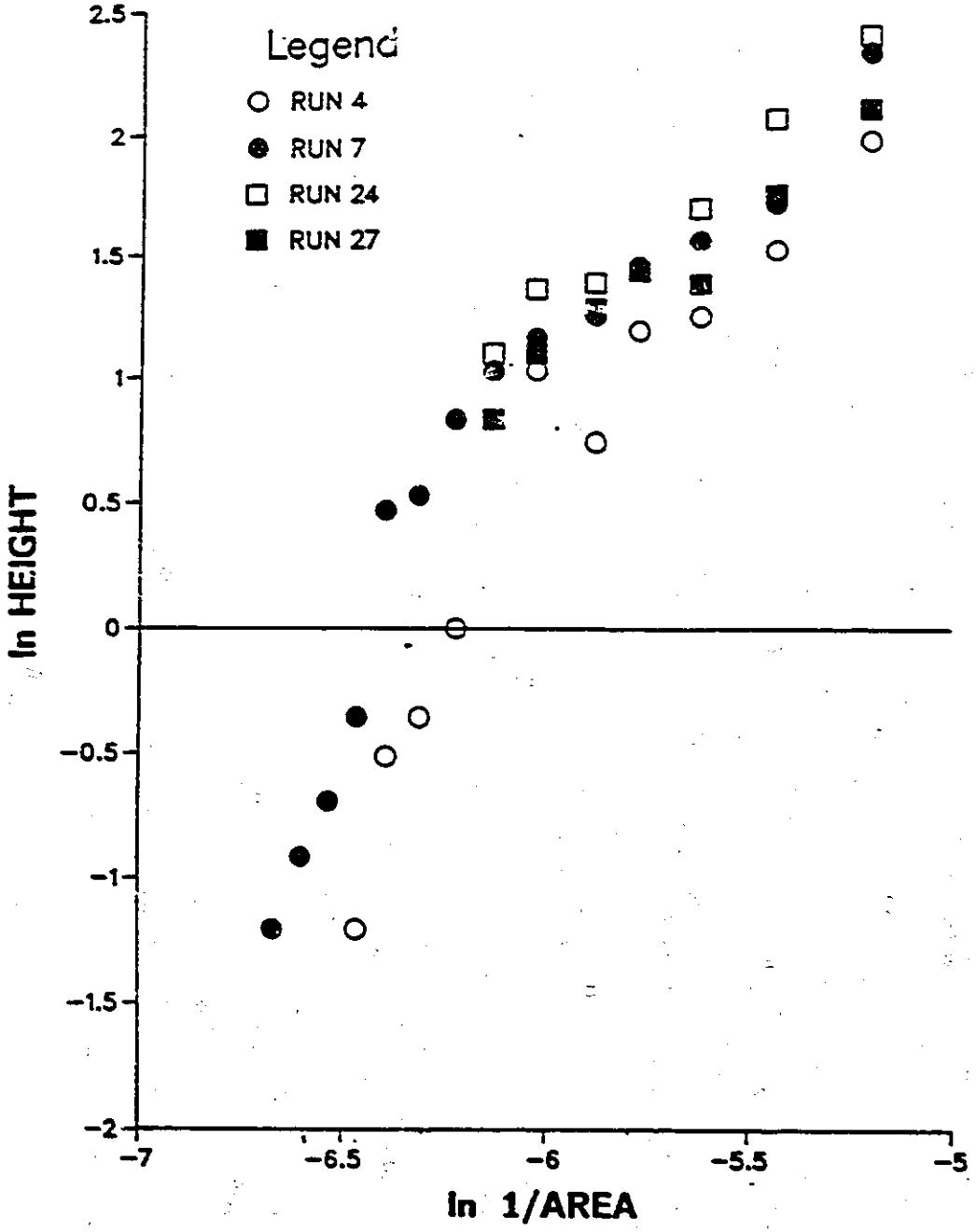

Figure No. 22: ln Height versus ln 1/area plot for the replicate run data at Q = 150 mL/min, RPM = 200, PR = 0.5

to model the data (see section 4.1). The parameters β_0 and β_1 are again expanded into polynomial form as:

$$\beta = a_0 + \sum_{i=1}^{3} a_i x_i + \sum_{i=1}^{3}\sum_{j=1}^{3} a_{ij} x_i x_j$$

The SAS procedure STEPWISE was used to determine the best model (see section 4.1). Coded variables were used for analysis and the subscripts 1, 2, and 3 represent Q, RPM, and PR respectively.

For the cylindrical mixer data the original parameters become:

$$\beta_0 = a_0 + a_1(Q) + a_2(RPM)$$

$$\beta_1 = b_0 + b_2(RPM)$$

The estimates for the secondary parameters are presented in Table 6.

Table 6: Parameter Estimates for the Cylindrical Mixer

parameter	Estimate and Std. Deviation
a_0	9.988 +/- 0.010
a_1	0.792 +/- 0.486
a_2	-1.107 +/- 0.4860
b_0	1.540 +/- 0.003
b_1	-0.278 +/- 0.0890

The final equation is of the form:

$$\ln H = (a_0 + a_1(Q) + a_2(RPM)) + (b_0 + b_2(RPM)) * \ln(1/A)$$

This model was then plotted against the experimental data. This is presented in Figures 23 to 25. These plots represent the extreme and centre point data from the experimental design (i.e. -1, -1, -1 and +1, +1, +1 and 0, 0, 0). A residual plot is shown in Figure 26. Figures 23 through 26 show that the model overpredicts the dispersion band heights for the cylindrical mixer configuration. Again, the lack of fit has several sources. The experimental and modelling weaknesses were discussed in the previous section (see Section 4.1) and equally apply for this set of data.

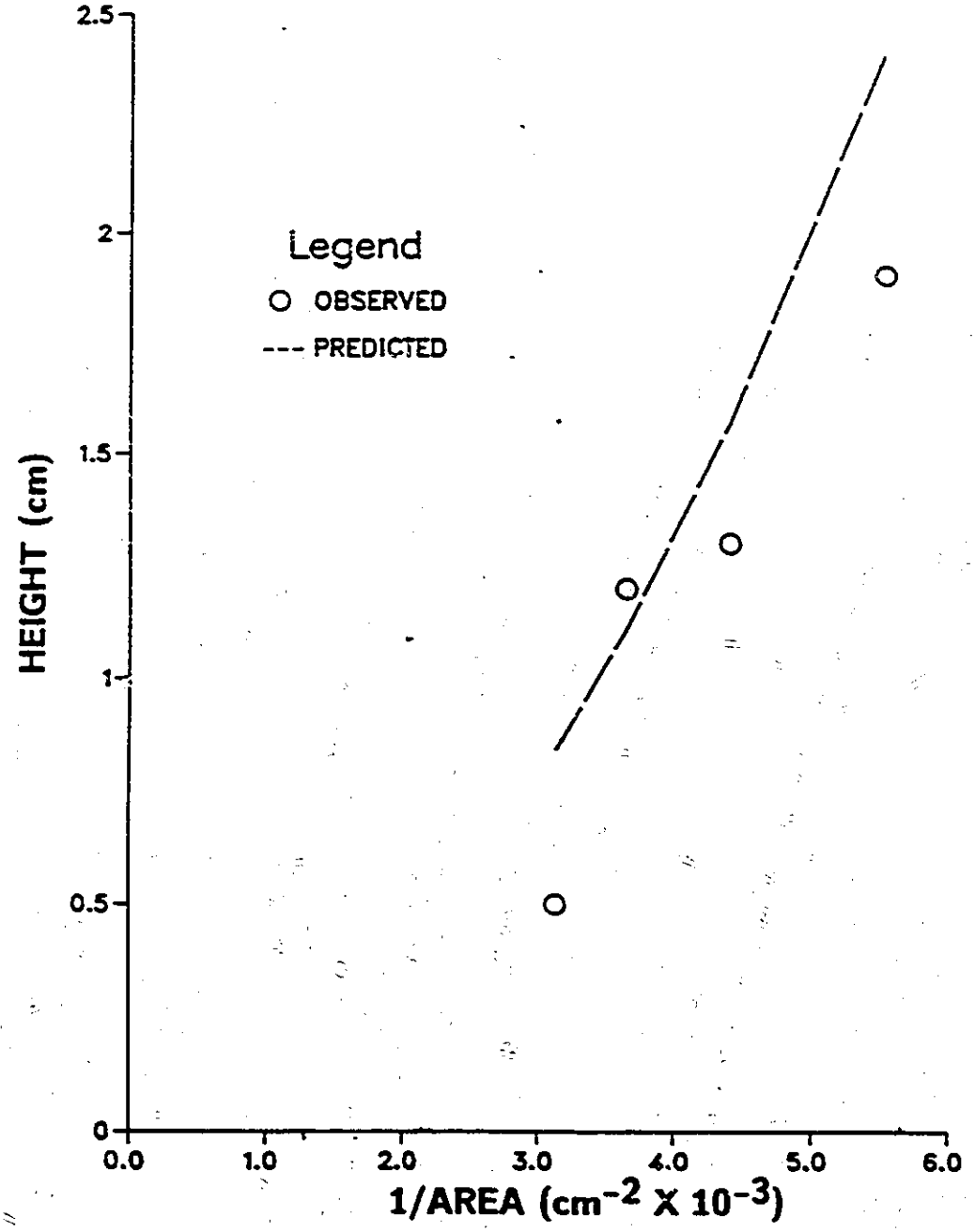

Figure No. 23: Observed and Predicted dispersion band heights versus 1/area for the cylindrical mixer. At Q = 1000 mL/min, RPM = 150 and PR = 0.4

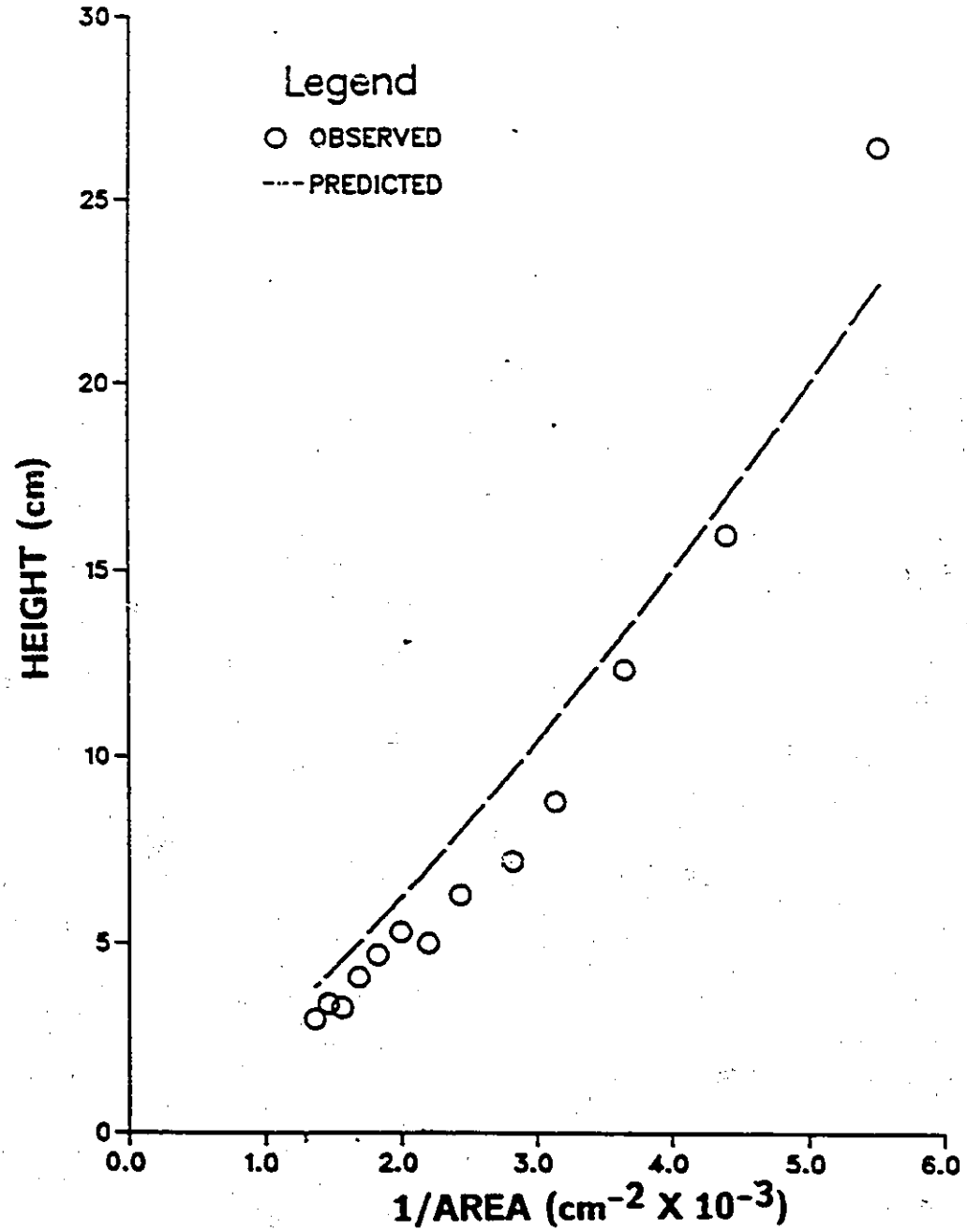

Figure No. 24: Observed and Predicted dispersion band heights versus 1/area for the cylindrical mixer. At Q = 2000 mL/min, RPM = 250 and PR = 0.6

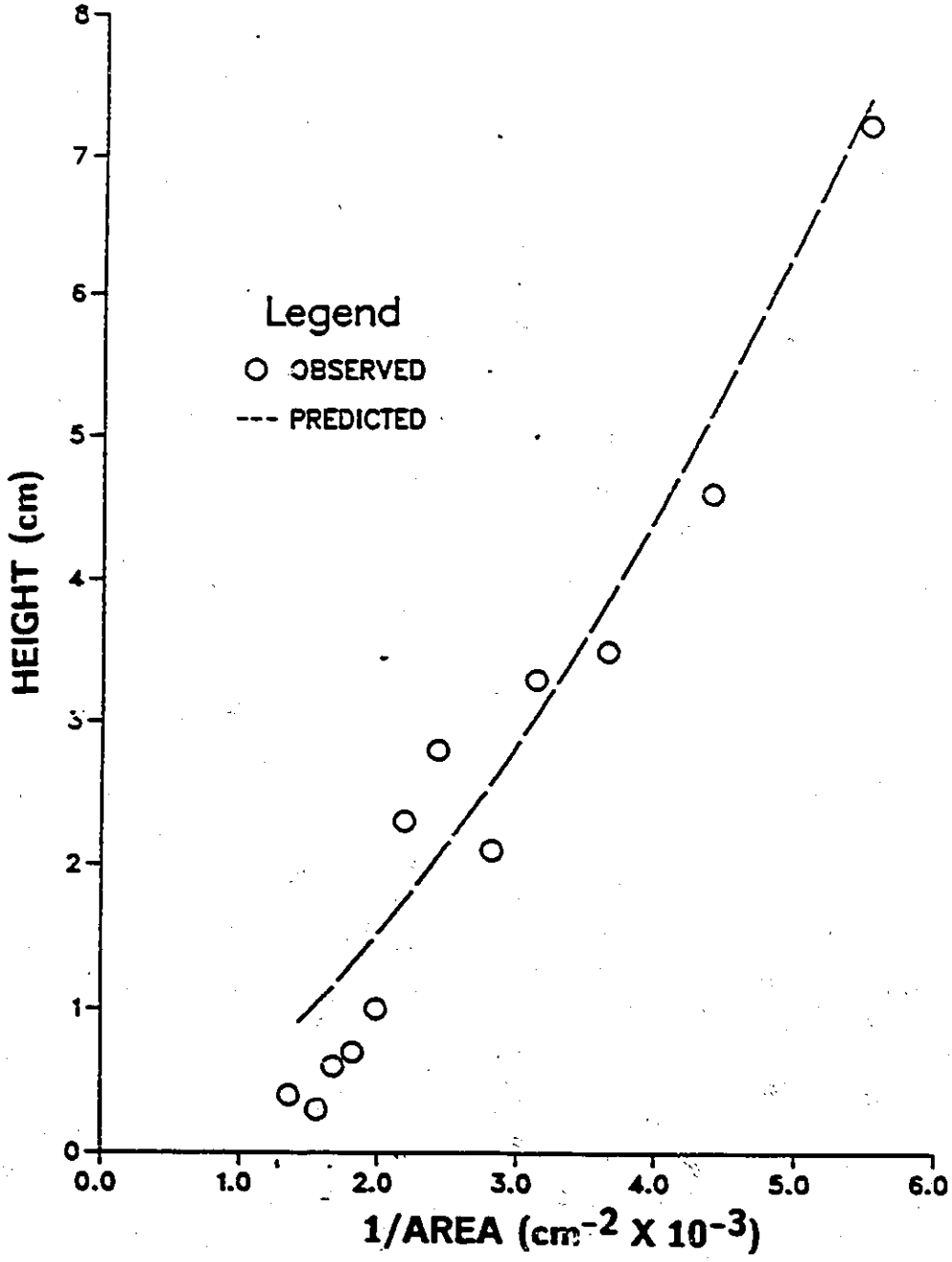

Figure No. 25: Observed and Predicted dispersion band heights versus 1/area for the cylindrical mixer. At Q = 1500 mL/min, RPM = 200 and PR = 0.5

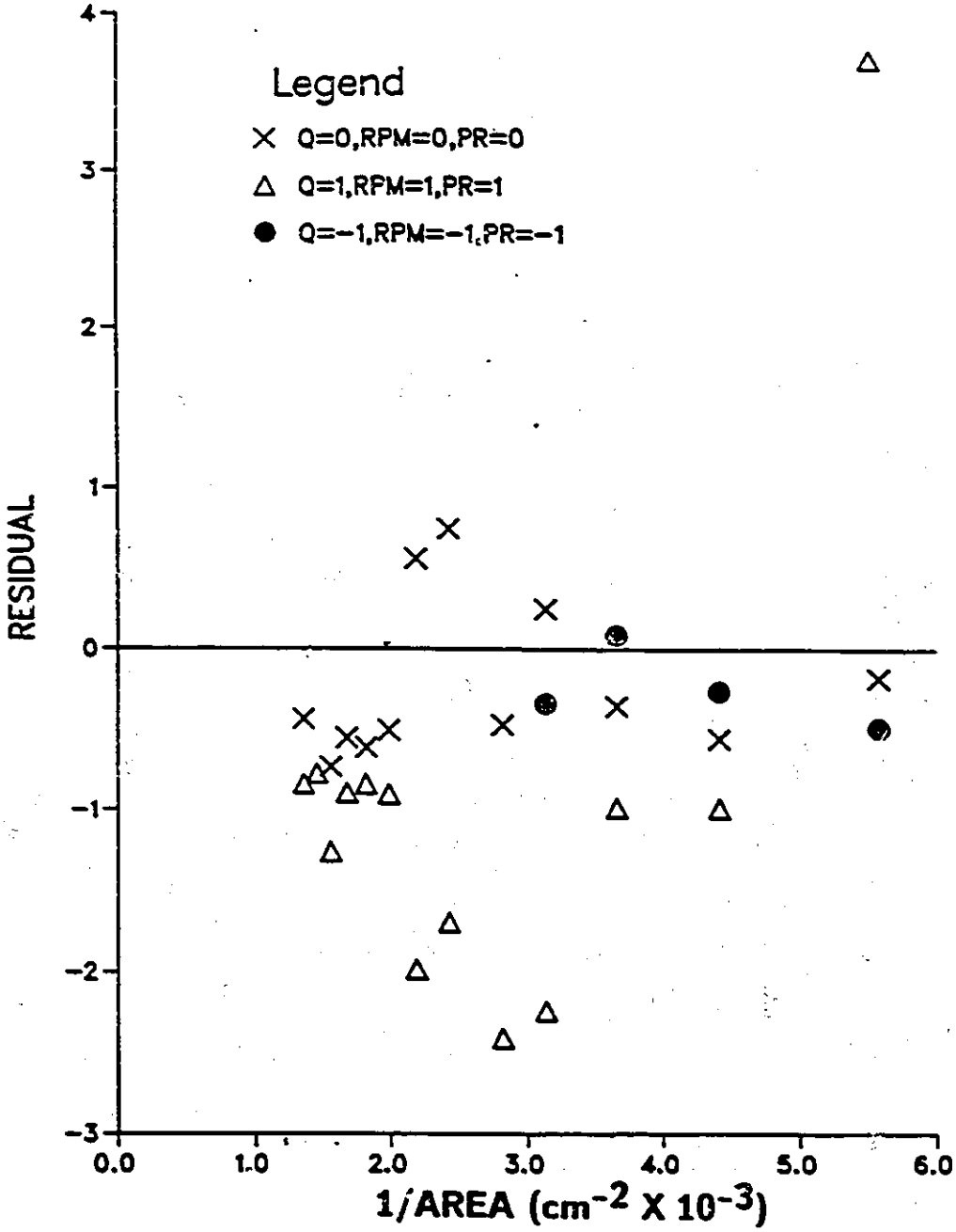

Figure No. 26: Residual Plot for the cylindrical mixer model

The inconsistent effect of agitation intensity must also be considered an additional source of model error. Respecting these sources for model error, a model for the cylindrical mixer data has been developed. This model allows for comparison with the square mixer model.

The cylindrical mixer model does not contain as many parameters (5 versus 9) as the square mixer model. Fewer parameters are desired, since an excessive number erodes the credibility of the model. Although the transformation selection procedure was identical for the two models, the difference in the number of parameters can be attributed to the use of different transformations. Recall that the square mixer utilized the transformation ln H versus 1/A, while the transformation ln H versus ln (1/A) was implemented for the cylindrical data. Since the reliability of R^2 values as a method of determining model adequacy is not known, applying the alternative transformation may prove advantageous.

The cylindrical mixer model did not show the dependence of dispersed phase ratio on dispersion band height. This contradicts the mechanism of dispsersion coalescence proposed by Barnea and Mizrahi [5]. The use of a larger dispersed phase ratio range must be tested to verify this result.

The effect of mixer configuration indicate that a simpler model can be developed for the cylindrical mixer. The effect of dispersed phase appears to be less pronounced for the cylindrical mixer configuration.

4.3 Closed Mixer Results and Modelling

A sealed baffled cylindrical mixer was used to study the effect of air entrainment on the dispersion band height in a gravity settler. The top of the mixer was sealed. The dispersion was forced through the small annulus between the shaft opening and the shaft itself. The dispersion flowed by gravity down a walled trough to the settler.

Determination of the correct agitation intensity was performed as detailed in Chapter 3. At an impeller speed of 150 RPM the phases inverted. Therefore, the speed was increased to prevent phase inversion. The lower limit was set at 200 RPM. Thus, center and upper limits became 250 and 300 RPM respectively.

The experimental data is presented in Figures 27 through 30 and Appendix B. The data is presented in the form: dispersion band height (H) versus the inverse of the area (1/A). The general shape of the plots is concave upward. Once again, the replicate run data, Figure 30, indicates a time trend for the data.

Plotting the experimental data in the form of the two transformations, ln H versus 1/A and ln H versus ln (1/A), yielded R^2 values for each run. These R^2 values were then used to select the most appropriate transformation for further modelling of the data. The R^2 values are listed in Table 7. Blocking the R^2 values into individual runs and calculating the difference between each transformation was used to calculate a 95% confidence interval for the difference between the two R^2 values. The 95% confidence interval for the difference between R^2 values was [-0.0102 to 0.0129]. In this case, the value of zero does lie within the interval. This result implies that there is no significant difference between the mean R^2 values of 0.9511 and 0.9497 representing the ln H versus 1/A and ln H versus ln (1/A) transformations. The selection process for the appropriate transformation was performed by comparison of R^2 values for each run. Recall that, higher R^2 values imply better model fit of the data. The transformation with the most 'winning' runs was then used for further modelling. From this the model selected for the closed mixer data was:

$$\ln H = \beta_0 + \beta_1(1/A)$$

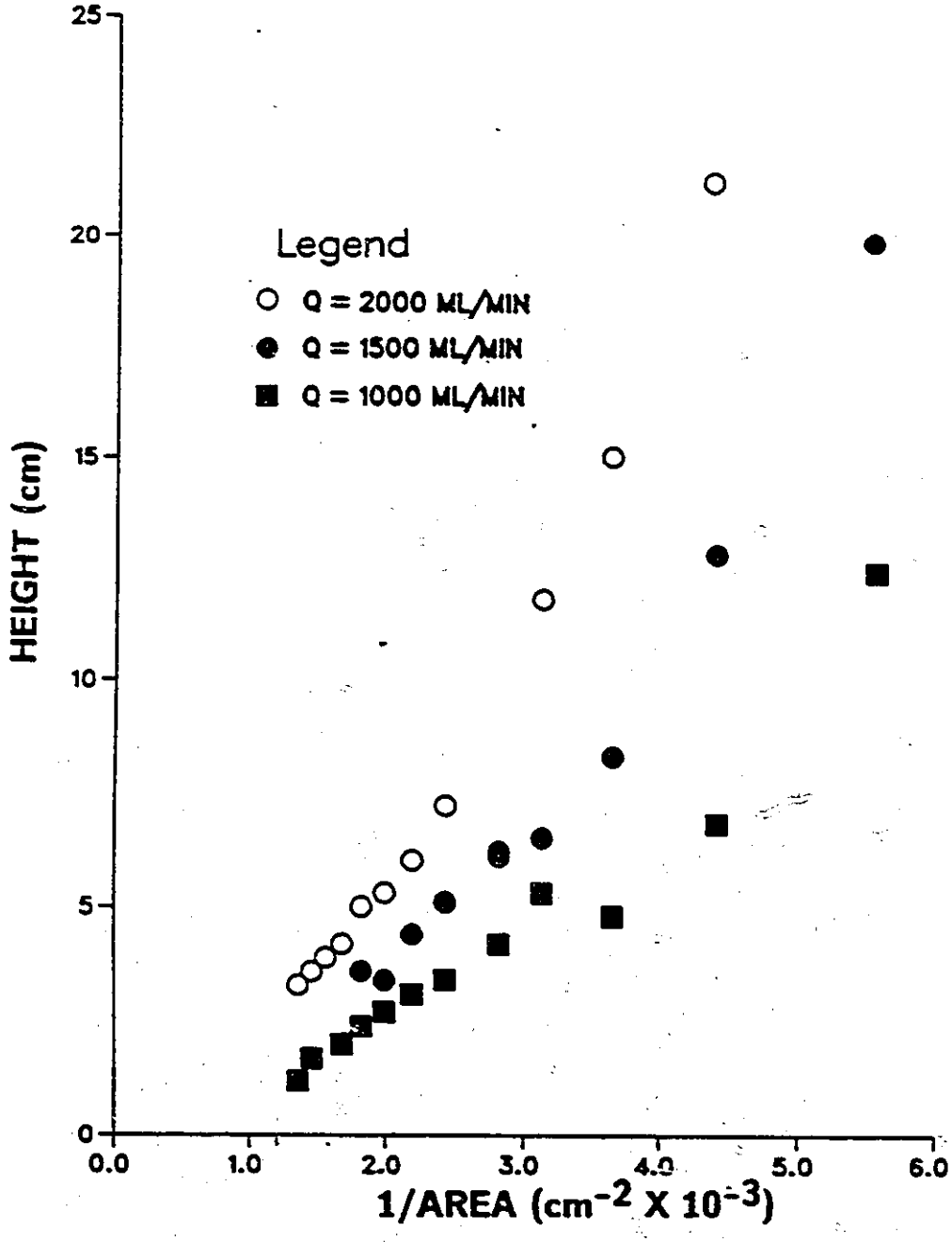

Figure No. 27: Experimental data for the closed mixer.
Dispersion band height vs. 1/area at RPM = 250 and PR = 0.6

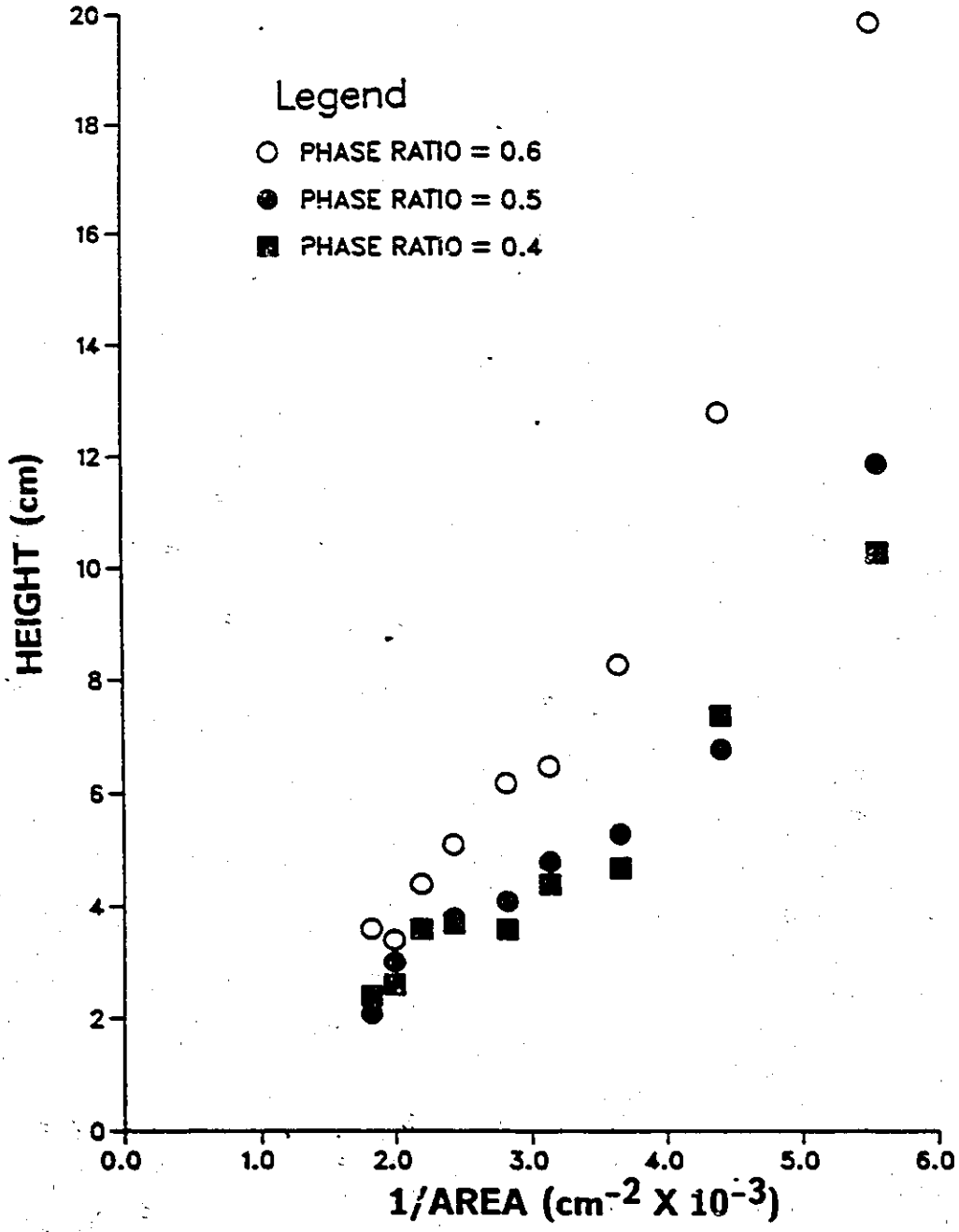

Figure No. 28: Experimental data for the closed mixer . Dispersion band height vs. 1/area at Q = 1500 mL/min and RPM = 250

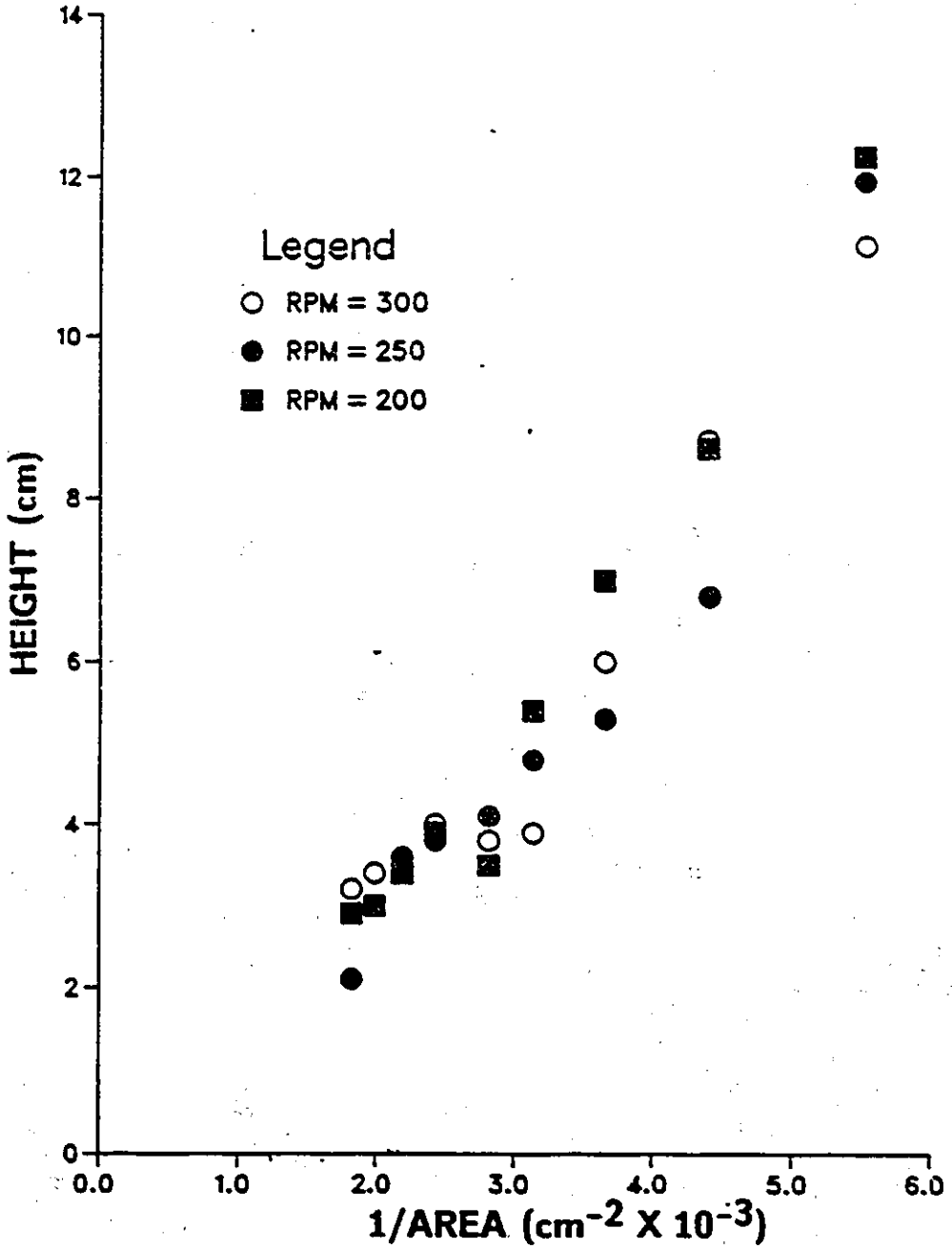

Figure No. 29: Experimental data for the closed mixer. Dispersion band height vs. 1/area at Q = 1500 mL/min and PR = 0.5

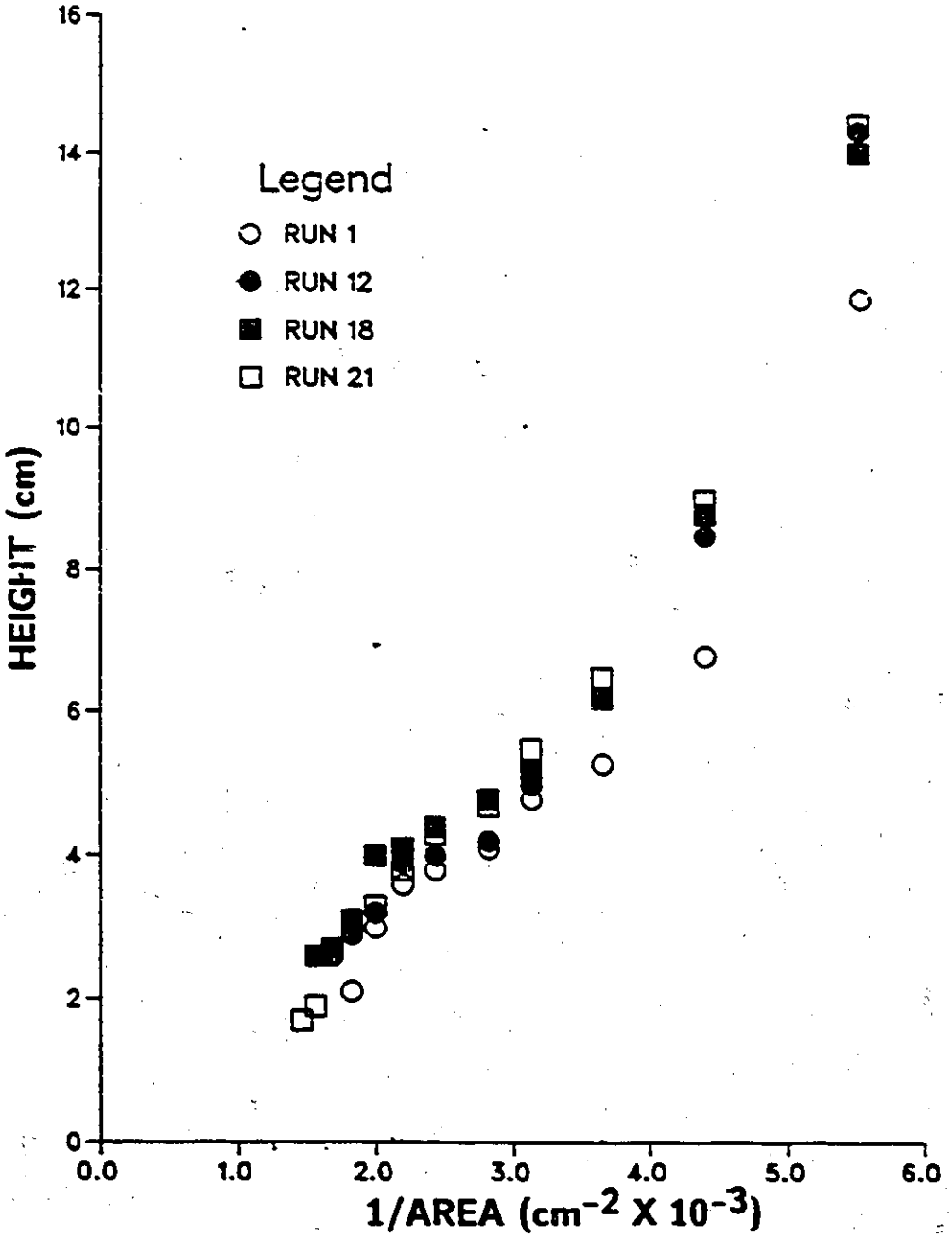

Figure No. 30: Replicate run data for the closed mixer. Dispersion band height vs. 1/area at Q = 1500 mL/min, RPM = 250 and PR = 0.5

Table 7: R^2 values for Closed Mixer data

Run No.	ln H vs. 1/A	ln H vs. ln(1/A)
1	0.9442	0.9445
2	0.9678	0.9683
3	0.8656	0.8240
4	0.9966	0.9662
5	0.8839	0.9537
6	0.9552	0.9419
7	0.9669	0.9595
8	0.9241	0.9664
9	0.7999	0.8755
10	0.9605	0.9413
11	0.9553	0.9826
12	0.9884	0.9607
13	0.8992	0.8572
14	0.9949	0.9793
15	0.9598	0.9537
16	0.9916	0.9724
17	0.9782	0.9892
18	0.9719	0.9604
19	0.9812	0.9917
20	0.9867	0.9771
21	0.9402	0.9740
22	0.9051	0.9259
23	0.9766	0.9722
24	0.9673	0.9866
25	0.9874	0.9758
26	0.9429	0.8923
27	0.9351	0.9269
28	0.9591	0.9516
29	0.9627	0.9879
30	0.9846	0.9329

The ln H versus 1/A graphs are presented in Figures 31 to 33 and Appendix C.

Implementing the expanded version of the Grid Technique (16), as mentioned in Sections 4.1 and 4.2, an appropriate model was developed. The original parameters , β_0 and β_1, were expanded according to the polynomial:

$$\beta = a_0 + \sum_{i=1}^{3} a_i x_i + \sum_{i=1}^{3}\sum_{j=1}^{3} a_{ij} x_i x_j$$

Using the SAS procedure STEPWISE (see Section 4.1) the most frugal model was developed. Coded variables were used for analysis and the subscripts 1, 2 and 3 represent Q, RPM and PR respectively.

For the closed cylindrical mixer data the original parameters become:

$$\beta_0 = a_0 + a_1(Q) + a_2(RPM) + a_{23}(RPM * PR) + a_{33}(PR)^2$$

$$\beta_i = b_0 + b_1(Q) + b_2(RPM) + b_3(PR)$$

The parameter estimates for the closed cylindrical data are listed in Table 8.

Table 8: Parameter Estimates for Closed Mixer data

parameter	Estimate and Std. Deviation
a_0	0.340 +/- 0.002
a_1	0.0925 +/- 0.0313
a_2	0.0475 +/- 0.0313
a_{23}	-0.0796 +/- 0.03830
a_{33}	-0.109 +/- 0.0495
b_0	415.54 +/- 3.01
b_1	97.83 +/- 10.92
b_2	-18.35 +/- 10.920
b_3	54.44 +/- 10.92

This model was then plotted against the experimental data. The experimental data representing the extreme and centre point runs (i.e. -1, -1, -1 and +1, +1, +1 and 0, 0, 0) were used for comparison to the model. This is presented in Figures 34 to 36. A residual plot is shown in Figure 37.

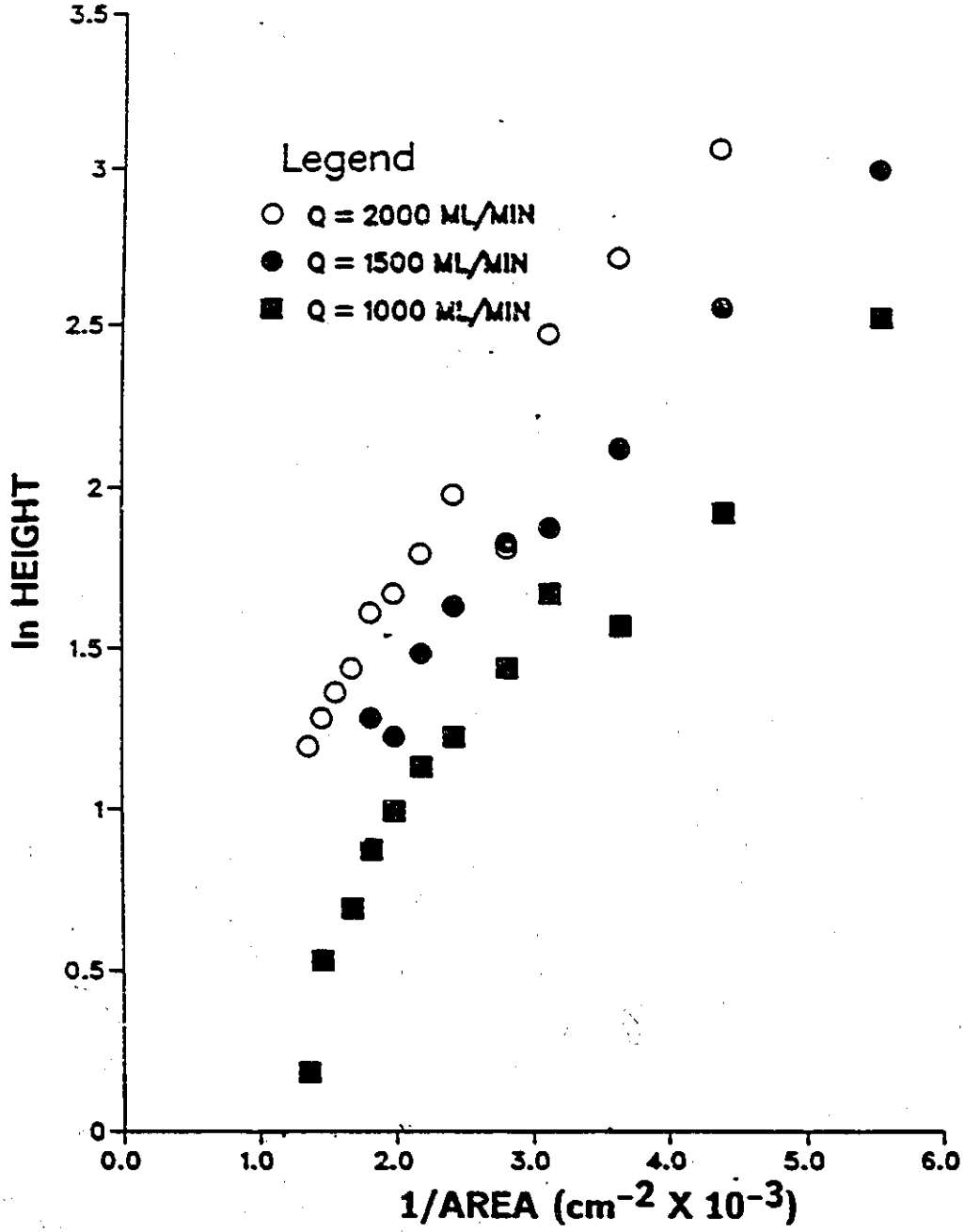

Figure No. 31: ln Height versus 1/area plot for the closed mixer data at RPM 250 and PR = 0.6

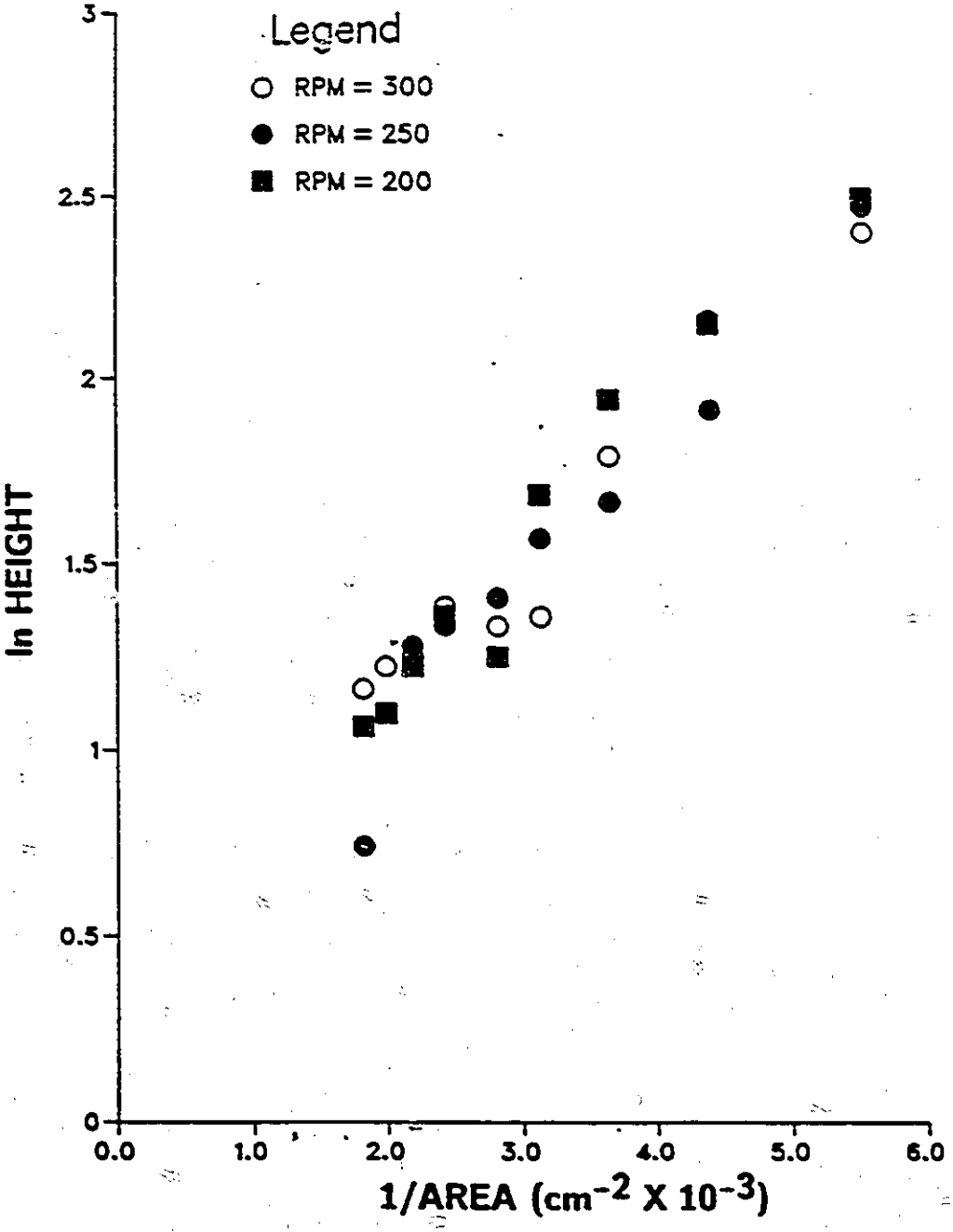

Figure No. 32: ln Height versus 1/area plot for the closed mixer data at Q = 1500 mL/min and PR = 0.5

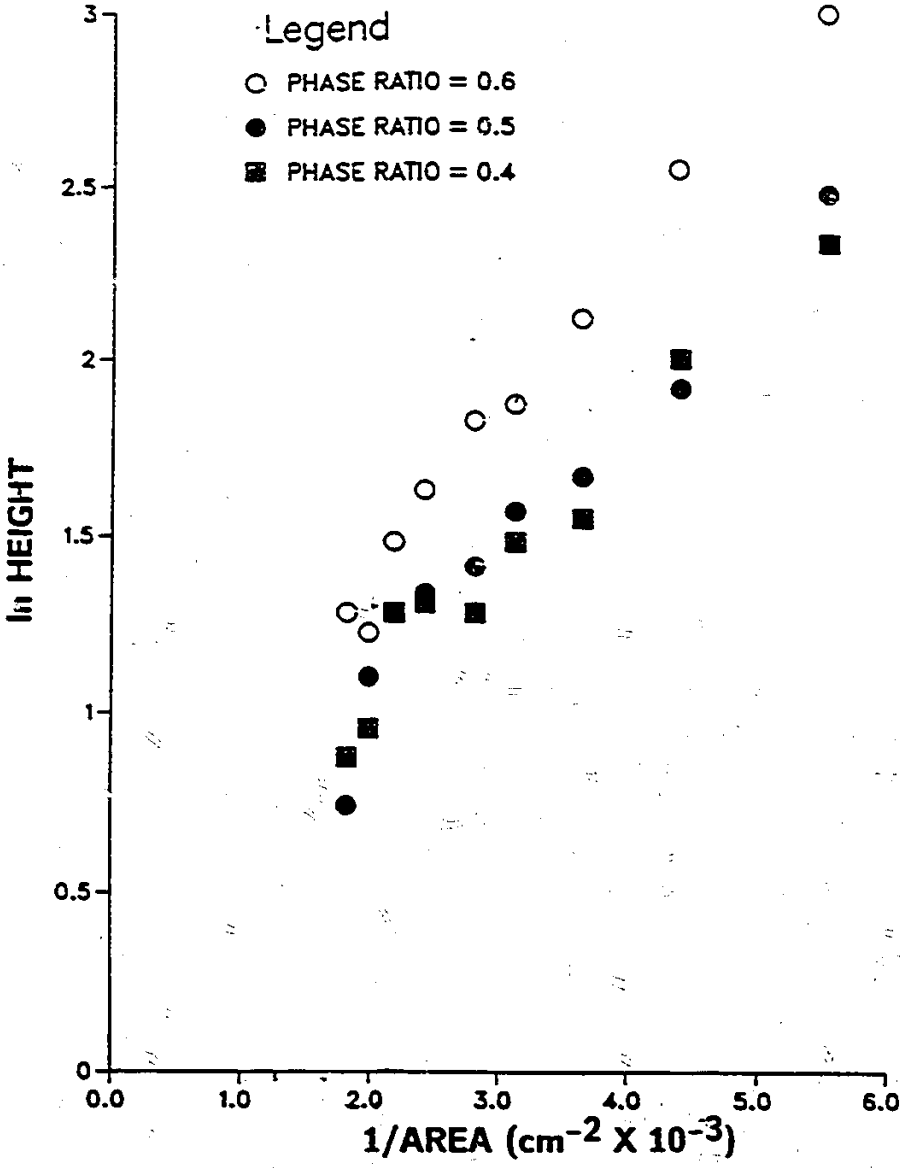

Figure No. 33: ln Height versus 1/area plot for the closed mixer data at Q = 1500 mL/min and RPM = 250.

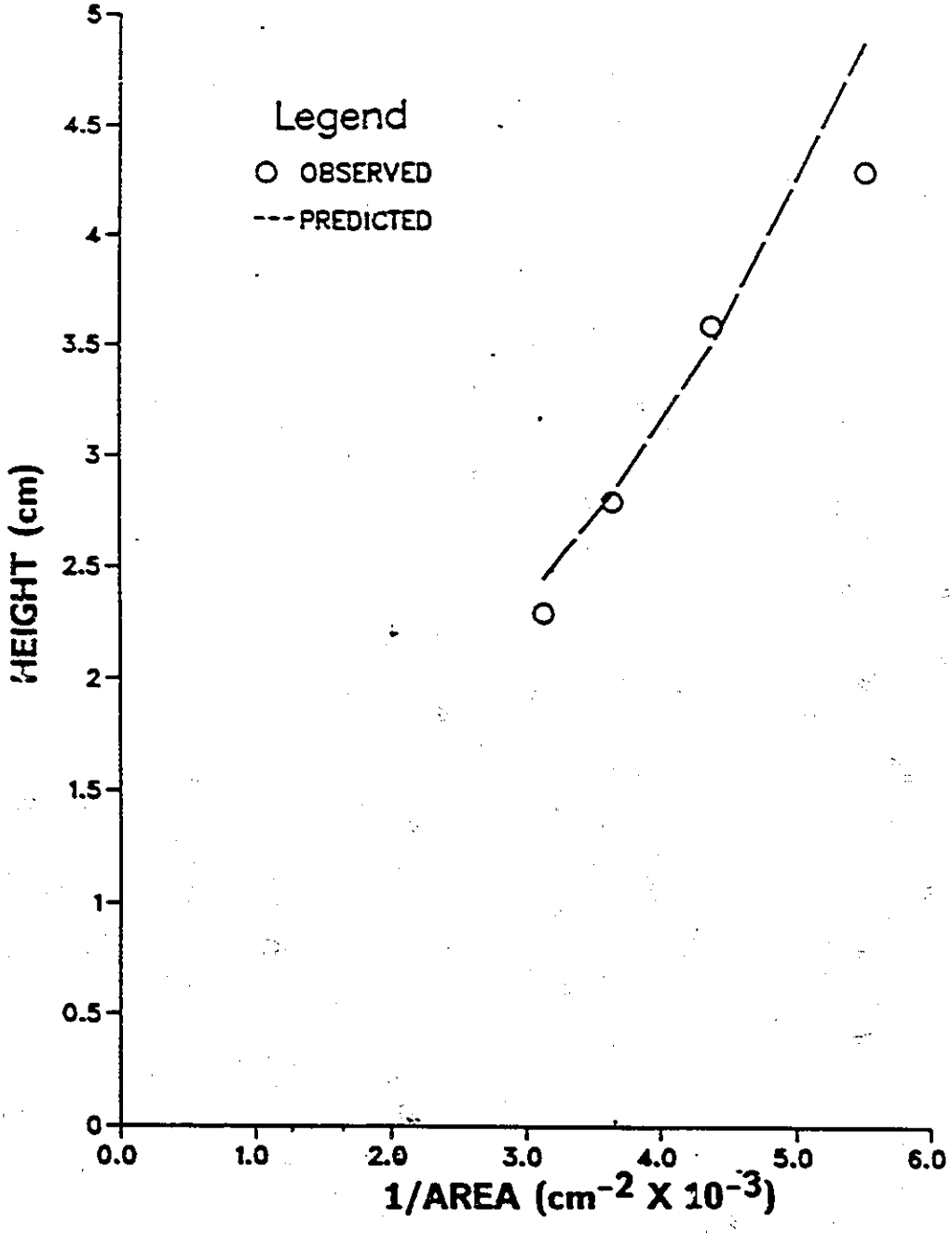

Figure No. 34: Observed and Predicted dispersion band heights versus 1/area for the closed mixer. At Q = 1000 mL/min, RPM = 200 and PR = 0.4

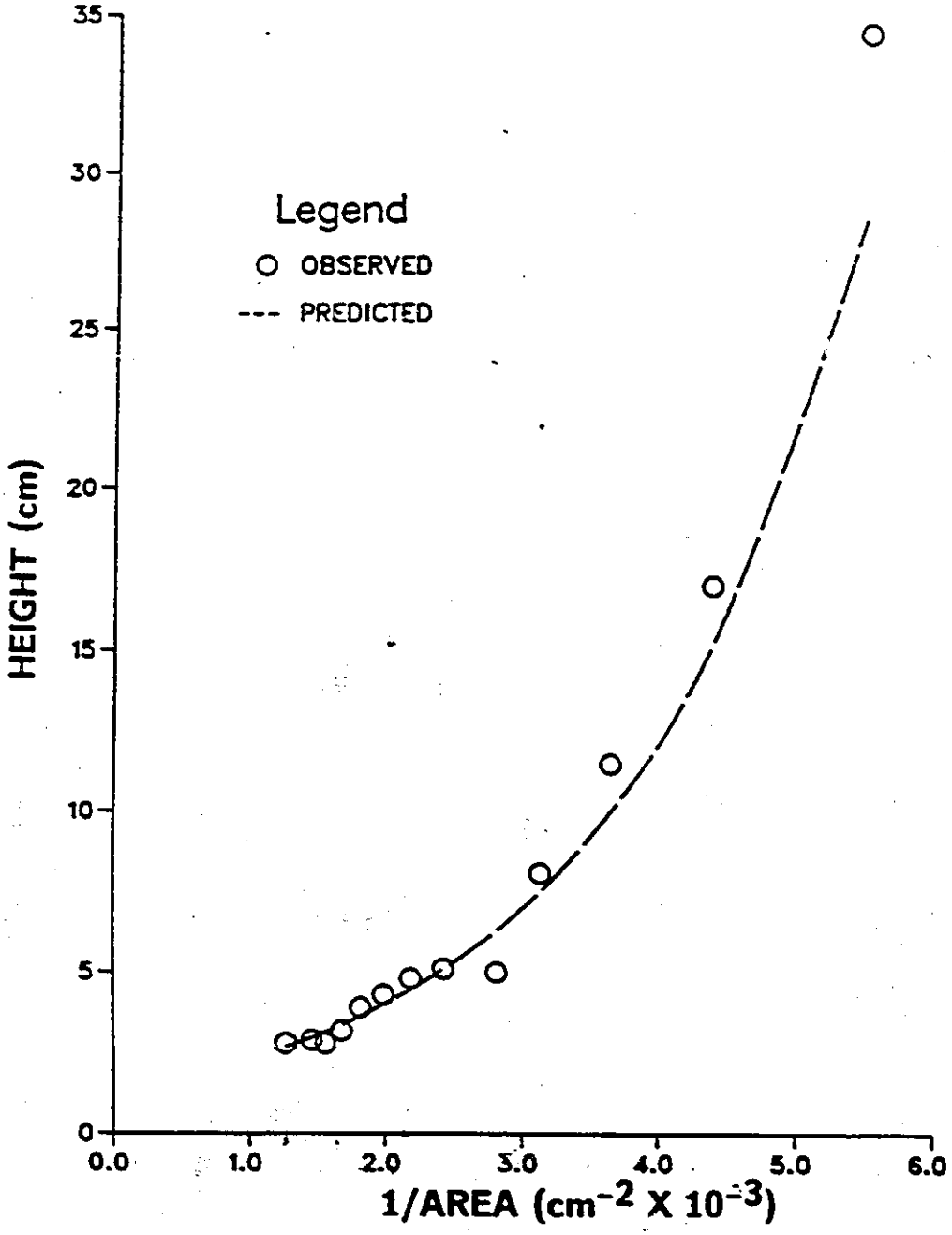

Figure No. 35: Observed and Predicted dispersion band heights versus 1/area for the closed mixer.
At Q = 2000 mL/min, RPM = 300 and PR = 0.6

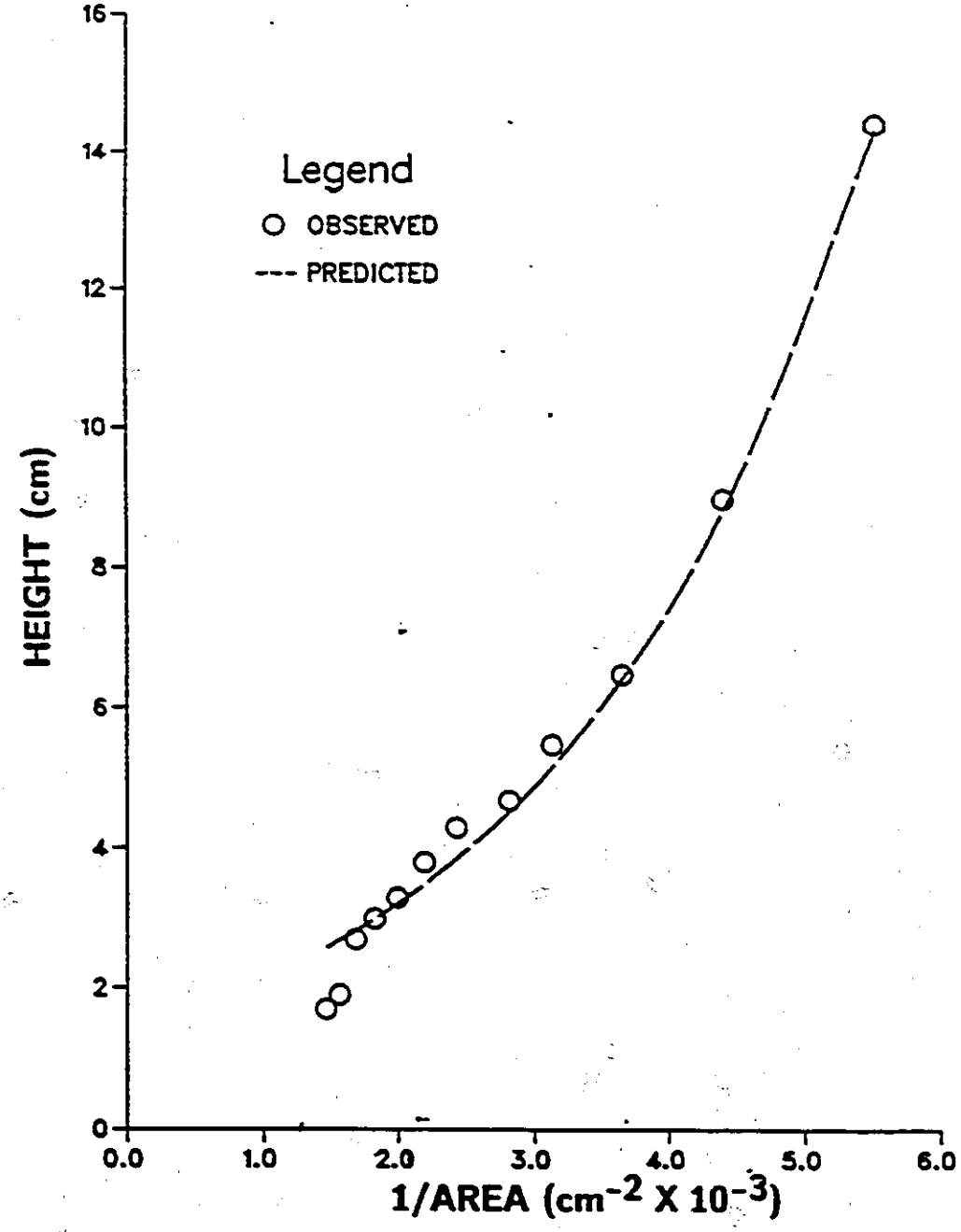

Figure No. 36: Observed and Predicted dispersion band heights versus 1/area for the closed mixer.
At Q = 1500 mL/min, RPM = 250 and PR = 0.5

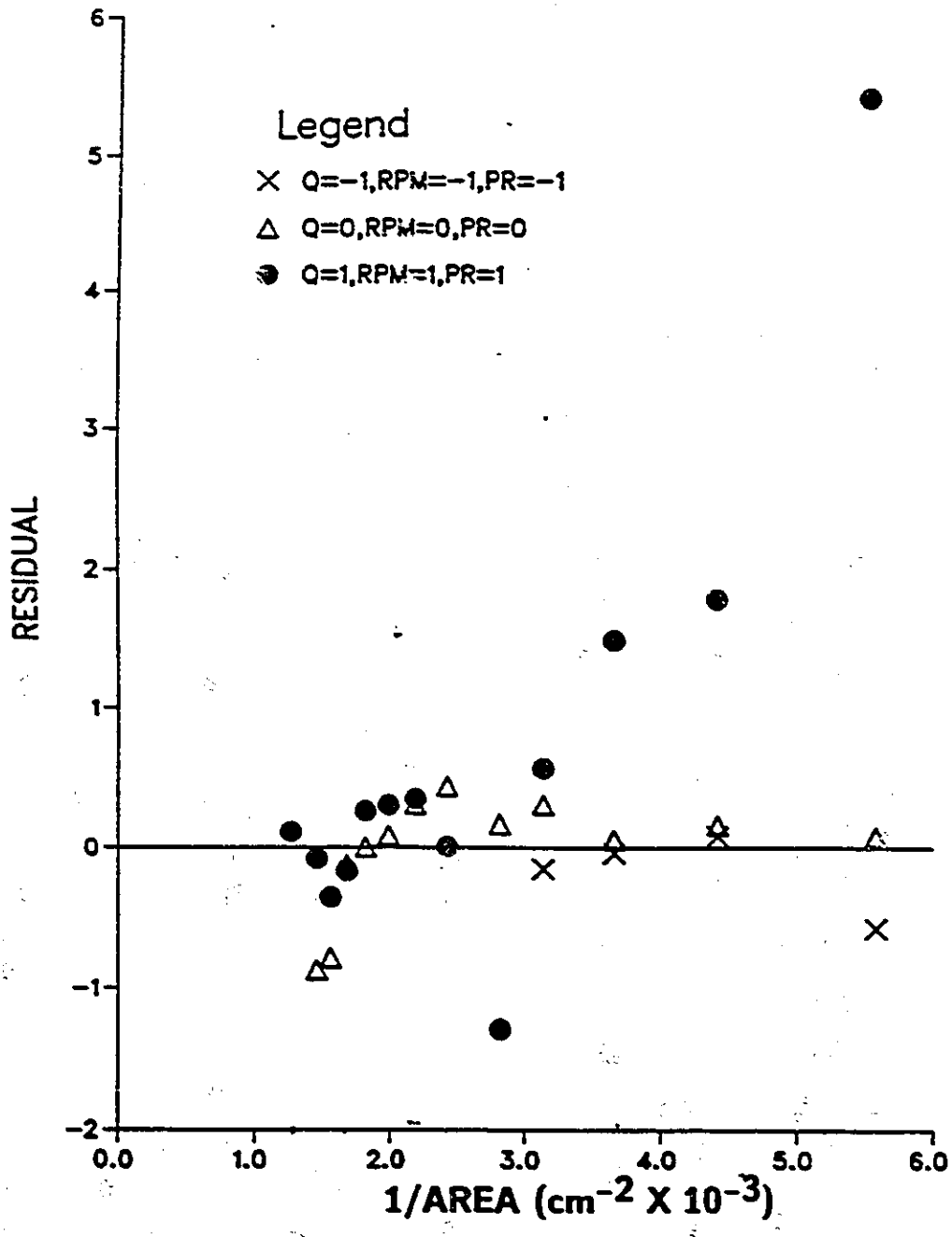

Figure No. 37: Residual plot for the closed mixer model

The model is shown to underpredict the actual dispersion band height. This lack of fit may derive from the experimental and modelling techniques employed. These have been discussed in Section 4.1.

A model was developed for the closed cylindrical mixer which does allow for comparison to other models. The model developed for the prediction of dispersion band heights in a mixer with no air entrainment indicated a dependence of all process variables investigated. This agrees with the mechanism for dispersion coalescence proposed by Barnea and Mizrahi [5].

Atkinson [1] also attempted to develop a closed cylindrical mixer model. Unfortunately, he developed three different models for each level of throughput. The present model then represents a significant advantage over Atkinsons' model.

The significant effect of air entrainment (or lack of air entrainment) was provided during testing for the appropriate agitation intensity levels. Recall that, agitation intensity was raised to prevent phase inversion in the 'air free' mixer. This can be explained in the following manner. Lack of air in the mixer increases the bulk solution viscosity and density, making thorough mixing more difficult for the same power input. The impeller tip speed (or power number) would decrease, thus lowering the energy transferred to the solution. A minimum amount of energy is required to maintain organic phase continuous operation in a mixer. If the minimum is not attained the phases will invert to aqueous phase continuous operation. Simply put, aqueous phase continuous operation requires less energy than organic phase continuous operation. The effect of air entrainment then, was to decrease the power requirement to the mixer.

Another difference between the cylindrical and closed mixer models were the number of parameters in each model. There were nine parameters in the closed mixer model as opposed to five for the cylindrical mixer model. As explained before this was not desired, since models with large numbers of parameters lose their credibility. Recall that, the effect of dispersed phase ratio was absent for the cylindrical mixer model. This was not the case for the closed mixer model.

Comparison of the closed mixer and square mixer models show that interactive and quadratic effects of process variables appear in different parameters (i.e. β_0 or

β_1). However, the effects of both mixer configuration and air entrainment do not allow for proper comparison of the two models.

4.4 Spiked Key Lake Raffinate Results

To test the proposed model developed using simulated phases, a Key Lake Raffinate solution was 'spiked' with Uranium to produce a leach liquor. The raffinate was reconcentrated with yellow cake. The composition of the leach liquor is given in Table 9. The open cylindrical mixer configuration was selected because its' model

Table 9: Spiked Key Lake Raffinate Composition

element	Concentration (g/l)
U	2.500
Ni	2.000
Co	0.047
Fe	1.930
Al	1.110
Mg	0.690
Si	0.380
Ca	0.620
Na	0.032
Zn	0.057

contained the fewest parameters, as well, the conspicuous absence of a dispersed phase ratio term allowed for testing the leach liquor at a fixed dispersed phase ratio of 0.5. The experimental design required only nine (3^2, two variables at three levels) plus three additional zero point runs, saving a considerable amount of time.

Operation of the individual runs revealed that the system was subject to phase inversion at certain combinations of flowrate (Q) and agitation intensity (RPM). The operating region is presented in Figure 38, where the open circle represents organic phase continuous operation and the filled circle indicates phase inversion or aqueous phase continuous operation.

Observation of continuous mixer-settler operation for the Key Lake system also reveals differences between aqueous and organic continuous operation. This is presented in Figures 39 through 42. Figure 39 shows a small dispersion band at mid-height in the settler. This represents organic continuous operation. With the phases inverted the dispersion band grew (Figures 40 and 41), and a stable emulsion was

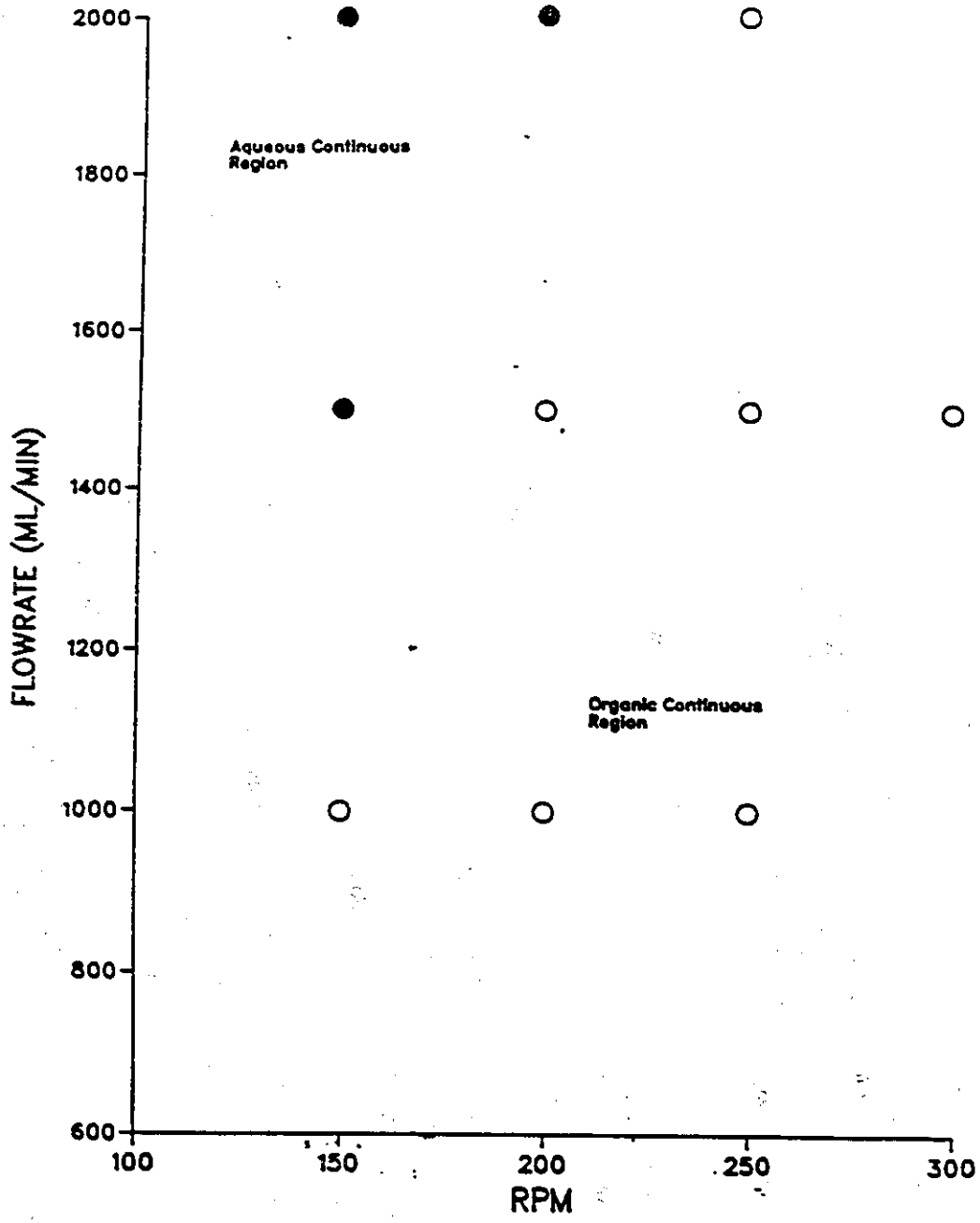

Figure No. 38: Operating region for the spiked Key Lake raffinate

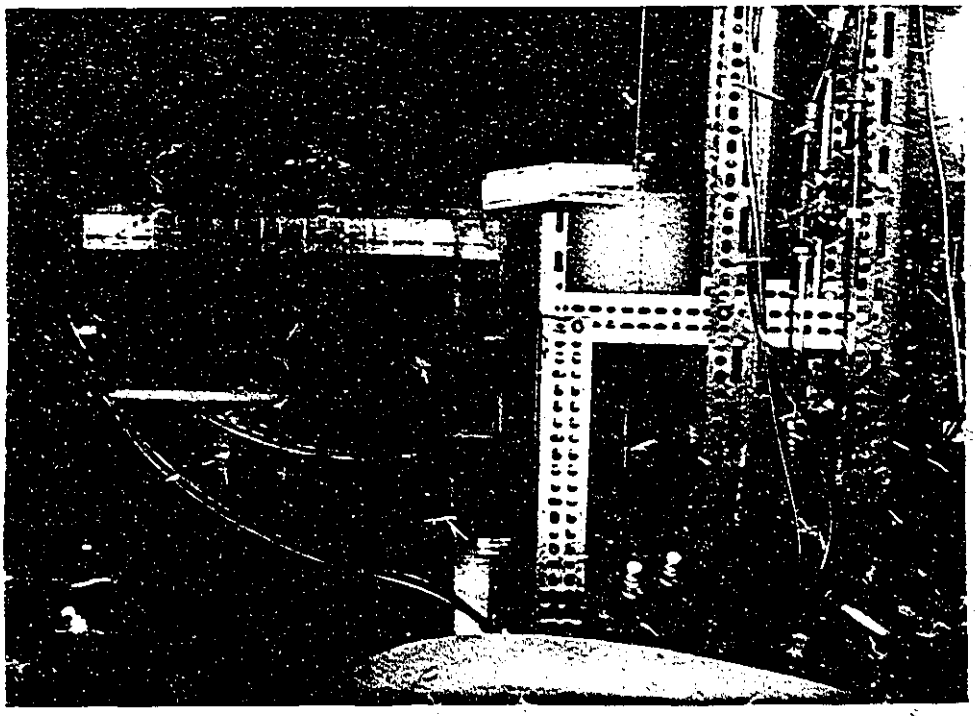

Figure No. 39: Organic continuous operation.

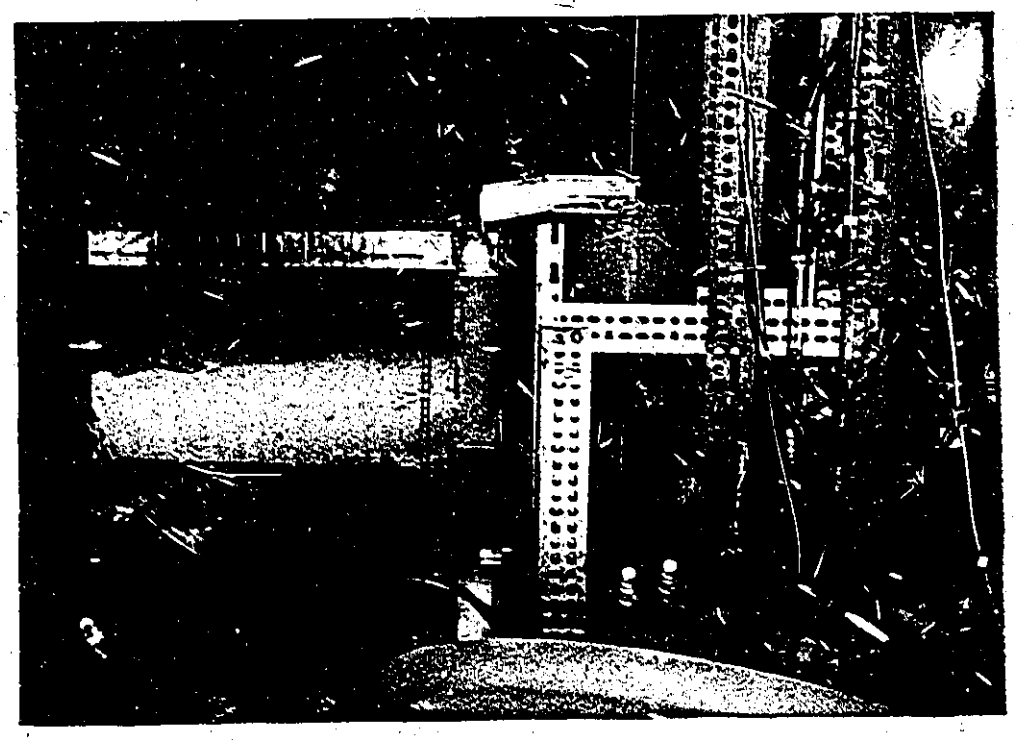

Figure No. 40: Aqueous continuous operation

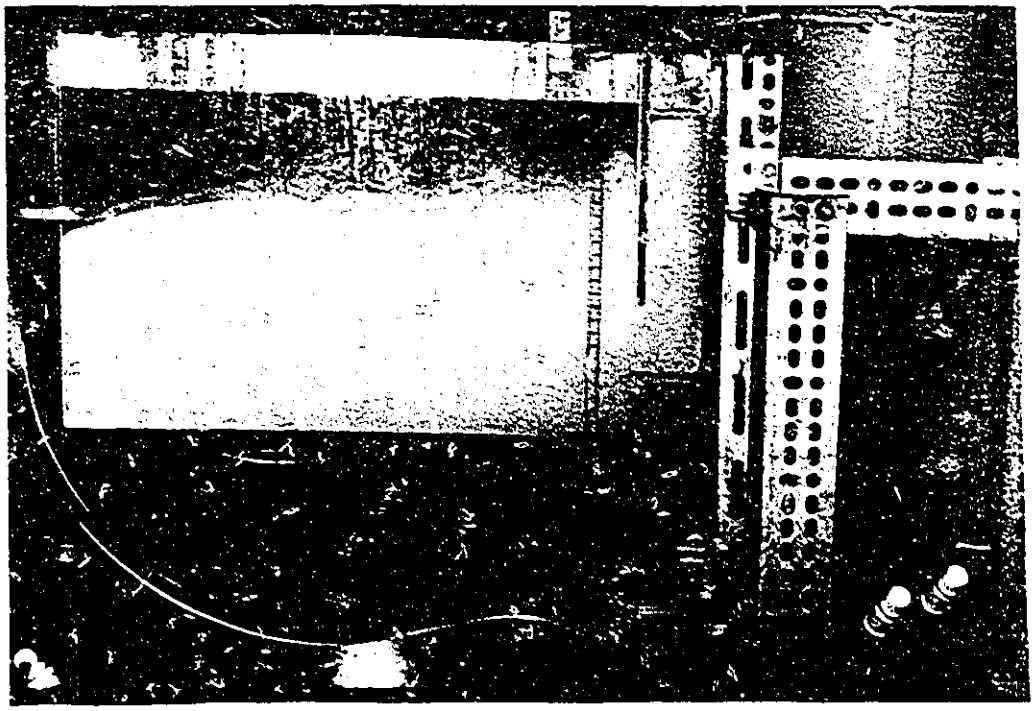

Figure No. 41: Aqueous continuous operation

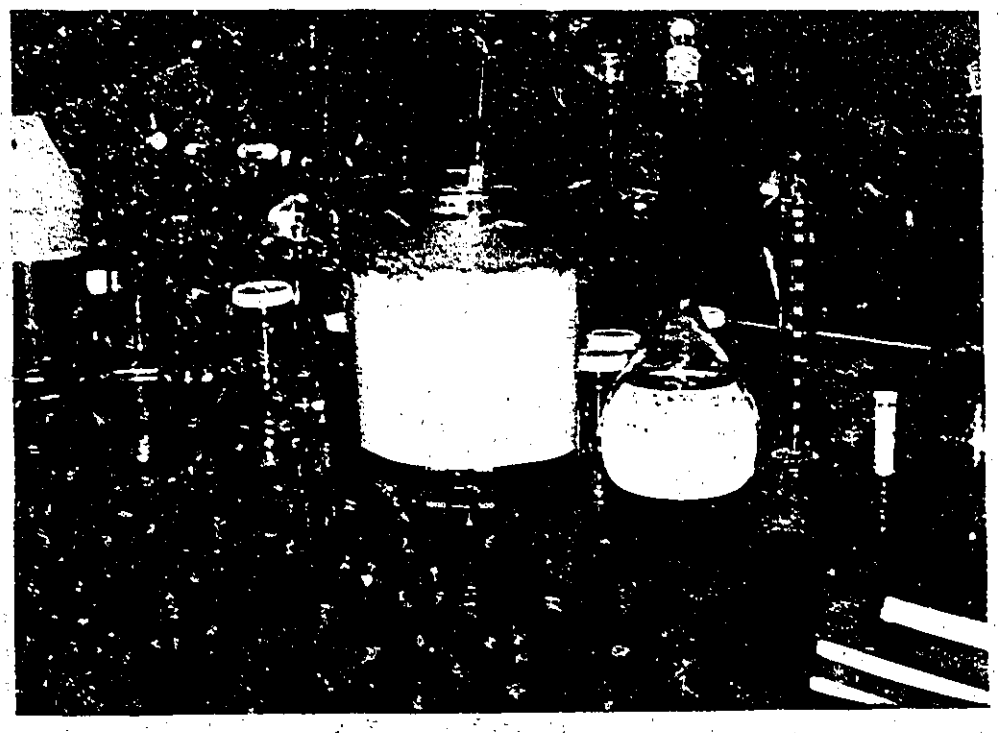

Figure No. 42: Six day-old emulsion

formed. Six days later the emulsion still had not separated. This is shown in Figure 42.

The observed and predicted dispersion band heights, for organic phase continuous operation, are presented in Figures 43 through 49. The data is presented in the form: dispersion band height (H) versus the inverse of settler area (1/A). The predicted dispersion band heights were calculated from the model developed with an open cylindrical mixer. Bear in mind that synthetic phases were used to develop the model.

For most of the plots it can be seen that predicted band heights were generally higher than observed values. The residual plot, Figure 50, confirms this.

Inspection of centre point runs (see Appendix A Table 4) along with Figure 50 revealled a time trend for the observed data, which confirmed earlier findings of solvent degradation.

The various experimental and modelling techniques contribute to the models lack of fit. The use of R^2 values, Stepwise regression coupled with solvent degradation and correlated areas all contribute to model inadequacy.

Introducing an actual leach liquor, with its many chemical impurities only enhances the models' weaknesses. Another source of lack of fit, may be the use of the cylindrical mixer model itself. The possibility of using a square mixer model was not investigated. The use of the closed mixer model was not practical from an industrial point of view, since larger power requirements increase operating costs.

Although the lack of fit is evident in Figures 43 to 49, a model was developed for the uranyl-sulphate-Adogen 364 system. However, using this model for design would over-estimate settler area.

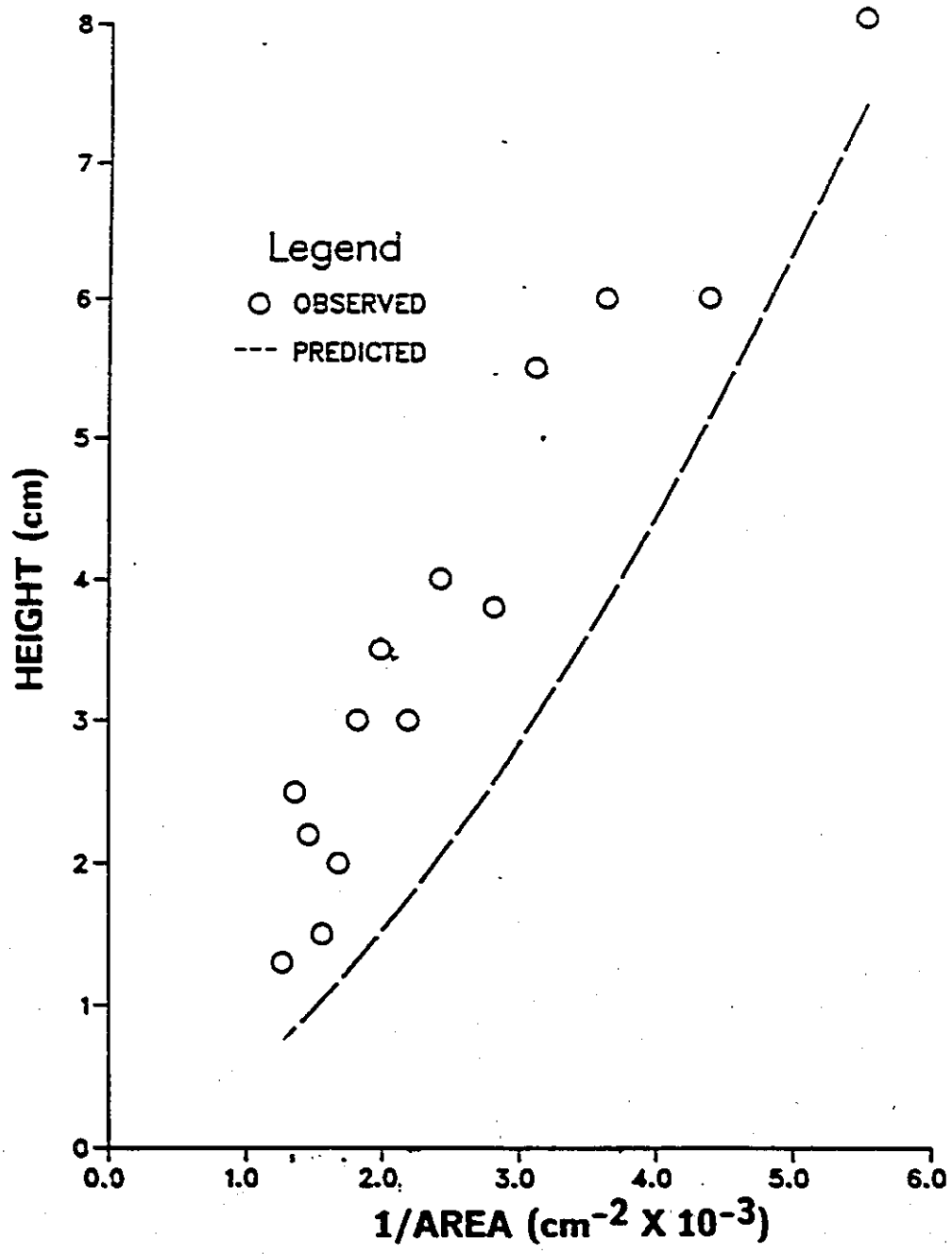

Figure No. 43: Observed and Predicted dispersion band heights versus 1/area for the spiked Key Lake raffinate. At Q = 1500 mL/min, RPM = 200 and PR = 0.5

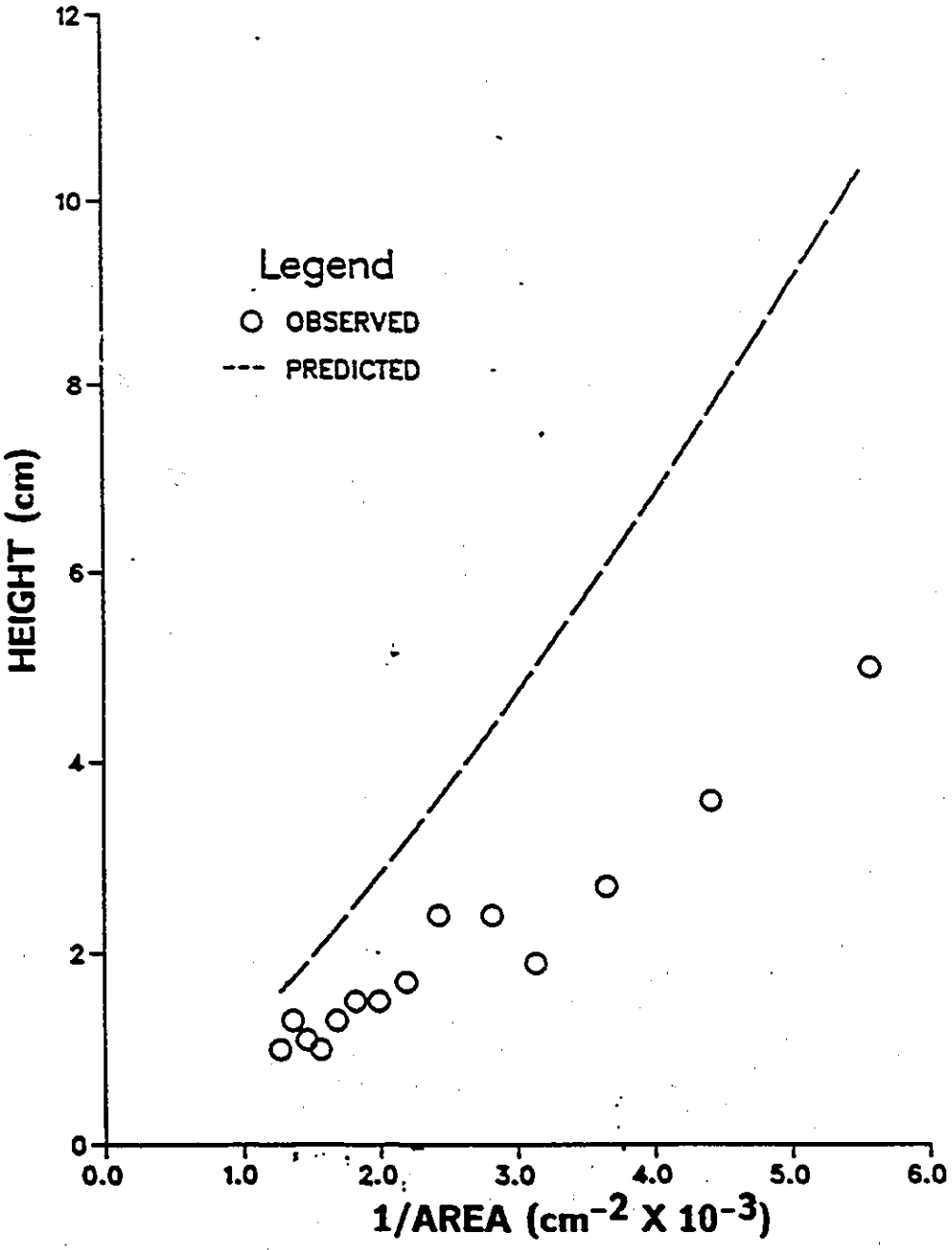

Figure No. 44: Observed and Predicted dispersion band heights versus 1/area for the spiked Key Lake raffinate. At Q = 1500 mL/min, RPM = 250 and PR = 0.5

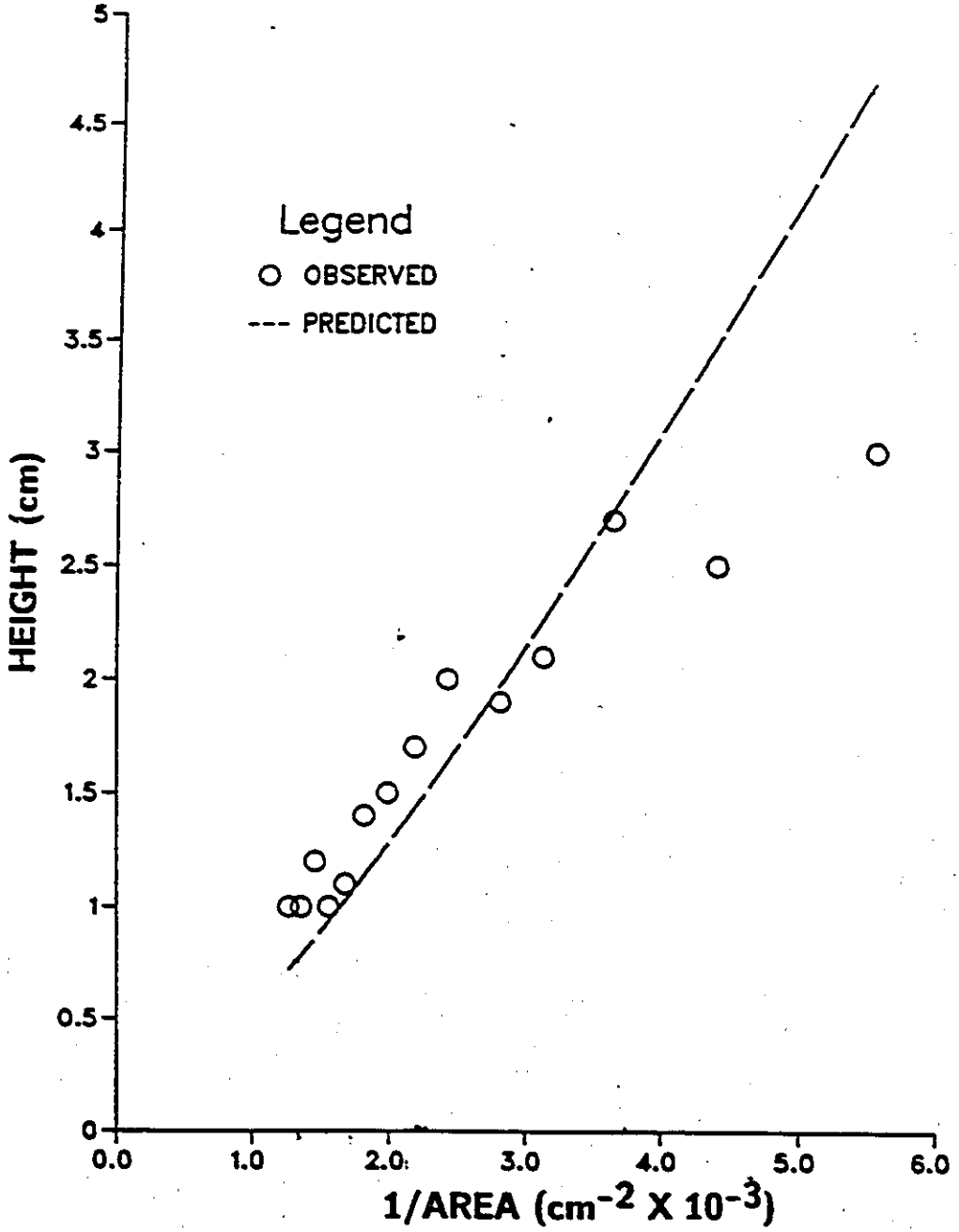

Figure No. 45: Observed and Predicted dispersion band heights versus 1/area for the spiked Key Lake raffinate. At Q = 1000 mL/min, RPM = 250 and PR = 0.5

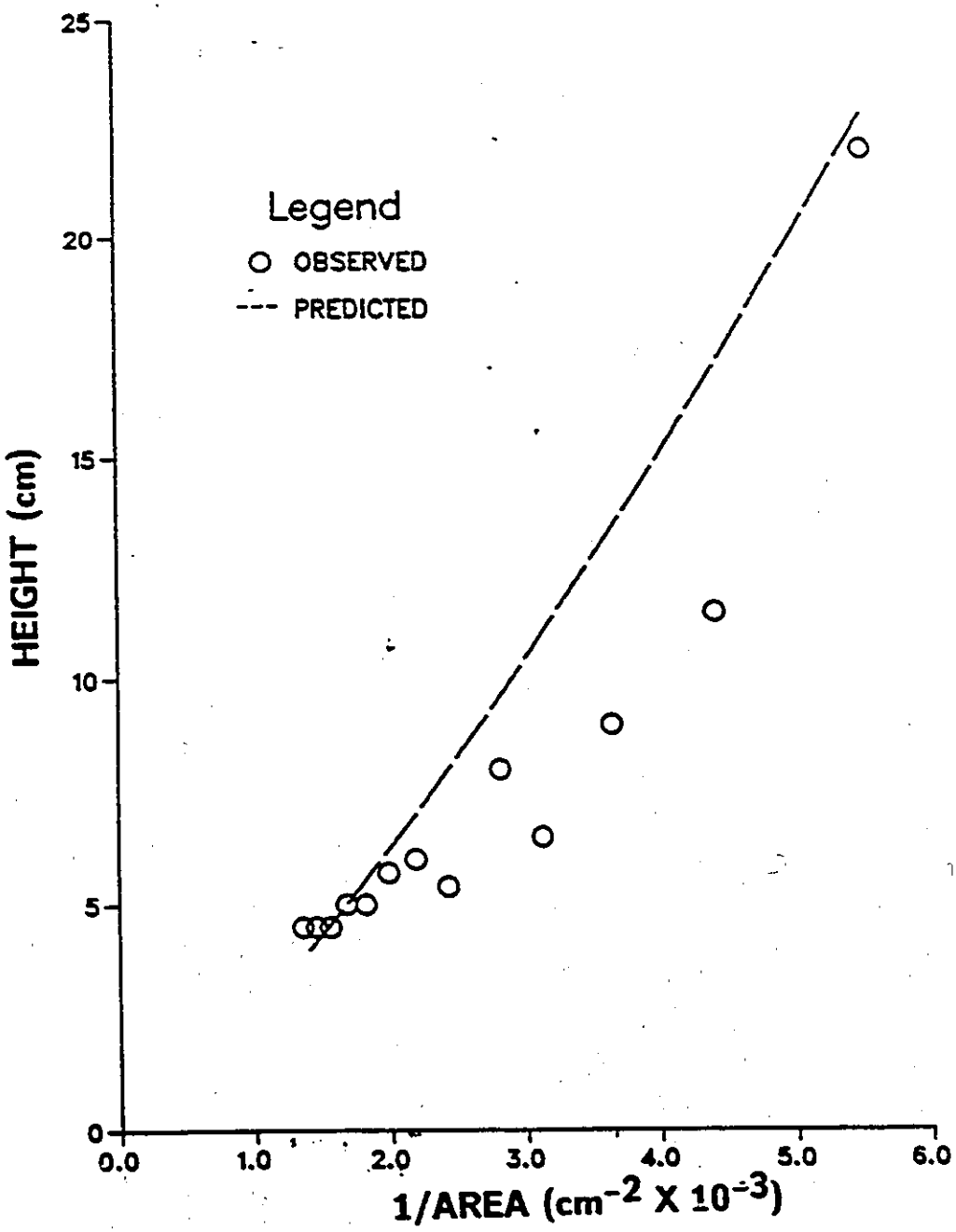

Figure No. 46: Observed and Predicted dispersion band heights versus 1/area for the spiked Key Lake raffinate. At Q = 2000 mL/min, RPM = 250 and PR = 0.5

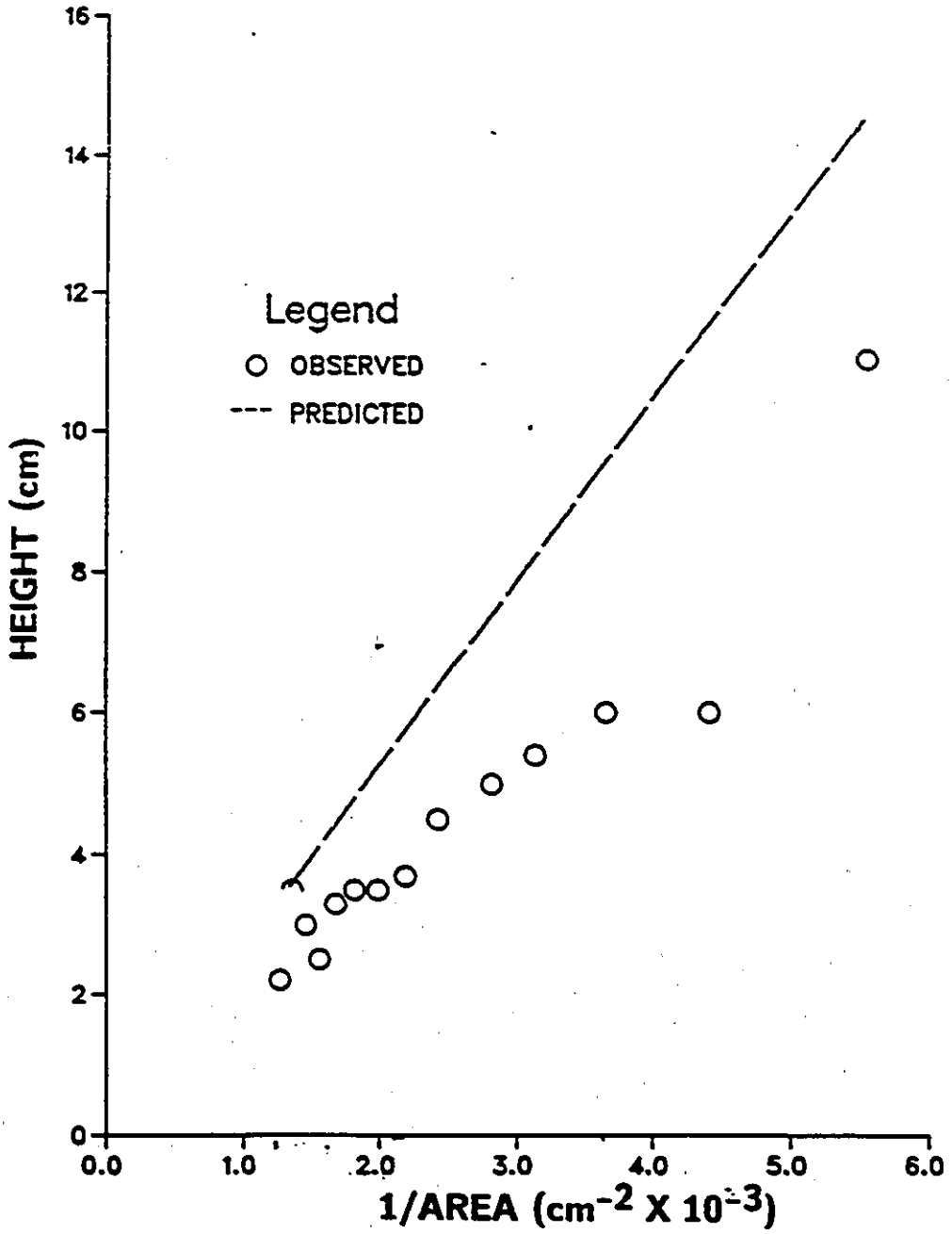

Figure No. 47: Observed and Predicted dispersion band heights versus 1/area for the spiked Key Lake raffinate. at Q = 1500 mL/min, RPM = 300 and PR = 0.5

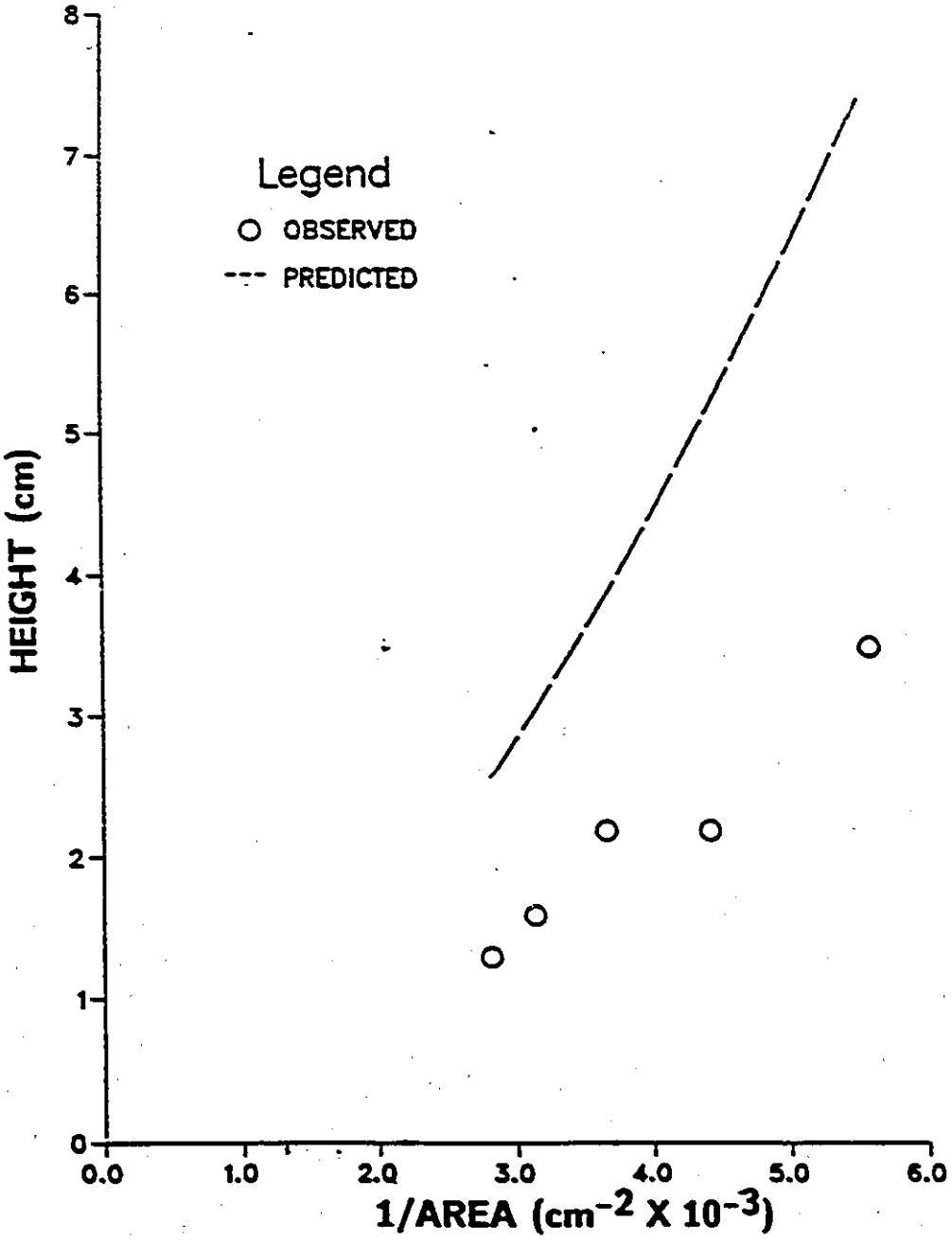

Figure No. 48: Observed and Predicted dispersion band heights versus 1/area for the spiked Key Lake raffinate. At Q = 1500 mL/min, RPM = 200 and PR = 0.5

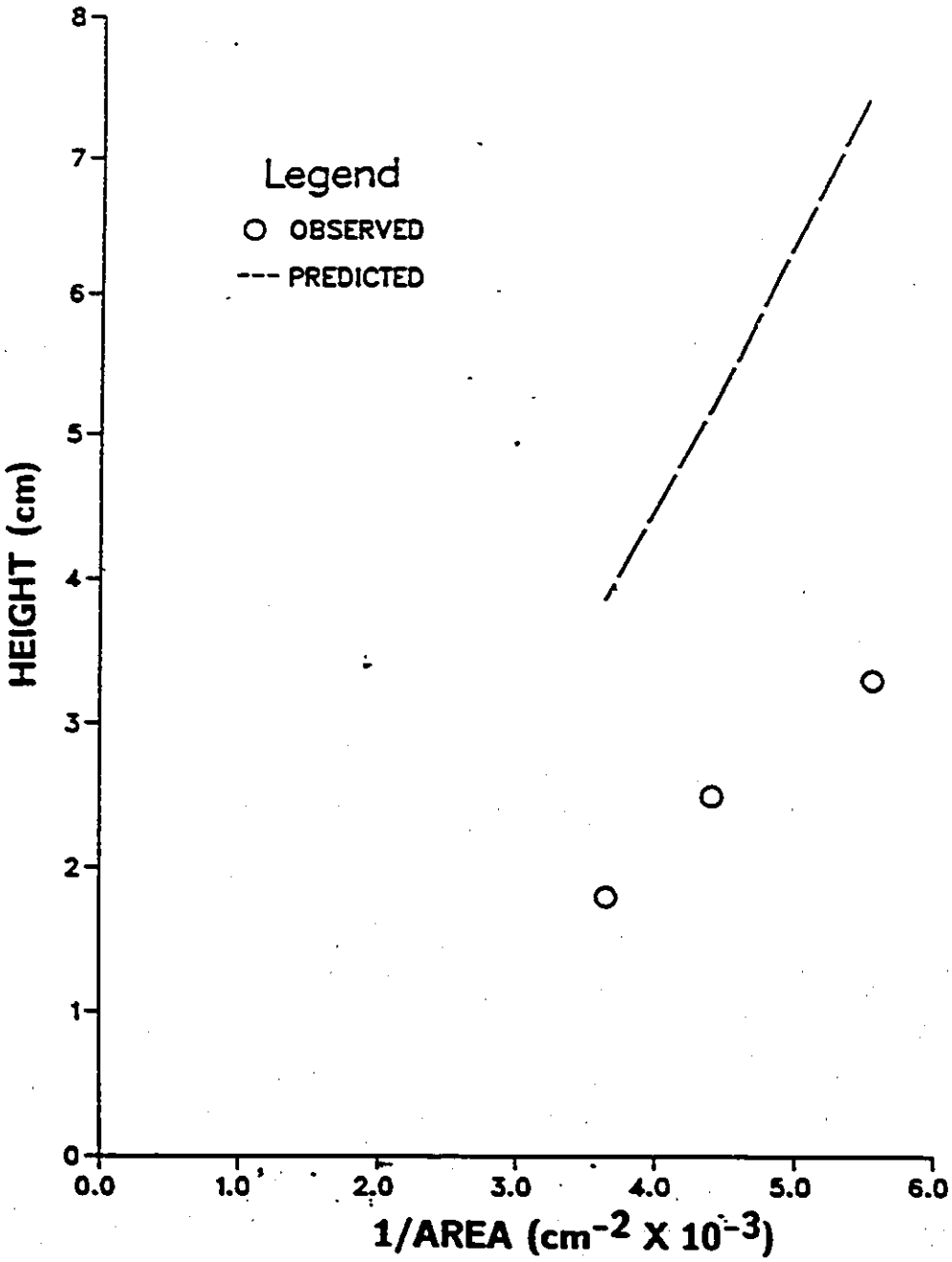

Figure No. 49: Observed and Predicted dispersion band heights versus 1/area for the spiked Key Lake raffinate. .
At Q = 1500 mL/min, RPM = 200 and PR = 0.5

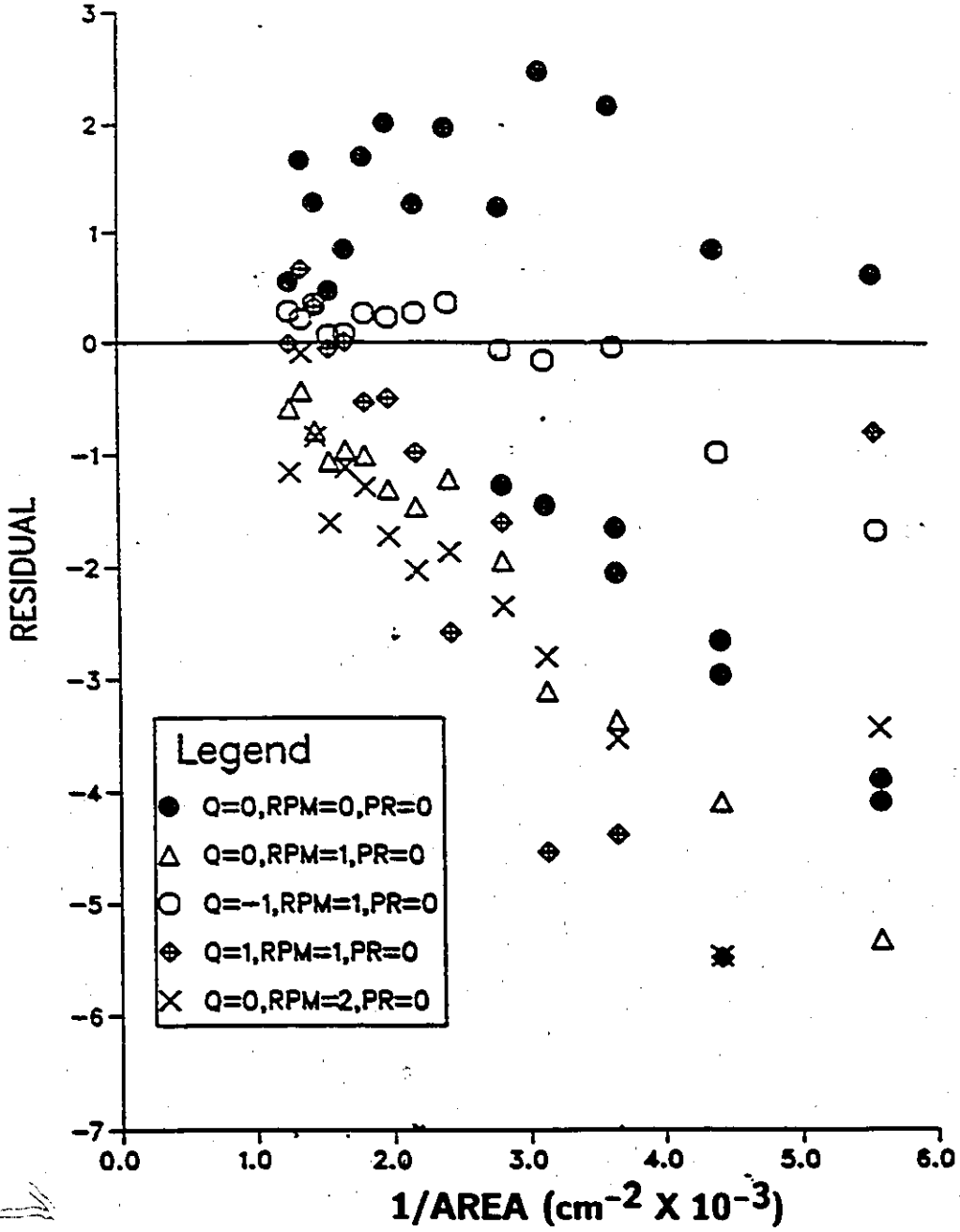

Figure No. 50: Residual plot for Key Lake data.

Chapter 5

Conclusions and Recommendations

Mathematical models for the prediction of dispersion band heights were developed for the; 1) square mixer, 2) cylindrical mixer, and the 3) closed cylindrical mixer configurations. The effect of process variables, throughput, agitation intensity and dispersed phase ratio were evident, with one notable exception, the cylindrical mixer model did not contain a dispersed phase ratio term. In general, the models support the proposed mechanism for the coalescence of a dispersion.

These models were not without weaknesses as a result of experimental procedure or modelling technique. Time trends were noted for the experimental data which indicates solvent degradation. In future studies, this may be overcome with the periodic addition of fresh organic. As well, the data collection procedure does not eliminate area correlation. Since the process variables, throughput, agitation intensity, and dispersed phase ratio were held constant while the areas were randomly varied, correlation of the areas occurs. This can be corrected by randomly selecting all of the variables including area for each dispersion band height recorded. However, this would be very time consuming.

The use of R^2 values to determine the best transformation was suspect. The use of other qualitative/quantitative methods may improve selection of the best transformation. With this in mind, it would be recommended that the alternative

transformation be implemented for comparison purposes. This is especially important for the closed cylindrical mixer model because no difference between the two transformations was detected using R^2 values. The use of Stepwise regression to determine the best model does not necessarily produce the fitted model with the fewest terms nor even the combination of a specified number of terms that provides the best fit to the data. Alternative model selection methods should be investigated.

Atkinson[1] was not able to develop a complete model for the closed cylindrical mixer configuration. The present study did accomplish this, suggesting better modelling techniques were utilized or differences in aqueous/organic continuous phase operation. The square mixer model developed by Atkinson was not compared to data collected from an actual leach liquor system.

Comparison of the models developed suggested an effect of mixer configuration. The adequacy of each model would be better studied by comparing the square mixer and closed cylindrical mixer models to the Key Lake dispersion band height data. The use of alternative leach liquors to test the selected model is also recommended.

Organic phase continuous operation of the mixer indicated the necessity of air entrainment to minimize power requirements. Eliminating air entrainment required additional power input to the mixer for the prevention of phase inversion. Phase inversion (aqueous continuous operation) was shown to induce flooding conditions in the settler and therefore should be avoided for this system.

Finally, comparison of the Key Lake liquor indicated that the cylindrical mixer model would overpredict dispersion band heights, thereby giving conservative settler design using this equation.

References

[1] Atkinson, J., M.A.Sc. Thesis, University of Ottawa, 1985.

[2] Ritcey, G.M. and A.W. Ashbrook, *Solvent Extraction Principles and Applications to process Metallurgy*, Part I, Elsevier, 1979.

[3] Hopkins, J. S., Golding, J. A. and G. M. Ritcey, Hydrometallurgy, 17, pp.315-334, (1987).

[4] Ryon, A. D., Daley, F. L. and R. S. Lowrie, Chem. Eng. Prog., 55, 70, (1959).

[5] Barnea, E. and J. Mizrahi, Trans. Instn. Chem. Engrs., 53, 61, Parts I to IV, (1975).

[6] Gondo, S. and K. Kusunoki, Hydrocarbon Processing, 48, 209, (1969).

[7] Smith, D. V. and G. A. Davies, Can. J. Chem. Eng., 48, 628, (1970).

[8] Allak, A. M. A. and G. V. Jeffreys, AIChE Journal, 20, 564, (1974).

[9] Golob, J. and R. Modic, Trans. Instn. Chem. E., 55, 207, (1977).

[10] Vieler, A. M. S., Glasser, D. and A. W. Bryson, Proceedings of ISEC (1977) p.399, Toronto.

[11] Jeelani, S. A. K. and S. Hartland, Chem. Eng. Res. Des., 64, 134, (1986) Institution of Chem. Engrs.

[12] Slater, M. J., Ritcey, G. M. and R. F. Pilgrim, Proceedings of ISEC, Lyon, Vol. 1, p.107, Pub. Soc. Chem. Industry, London (1974).

[13] Bouyatiotis, B. A. and J. D. Thornton, I. Chem. E. Symposium Series, No. 26, p.43 (1967) Trans. Inst. Chem. Eng.

[14] SAS Institute Inc. SAS User's Guide: Statistics, Version 5 Edition. Cary NC: SAS Institute Inc., 1985. p.486.

[15] Scott, R. R. and E. A. Sylvestre, J. Quality Tech., 11, 55, (1979).

[16] Bacon, D. W., *Collection and Interpretqtion of Industrial Data*, Dept. of Chem. Eng., Queen's University, Kingston, Canada. p.106.

Appendix A

Experimental Data

Table 1: Square Mixer Dispersion Band Heights

Run	Q	RPM	PR	A1	A2	A3	A4	A5	A6	A7	A8	A9	A10	A11	A12	A13	A14	A15
33	2000	250	0.6	—	26.5	15.7	12.4	8.3	6.2	5.9	4.8	3.8	3.6	3.2	3.4	2.9	2.6	2.3
10	2000	250	0.5	—	19.5	10.5	8.0	6.0	5.0	4.5	—	4.0	3.3	3.0	3.0	2.8	2.8	2.5
25	2000	250	0.4	27.0	11.0	7.5	5.5	4.1	3.7	3.4	3.1	2.8	2.1	2.0	1.9	—	—	—
17	2000	200	0.6	—	21.0	10.0	7.0	4.0	4.3	3.5	3.1	2.8	2.2	2.2	2.0	2.1	2.1	2.1
13	2000	200	0.5	36.0	16.5	10.0	7.0	5.0	4.5	3.4	3.8	3.5	2.5	—	—	—	—	—
15	2000	200	0.4	16.5	4.7	3.5	3.4	2.3	1.8	2.0	2.0	—	—	—	—	—	—	—
18	2000	150	0.6	22.5	10.9	6.9	3.7	3.5	3.2	2.3	2.5	2.0	—	—	—	—	—	—
11	2000	150	0.5	18.5	11.5	7.0	3.5	4.0	3.5	2.8	3.0	3.0	—	—	—	—	—	—
19	2000	150	0.4	6.9	4.3	3.5	2.2	2.2	2.0	—	—	—	—	—	—	—	—	—
7	1500	250	0.6	12.0	9.5	6.5	4.3	4.3	3.0	2.5	2.8	2.3	2.1	2.0	2.0	1.8	1.8	1.5
4	1500	250	0.5	19.0	8.0	5.5	4.0	3.5	3.0	2.5	2.5	2.5	2.0	2.0	2.0	1.5	1.5	1.0
21	1500	250	0.4	11.0	4.4	3.9	3.3	2.8	2.6	2.5	2.3	1.6	—	—	—	—	—	—
30	1500	200	0.6	24.7	13.2	9.0	4.3	5.2	3.8	3.3	3.6	2.9	2.3	2.0	—	—	—	—
28	1500	200	0.5	17.5	9.5	6.3	3.8	4.1	3.0	2.4	2.2	1.9	—	—	—	—	—	—
16	1500	200	0.4	5.5	3.8	3.3	2.7	2.2	2.0	1.8	1.5	1.3	—	—	—	—	—	—
1	1500	150	0.6	4.5	3.5	2.5	1.5	2.0	1.5	1.0	1.0	1.0	1.0	1.0	1.0	1.0	1.0	1.0
24	1500	150	0.5	7.7	4.0	3.2	2.1	2.0	1.6	—	—	—	—	—	—	—	—	—
26	1500	150	0.4	4.3	3.1	3.0	2.0	1.8	1.5	1.0	1.0	—	—	—	—	—	—	—
31	1000	250	0.6	19.2	9.7	6.4	4.7	4.4	3.3	3.2	2.7	2.4	2.3	1.8	1.6	—	—	—
8	1000	250	0.5	8.4	4.9	4.0	3.5	3.0	2.4	2.5	2.0	1.9	2.0	1.9	1.8	1.9	1.7	1.5
14	1000	250	0.4	4.0	2.5	2.0	2.0	1.5	1.3	1.5	1.5	—	—	—	—	—	—	—
22	1000	200	0.6	10.4	4.8	2.4	3.2	2.8	2.5	2.0	1.7	—	—	—	—	—	—	—
9	1000	200	0.5	8.5	5.0	4.5	3.1	2.7	2.8	2.2	2.3	2.3	—	—	—	—	—	—
32	1000	200	0.4	8.2	4.0	3.7	3.5	2.6	2.3	1.9	1.6	—	—	—	—	—	—	—
12	1000	150	0.6	4.5	3.3	3.0	1.5	1.8	1.3	0.5	0.8	0.5	—	—	—	—	—	—
29	1000	150	0.5	4.0	2.8	2.2	1.9	1.3	1.3	1.0	—	—	—	—	—	—	—	—
23	1000	150	0.4	3.0	2.0	2.0	2.0	1.2	1.0	—	—	—	—	—	—	—	—	—
27	1500	200	0.5	17.0	8.3	6.1	4.4	3.6	3.1	2.7	2.2	1.8	1.2	1.2	1.0	—	—	—
34	1500	200	0.5	25.0	12.0	8.5	5.8	4.4	3.8	3.4	3.1	2.3	—	—	—	—	—	—
20	1500	200	0.5	15.0	6.9	4.9	3.8	3.0	2.8	2.2	2.0	—	—	—	—	—	—	—

Table 2: Cylindrical Mixer Dispersion Band Heights

Run	Q	RPM	PR	A1	A2	A3	A4	A5	A6	A7	A8	A9	A10	A11	A12	A13	A14	A15
30	2000	250	0.6	—	26.5	16.0	12.4	8.8	7.2	6.3	5.0	5.3	4.7	4.1	3.3	3.4	3.0	—
21	2000	250	0.5	—	11.9	6.1	4.4	4.3	4.0	3.9	3.7	3.1	—	—	—	—	—	—
17	2000	250	0.4	—	13.5	8.3	5.9	4.8	4.5	4.0	3.2	—	—	—	—	—	—	—
12	2000	200	0.6	—	19.5	11.3	8.1	6.8	6.2	5.8	4.6	4.2	2.9	2.6	—	—	—	—
14	2000	200	0.5	—	11.4	7.0	4.7	4.1	3.6	3.8	2.8	2.4	1.5	—	—	—	—	—
1	2000	200	0.4	25.7	12.4	8.1	6.0	4.2	3.2	4.0	3.1	2.2	2.2	1.9	—	—	—	—
25	2000	150	0.6	—	10.8	7.0	5.2	4.0	2.9	2.2	—	—	—	—	—	—	—	—
11	2000	150	0.5	—	10.2	5.0	3.4	4.0	3.3	3.0	—	—	—	—	—	—	—	—
20	2000	150	0.4	—	4.8	3.0	2.4	—	—	—	—	—	—	—	—	—	—	—
6	1500	250	0.6	—	12.2	7.3	5.1	5.0	3.9	3.6	3.3	2.9	2.5	2.7	—	—	—	—
22	1500	250	0.5	—	9.0	6.1	4.5	4.3	3.7	3.5	2.8	—	—	—	—	—	—	—
27	1500	250	0.4	—	8.4	5.3	4.7	3.8	3.4	3.4	2.8	2.2	—	—	—	—	—	—
28	1500	200	0.6	—	13.5	8.7	6.2	5.8	4.2	4.2	3.4	3.1	—	—	—	—	—	—
24	1500	200	0.5	—	11.0	7.9	5.5	4.2	4.0	3.9	3.0	—	—	—	—	—	—	—
29	1500	200	0.4	—	7.2	5.9	4.3	3.8	3.8	3.4	2.7	—	—	—	—	—	—	—
10	1500	150	0.6	—	9.0	3.5	2.9	2.2	2.0	2.4	—	—	—	—	—	—	—	—
5	1500	150	0.5	—	3.5	2.2	1.7	1.5	1.2	—	—	—	—	—	—	—	—	—
16	1500	150	0.4	—	3.3	2.6	—	—	—	—	—	—	—	—	—	—	—	—
18	1000	250	0.6	—	4.8	4.4	3.6	3.5	3.1	2.3	2.3	1.8	—	—	—	—	—	—
13	1000	250	0.5	—	5.1	4.2	4.3	3.3	3.5	2.2	2.5	—	—	—	—	—	—	—
3	1000	250	0.4	5.4	4.0	3.6	2.9	2.5	2.1	2.0	1.7	—	—	—	—	—	—	—
2	1000	200	0.6	12.0	6.5	5.1	3.5	2.7	2.6	2.4	2.5	2.5	—	—	—	—	—	—
8	1000	200	0.5	—	5.5	4.5	3.5	3.3	3.1	2.2	2.1	1.3	—	—	—	—	—	—
26	1000	200	0.4	—	4.3	4.3	3.4	2.3	2.5	—	—	—	—	—	—	—	—	—
9	1000	150	0.6	—	4.1	3.7	2.8	2.0	—	—	—	—	—	—	—	—	—	—
15	1000	150	0.5	—	1.9	1.2	0.5	—	—	—	—	—	—	—	—	—	—	—
19	1000	150	0.4	—	1.9	1.3	1.2	—	—	—	—	—	—	—	—	—	—	—
4	1500	200	0.5	—	7.2	4.6	3.5	3.3	2.1	2.8	2.3	—	—	—	—	—	—	—
7	1500	200	0.5	—	10.3	5.6	4.8	4.3	3.5	3.2	2.8	2.3	1.7	1.6	—	—	—	—
23	1500	200	0.5	—	8.2	5.8	4.0	4.2	3.6	3.0	2.3	—	—	—	—	—	—	—

Table 3: Closed Cylindrical Mixer Dispersion Band Heights

Run	Q	RPM	PR	A1	A2	A3	A4	A5	A6	A7	A8	A9	A10	A11	A12	A13	A14	A15
30	2000	300	0.6	—	34.2	17.0	11.5	8.1	5.0	5.1	4.8	4.3	3.9	3.2	3.2	2.9	2.8	2.8
16	2000	300	0.5	—	25.5	14.5	10.1	8.1	6.5	5.3	4.8	4.2	3.7	4.1	3.2	2.9	—	—
3	2000	300	0.4	—	13.4	6.8	5.0	3.0	4.3	4.2	2.4	3.0	—	—	—	—	—	
10	2000	250	0.6	—	—	21.2	15.0	11.8	6.1	7.2	6.0	5.3	5.0	4.2	3.9	3.6	—	—
4	2000	250	0.5	—	24.7	13.7	9.6	7.6	6.0	5.3	5.1	4.3	3.9	3.6	—	—	—	—
27	2000	250	0.4	—	15.6	9.6	6.9	5.4	3.3	4.4	3.8	3.6	3.2	2.8	2.0	2.0	—	—
13	2000	200	0.6	—	—	20.8	11.0	6.3	5.0	5.5	7.2	4.8	3.7	3.2	—	—	—	—
23	2000	200	0.5	—	28.0	15.0	11.0	9.3	6.5	6.1	5.0	5.2	4.4	4.1	3.2	2.8	—	—
15	2000	200	0.4	—	16.3	10.8	7.9	5.2	4.8	4.4	4.2	3.4	3.6	2.3	—	—	—	—
25	1500	300	0.6	—	19.3	11.2	8.2	6.6	5.2	4.5	3.5	3.9	3.0	—	—	—	—	—
26	1500	300	0.5	—	11.1	8.7	6.0	3.9	3.8	4.0	3.5	3.4	3.2	—	—	—	—	—
7	1500	300	0.4	—	9.2	6.4	4.5	4.4	3.6	3.5	3.3	2.8	2.3	—	—	—	—	—
20	1500	250	0.6	—	19.8	12.8	8.3	6.5	6.2	5.1	4.4	3.4	3.6	—	—	—	—	—
1	1500	250	0.5	—	11.9	6.8	5.3	4.8	4.1	3.8	3.6	3.0	2.1	—	—	—	—	—
6	1500	250	0.4	—	10.3	7.4	4.7	4.4	3.6	3.7	3.6	2.6	2.4	—	—	—	—	—
22	1500	200	0.6	—	19.6	12.5	9.8	6.9	5.5	5.6	4.7	4.5	2.1	3.2	—	—	—	—
28	1500	200	0.5	—	12.2	8.6	7.0	5.4	3.5	3.9	3.4	3.0	2.9	—	—	—	—	—
5	1500	200	0.4	—	9.9	6.8	5.3	4.4	3.4	3.6	2.8	2.4	2.0	1.4	1.1	—	—	—
24	1000	300	0.6	—	6.0	4.3	3.9	3.2	3.0	2.7	2.2	2.2	1.9	—	—	—	—	—
17	1000	300	0.5	—	7.3	5.0	4.3	3.8	3.4	2.7	2.5	2.3	—	—	—	—	—	—
9	1000	300	0.4	—	4.7	4.3	3.7	3.3	2.5	2.9	2.2	1.6	—	—	—	—	—	—
8	1000	250	0.6	—	12.4	6.8	4.8	5.3	4.2	3.4	3.1	2.7	2.4	2.0	—	—	—	—
29	1000	250	0.5	—	5.8	4.8	4.0	3.5	3.0	2.5	2.5	—	—	—	—	—	—	—
14	1000	250	0.4	—	6.0	4.1	3.5	2.8	2.5	2.3	2.1	—	—	—	—	—	—	—
2	1000	200	0.6	—	7.3	5.9	4.7	3.4	3.1	2.9	2.7	—	—	—	—	—	—	—
19	1000	200	0.5	—	6.9	5.0	4.0	3.3	2.6	2.4	2.1	—	—	—	—	—	—	—
11	1000	200	0.4	—	4.3	3.6	2.8	2.3	—	—	—	—	—	—	—	—	—	—
21	1500	250	0.5	—	14.4	9.0	6.5	5.5	4.7	4.3	3.8	3.3	3.0	2.7	1.9	1.7	—	—
12	1500	250	0.5	—	14.3	8.5	6.2	5.0	4.2	4.0	3.9	3.2	2.9	2.6	—	—	—	—
18	1500	250	0.5	—	14.0	8.8	6.2	5.2	4.8	4.4	4.1	4.0	3.1	2.7	2.6	—	—	—

Table 4: Spiked Key Lake Raffinate Dispersion Band Heights

Run	Q	RPM	PR	A1	A2	A3	A4	A5	A6	A7	A8	A9	A10	A11	A12	A13	A14	A15
10	2000	250	0.5	—	22.0	11.5	9.0	6.5	8.0	5.4	6.0	5.7	5.0	5.0	4.5	4.5	4.5	3.5
6[1]	2000	200	0.5	—	—	—	—	—	—	—	—	—	—	—	—	—	—	—
4[1]	2000	150	0.5	—	—	—	—	—	—	—	—	—	—	—	—	—	—	—
7	1500	250	0.5	—	5.0	3.6	2.7	1.9	2.4	2.4	1.7	1.5	1.5	1.3	1.0	1.1	1.3	1.0
5	1500	200	0.5	—	3.5	2.2	2.2	1.6	1.3	—	—	—	—	—	—	—	—	—
13[1]	1500	150	0.5	—	—	—	—	—	—	—	—	—	—	—	—	—	—	—
9	1000	250	0.5	—	3.0	2.5	2.7	2.1	1.9	2.0	1.7	1.5	1.4	1.1	1.0	1.2	1.0	1.0
3[2]	1000	200	0.5	—	1.9	—	—	—	—	—	—	—	—	—	—	—	—	—
2[2]	1000	150	0.5	—	—	—	—	—	—	—	—	—	—	—	—	—	—	—
1	1500	200	0.5	—	3.3	2.5	1.8	—	—	—	—	—	—	—	—	—	—	—
8	1500	200	0.5	—	8.0	6.0	6.0	5.5	3.8	4.0	3.0	3.5	3.0	2.0	1.5	2.2	2.5	1.3
12	1500	300	—	11.0	6.0	6.0	5.4	5.0	4.5	3.7	3.5	3.5	3.3	2.5	3.0	3.5	2.2	

1. Phases inverted.

2. Wedge shaped dispersion band.

Appendix B

Plots of Experimental Data

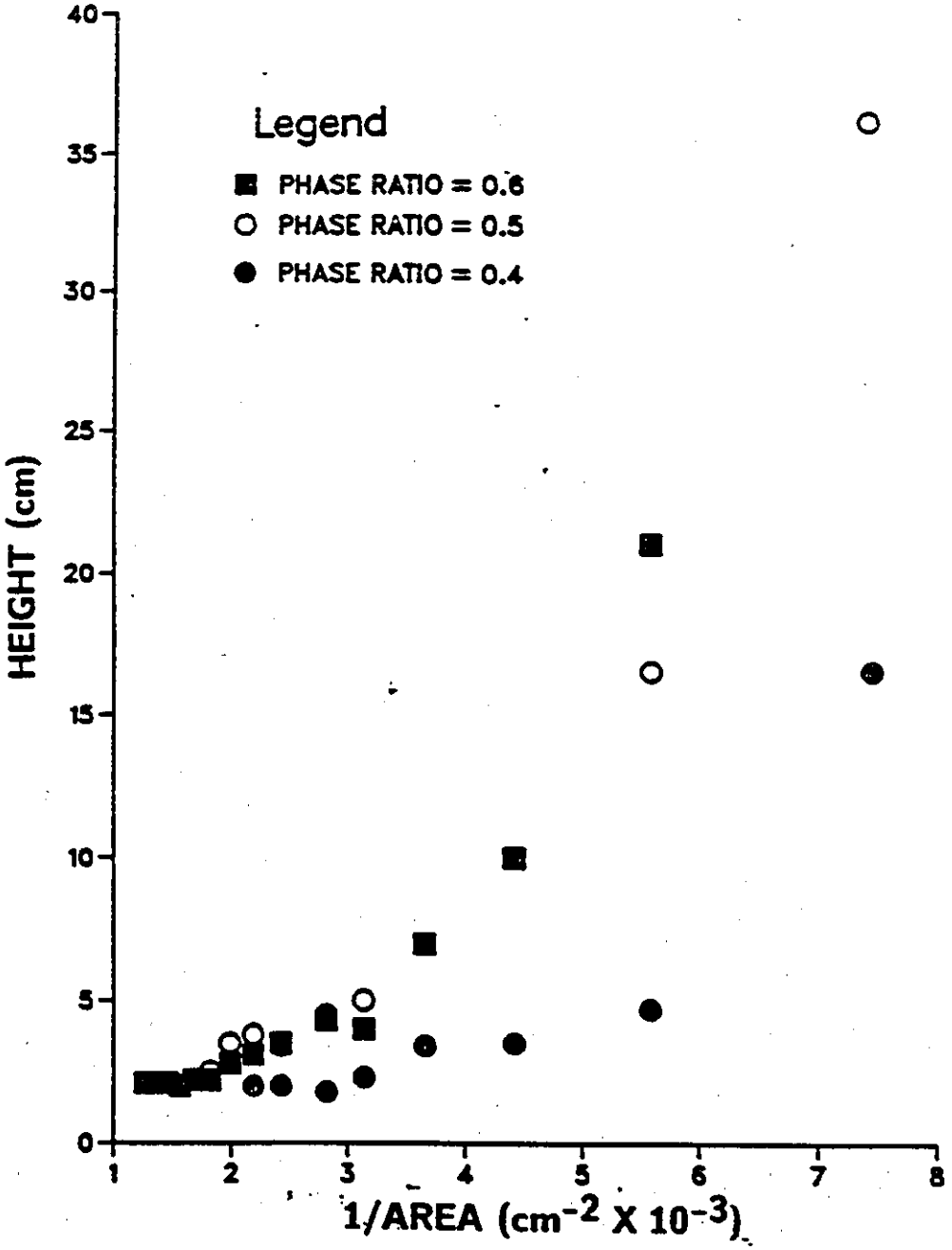

Figure No. 51: Experimental data for the square mixer. Dispersion band height versus 1/area at Q = 2000 mL/min and RPM = 200.

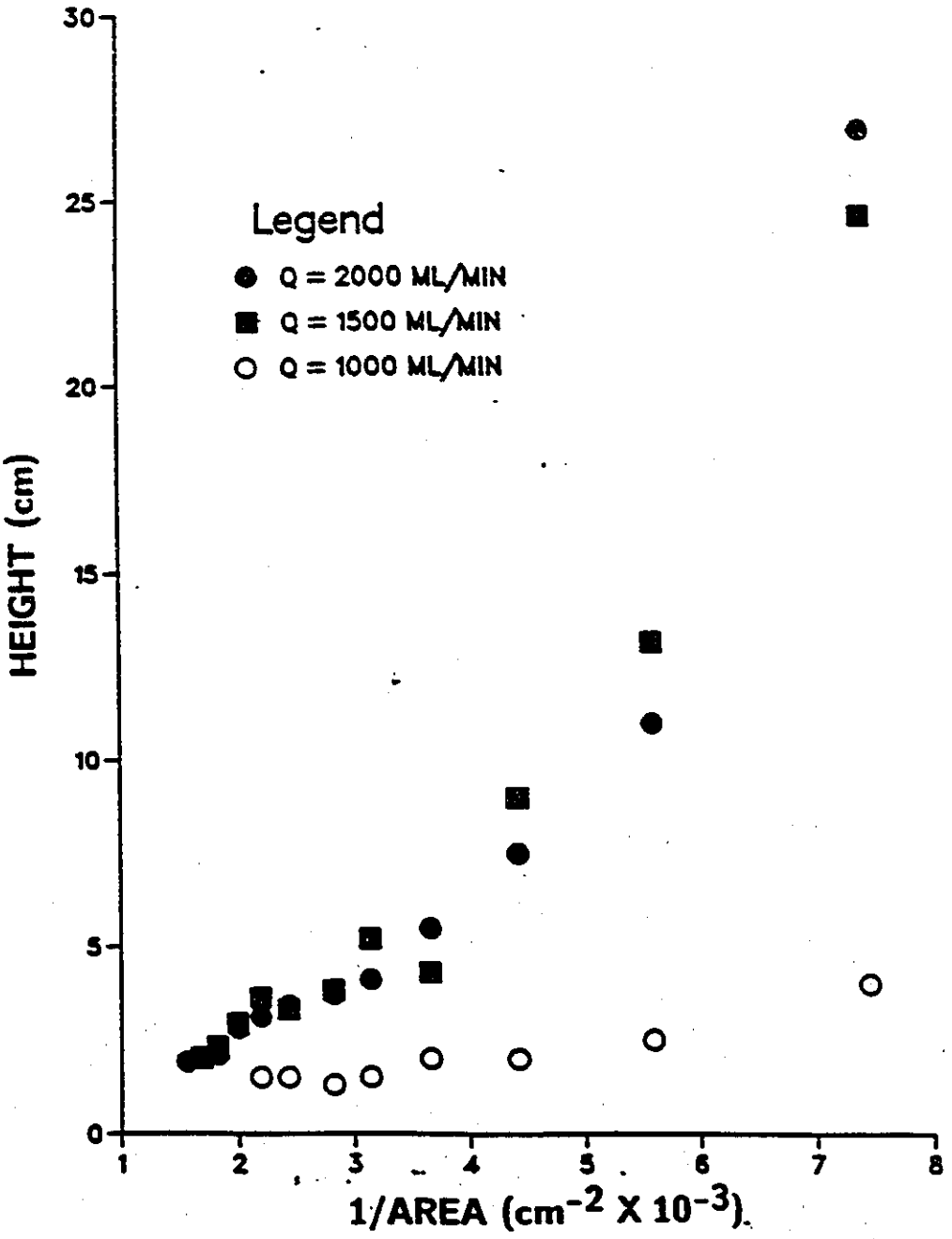

Figure No. 52: Experimental data for the square mixer. Dispersion band height versus 1/area at RPM = 250 and PR = 0.4.

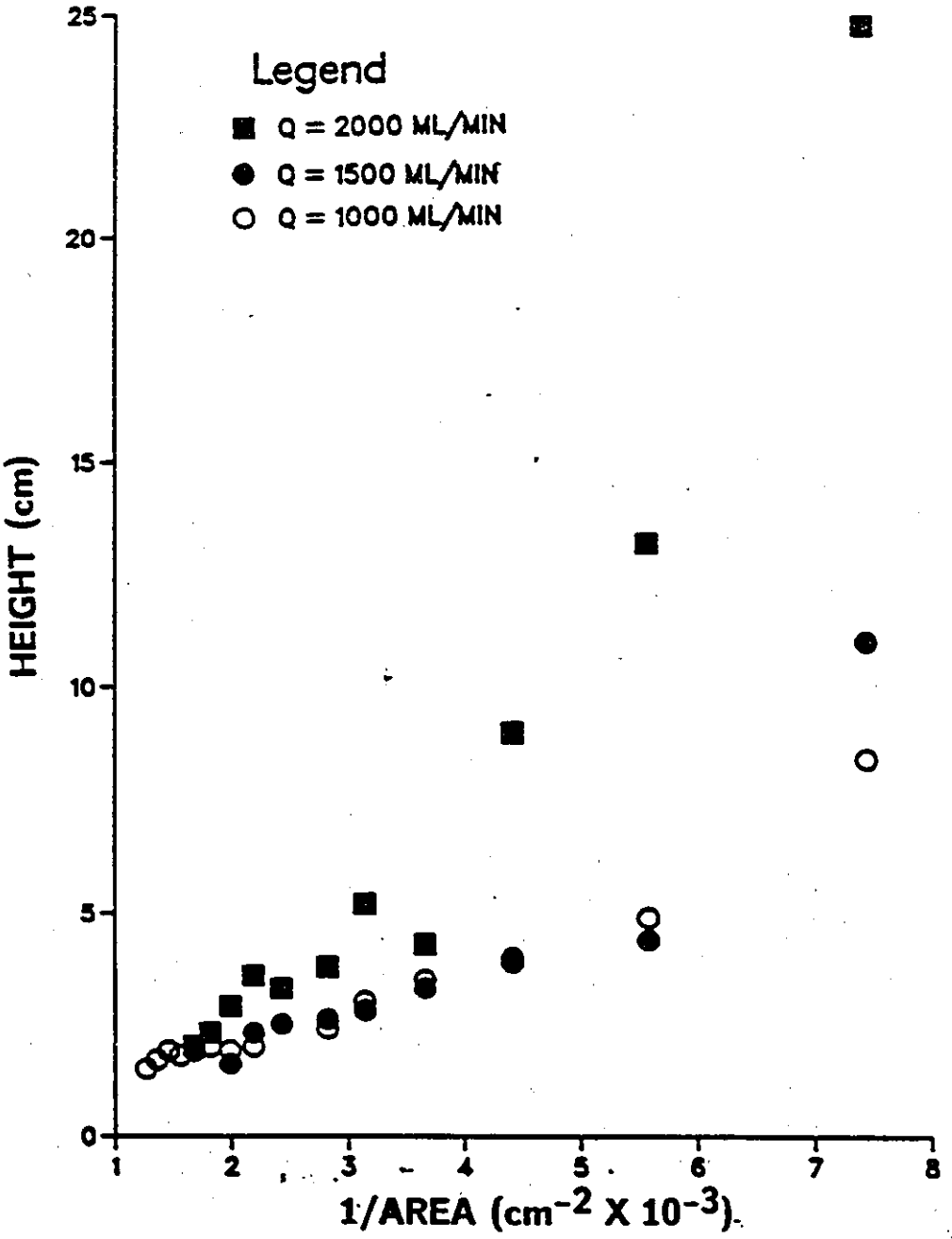

Figure No. 53: Experimental data for the square mixer. Dispersion band height versus 1/area at RPM = 250 and PR = 0.5.

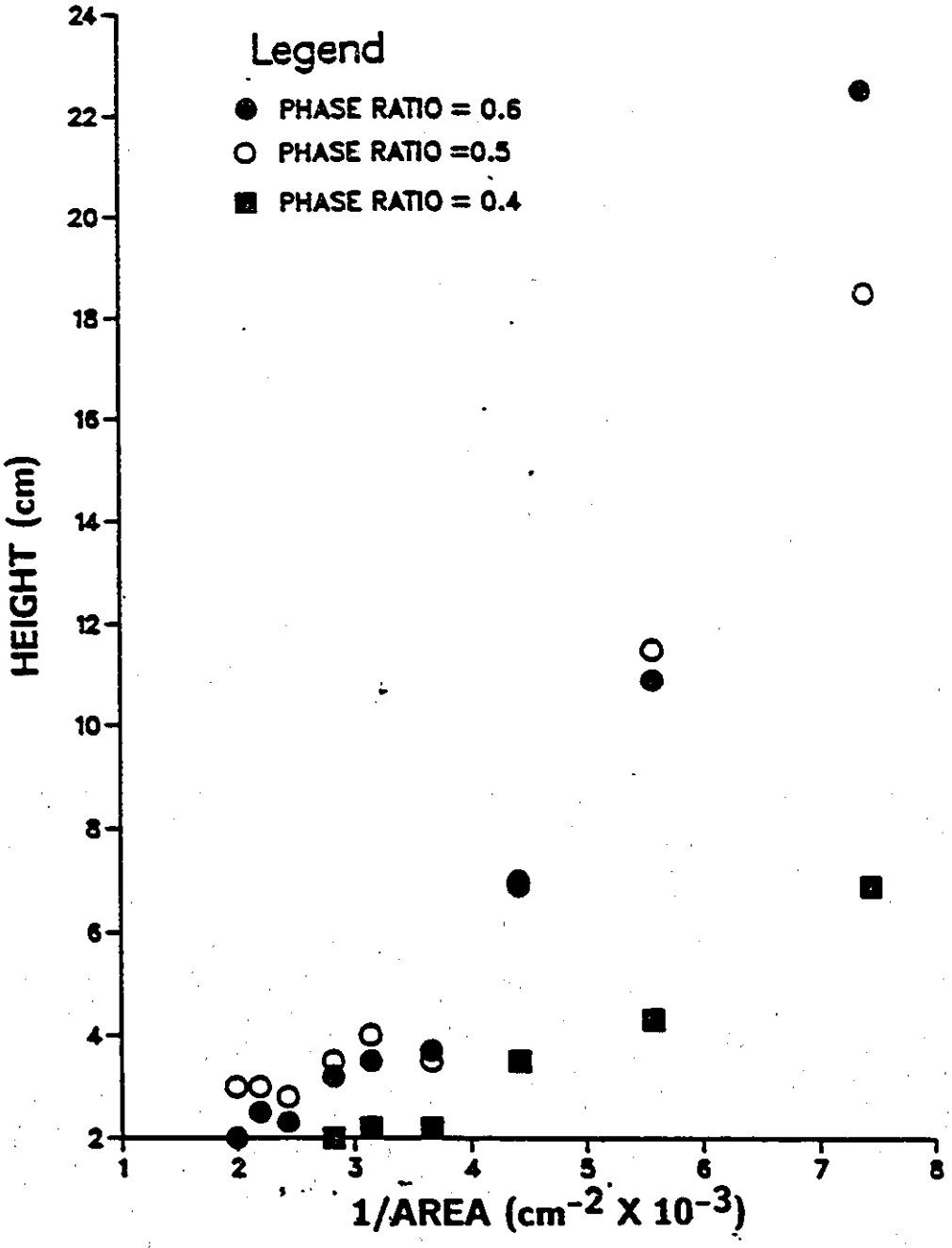

Figure No. 54: Experimental data for the square mixer. Dispersion band height versus 1/area at Q = 2000 mL/min and RPM = 150.

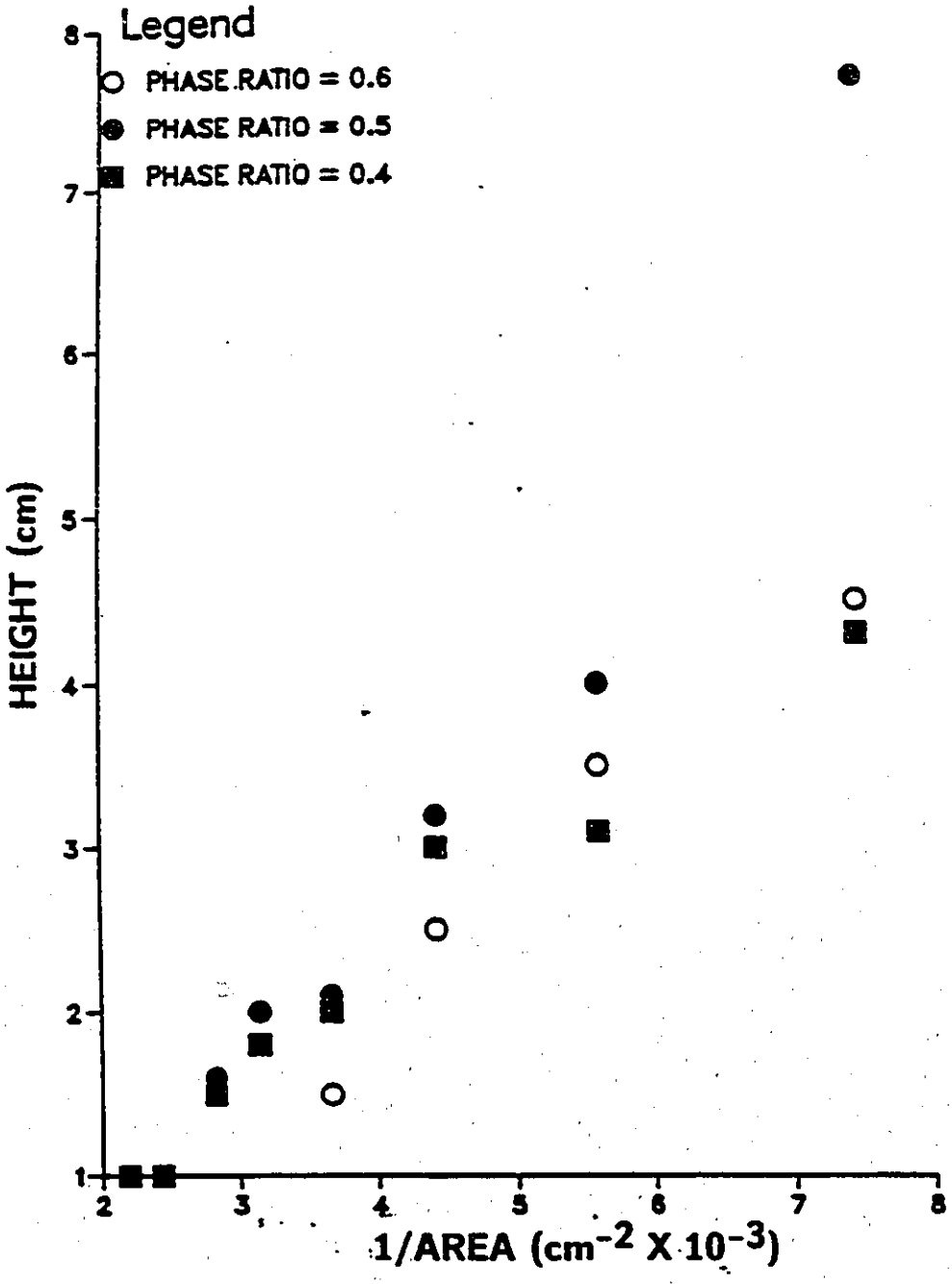

Figure No. 55: Experimental data for the square mixer. Dispersion band height versus 1/area at Q = 1500 mL/min and RPM = 150.

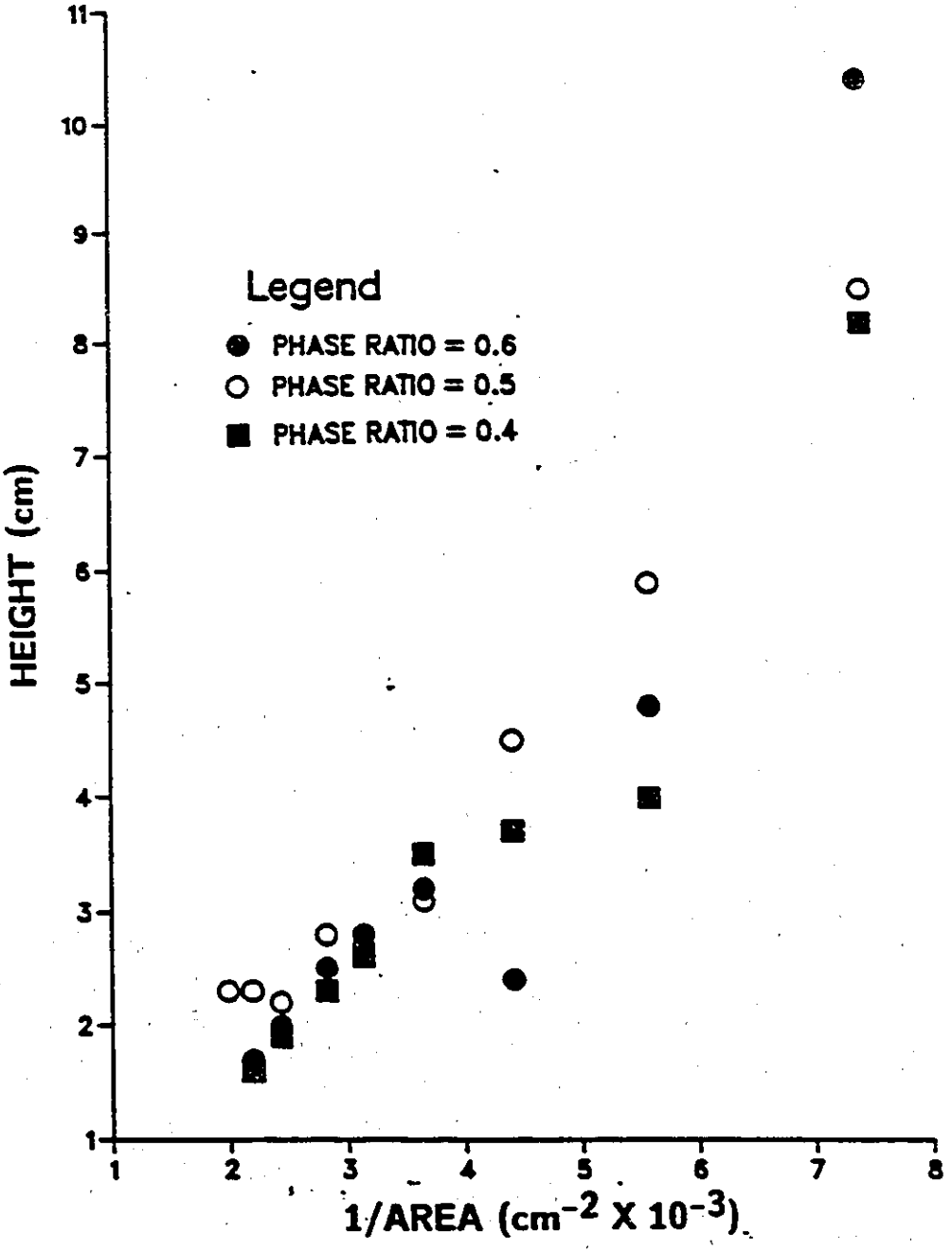

Figure No. 56: Experimental data for the square mixer. Dispersion band height versus 1/area at Q = 1000 mL/min and RPM = 200.

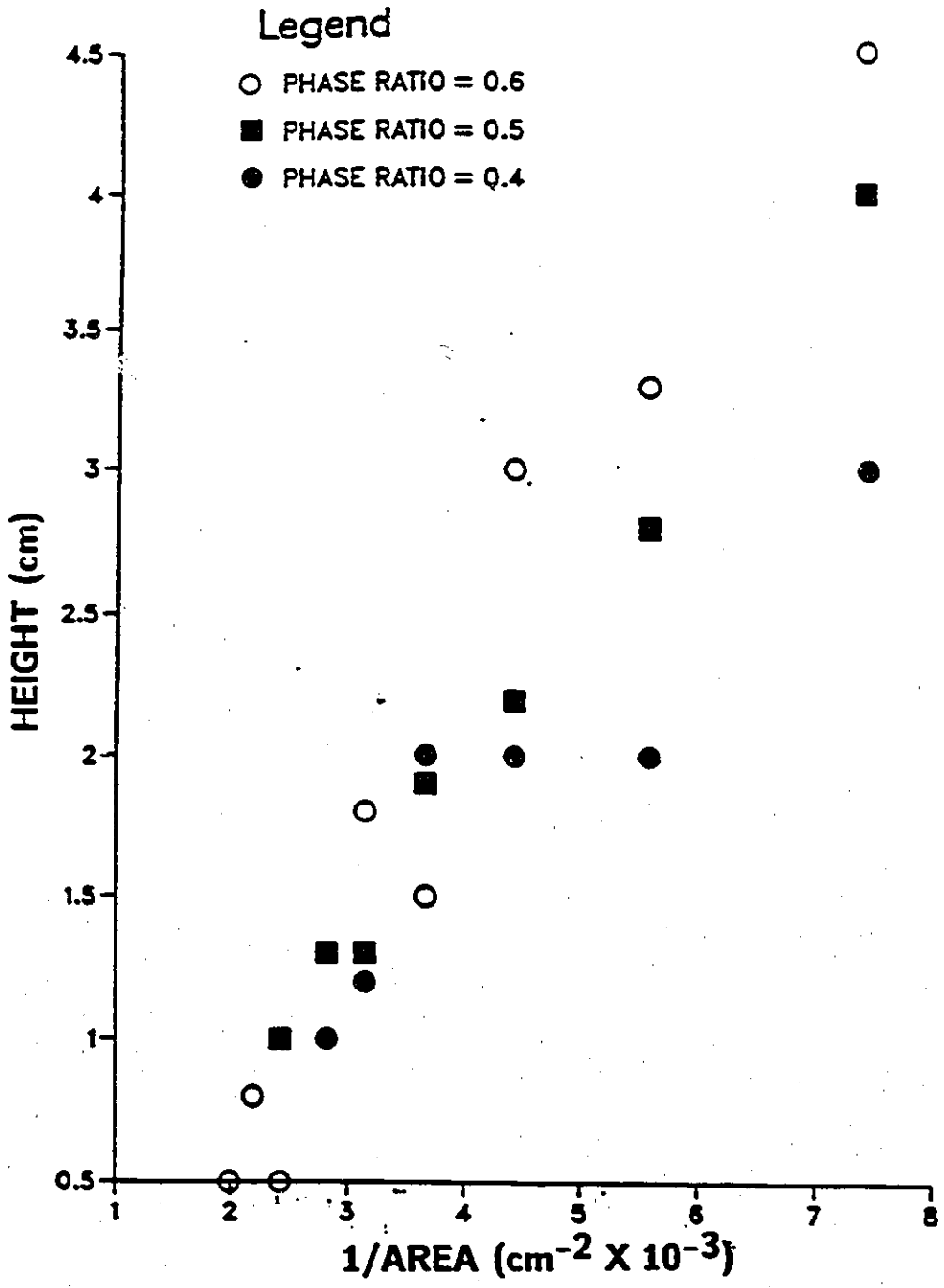

Figure No. 57:Experimental data for the square mixer. Dispersion band height versus 1/area at Q = 1000 mL/min and RPM = 150.

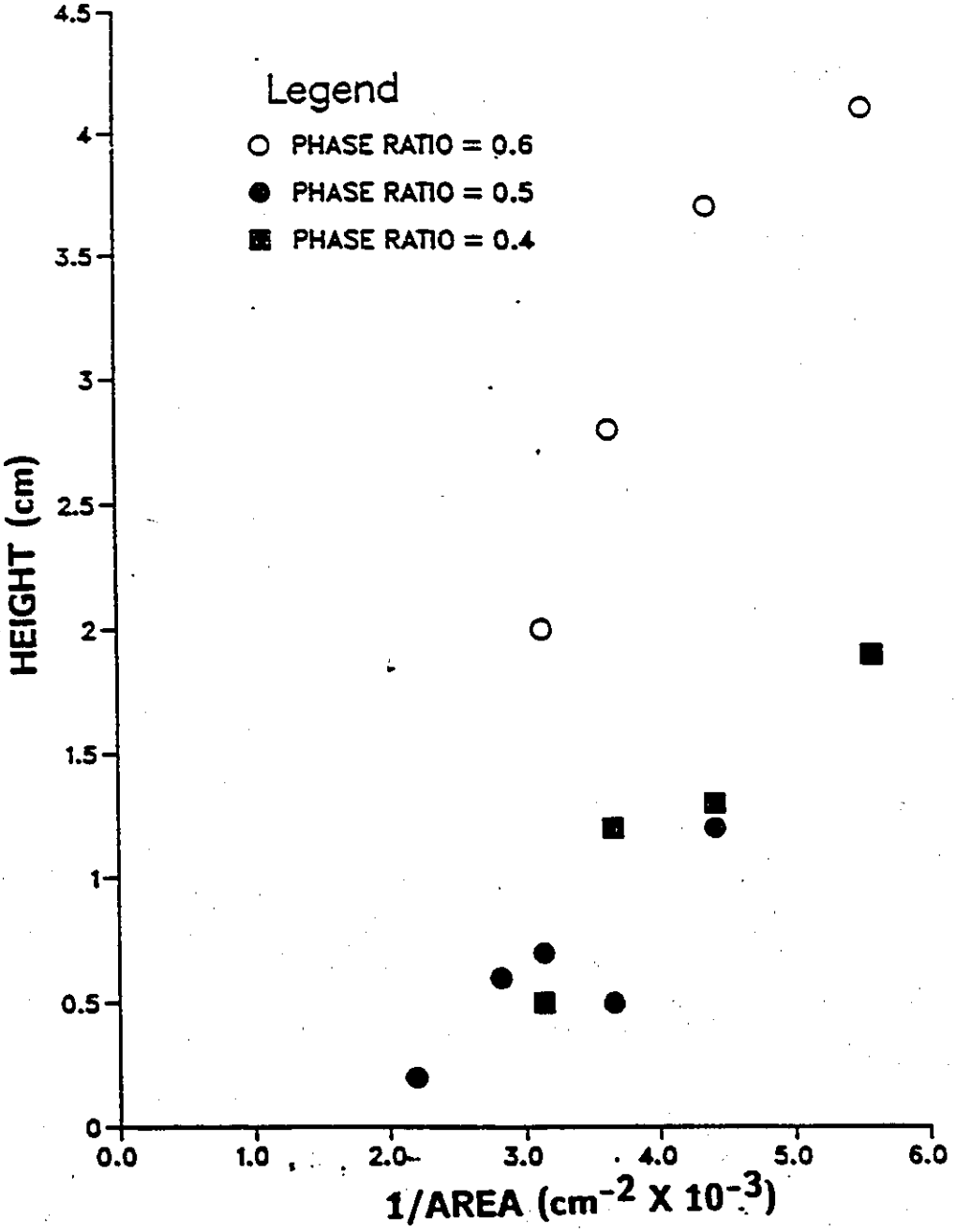

Figure No. 58: Experimental data for the cylindrical mixer. Dispersion band height versus 1/area at Q = 1000 mL/min and RPM = 150.

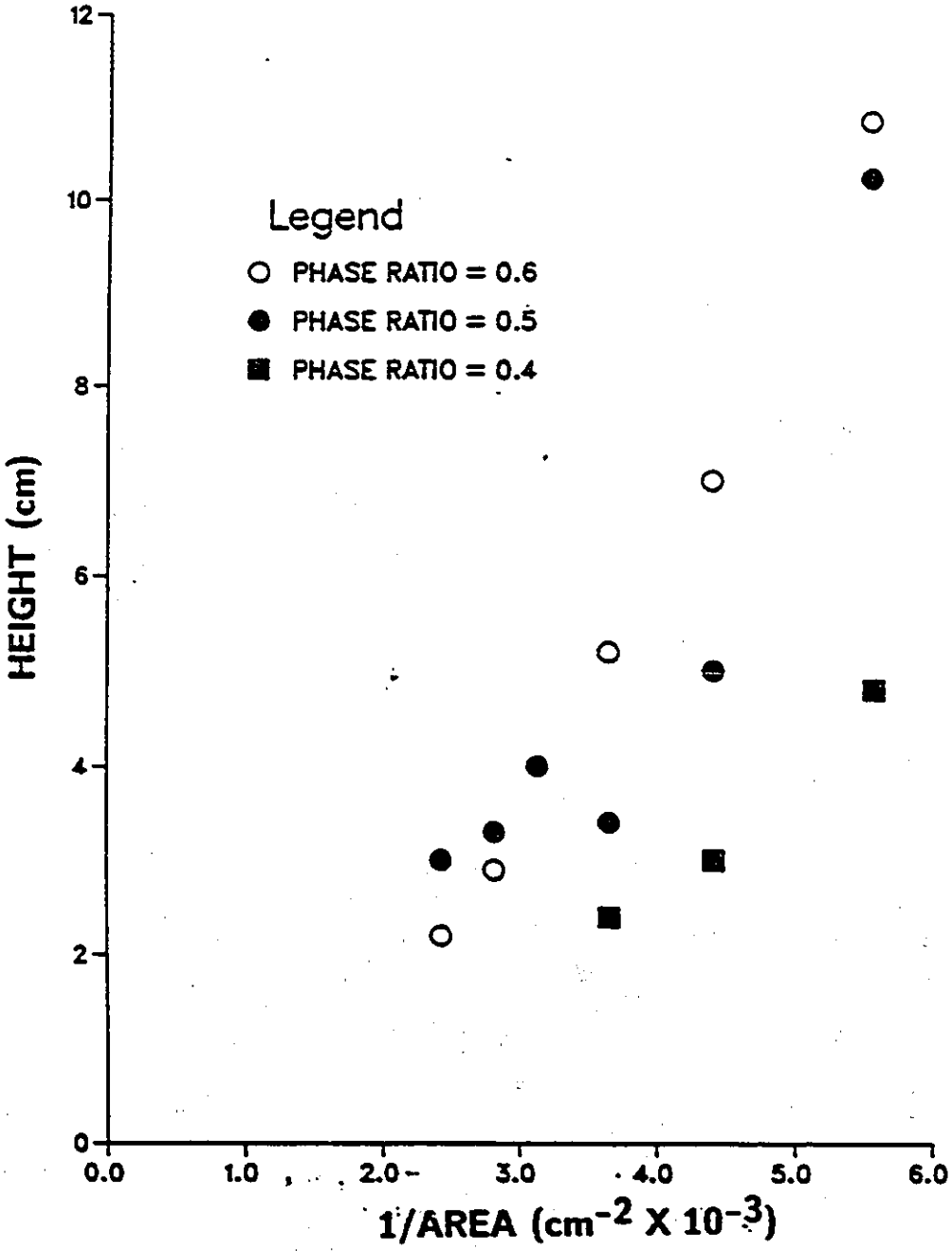

Figure No. 59: Experimental data for the cylindrical mixer. Dispersion band height versus 1/area at Q = 2000 mL/min and RPM = 150.

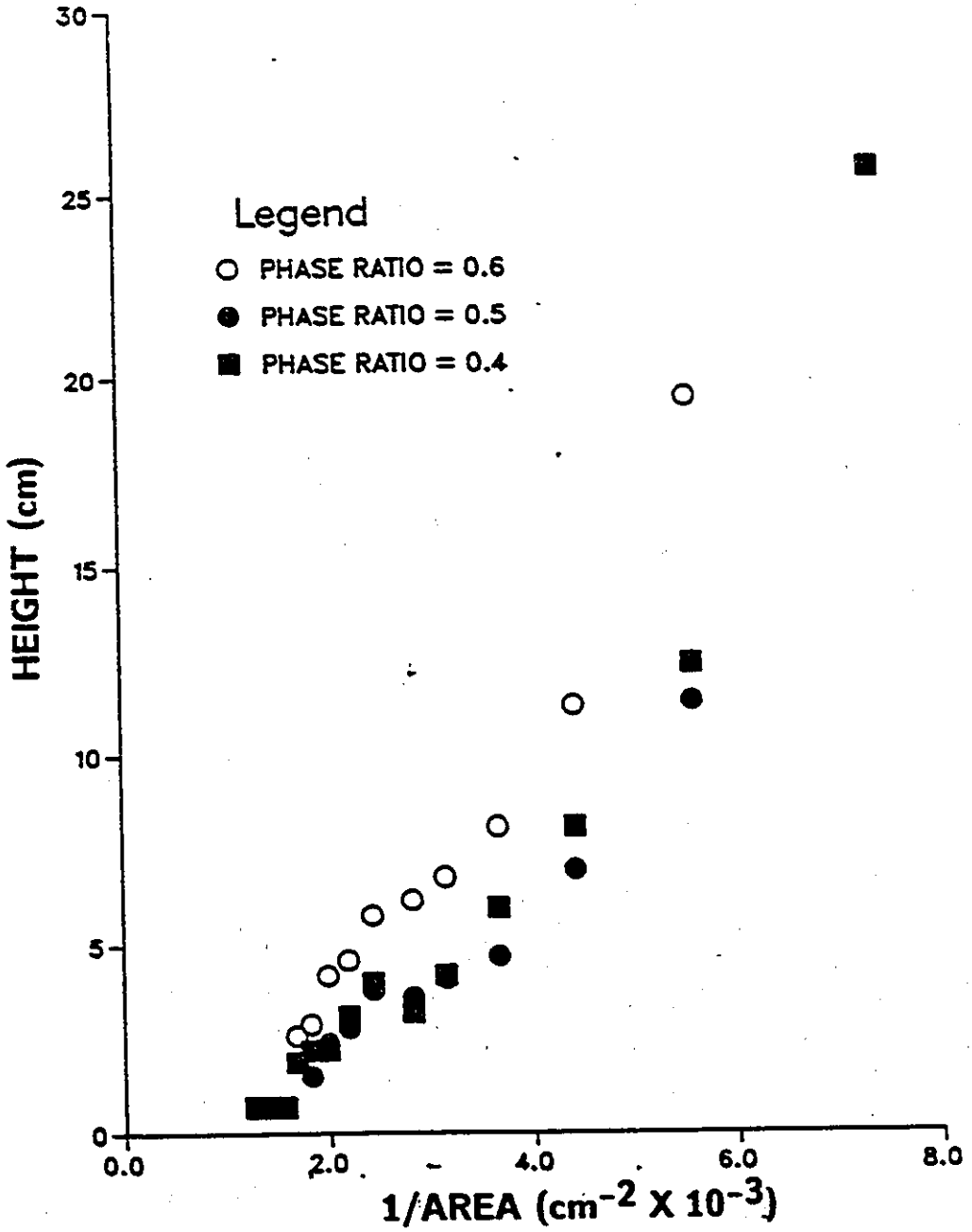

Figure No. 60: Experimental data for the cylindrical mixer. Dispersion band height 1/area at Q = 2000 mL/min and RPM = 200.

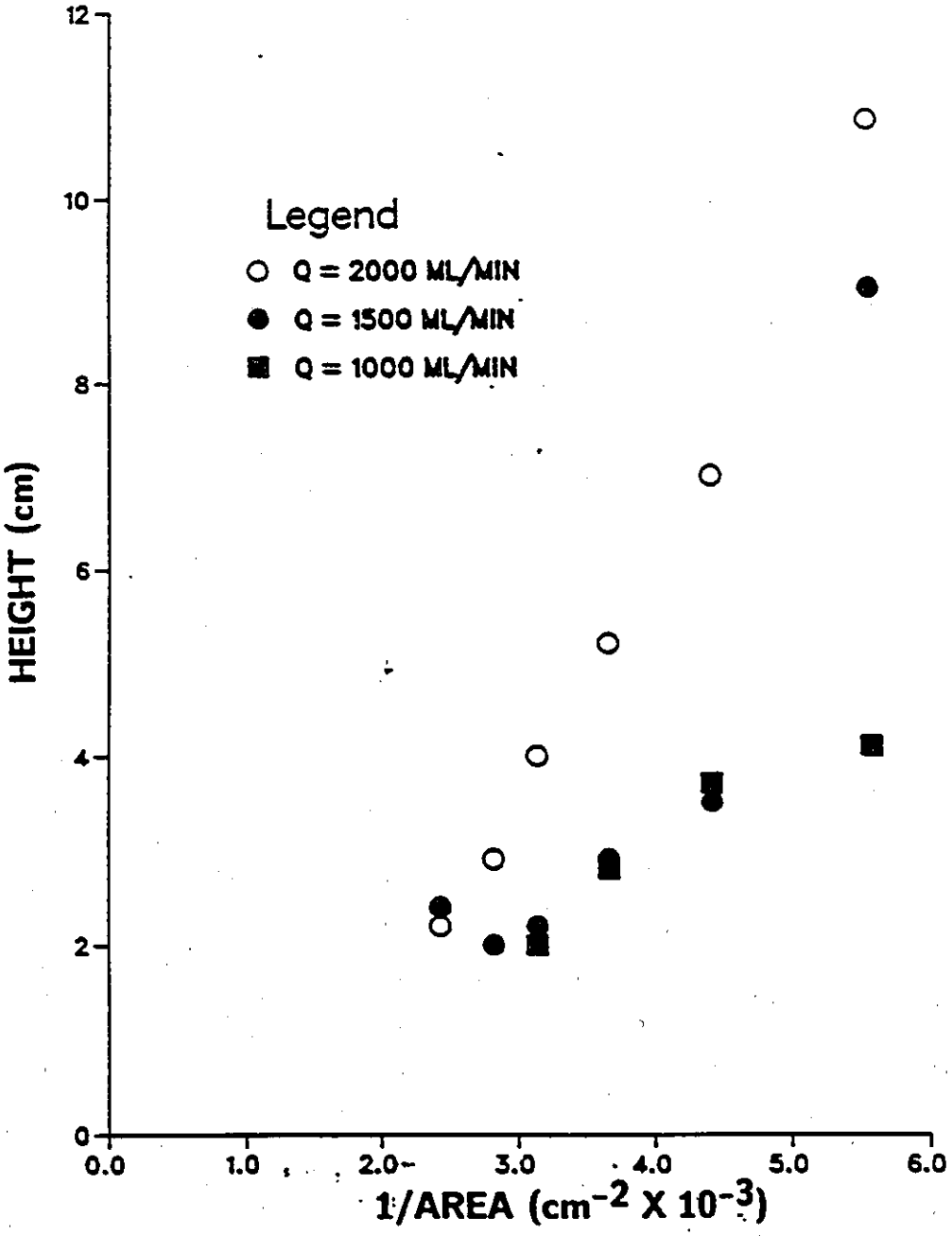

Figure No. 61: Experimental data for the cylindrical mixer. Dispersion band height versus 1/area at RPM = 150 and PR = 0.4.

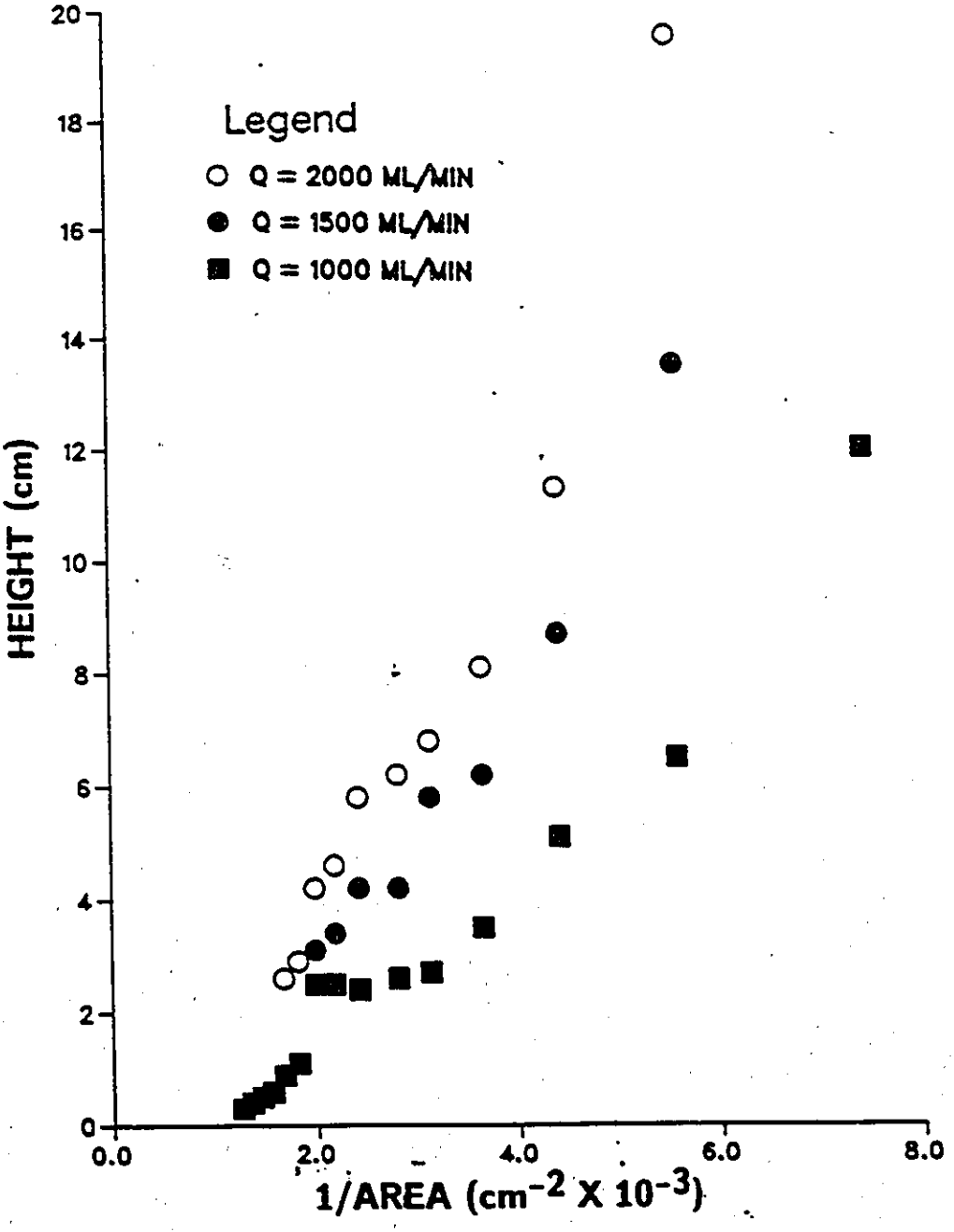

Figure No. 62: Experimental data for the cylindrical mixer. Dispersion band height versus 1/area at RPM = 200 and PR = 0.4

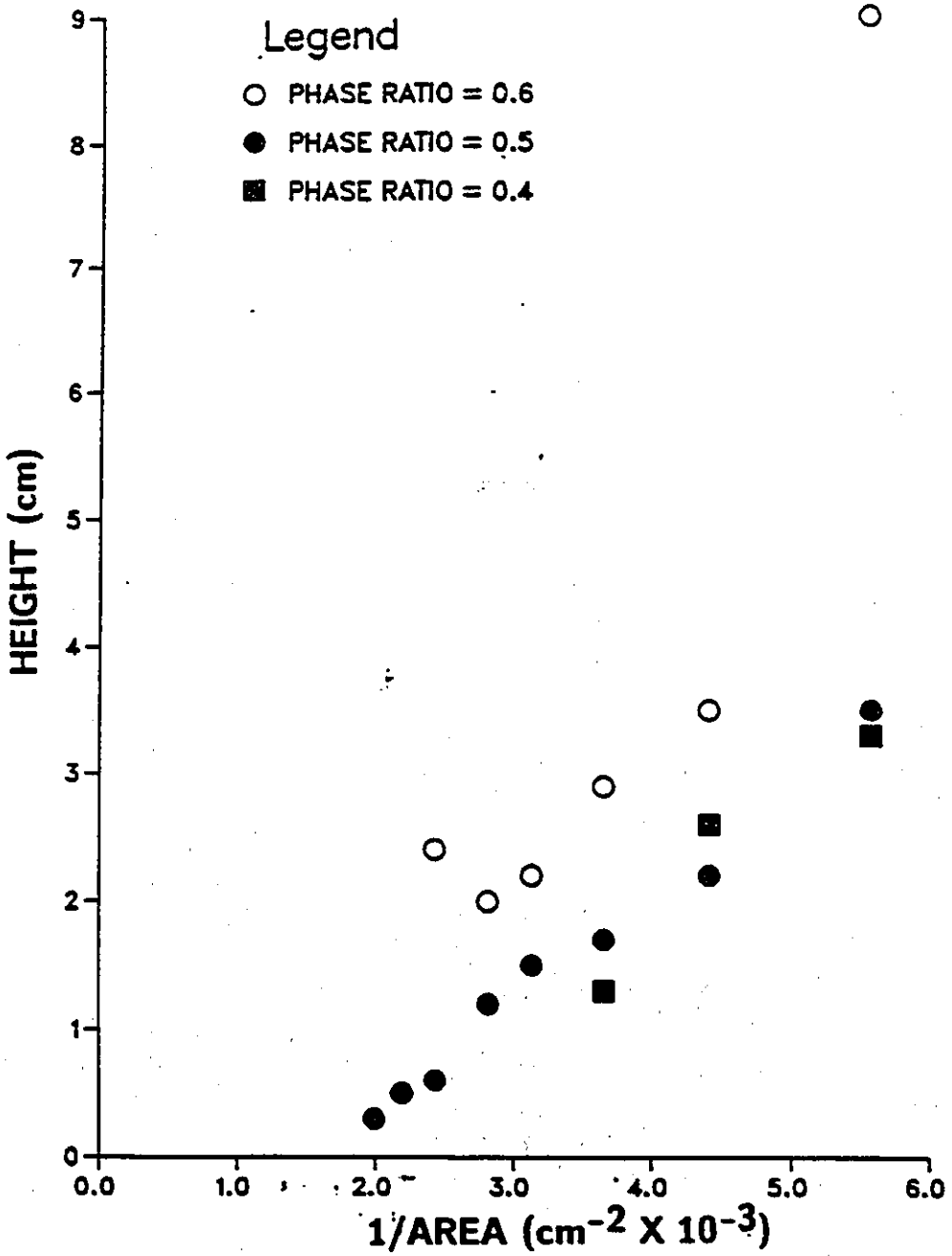

Figure No. 63: Experimental data for the cylindrical mixer. Dispersion band height versus 1/area at Q = 1500 mL/min and RPM = 150.

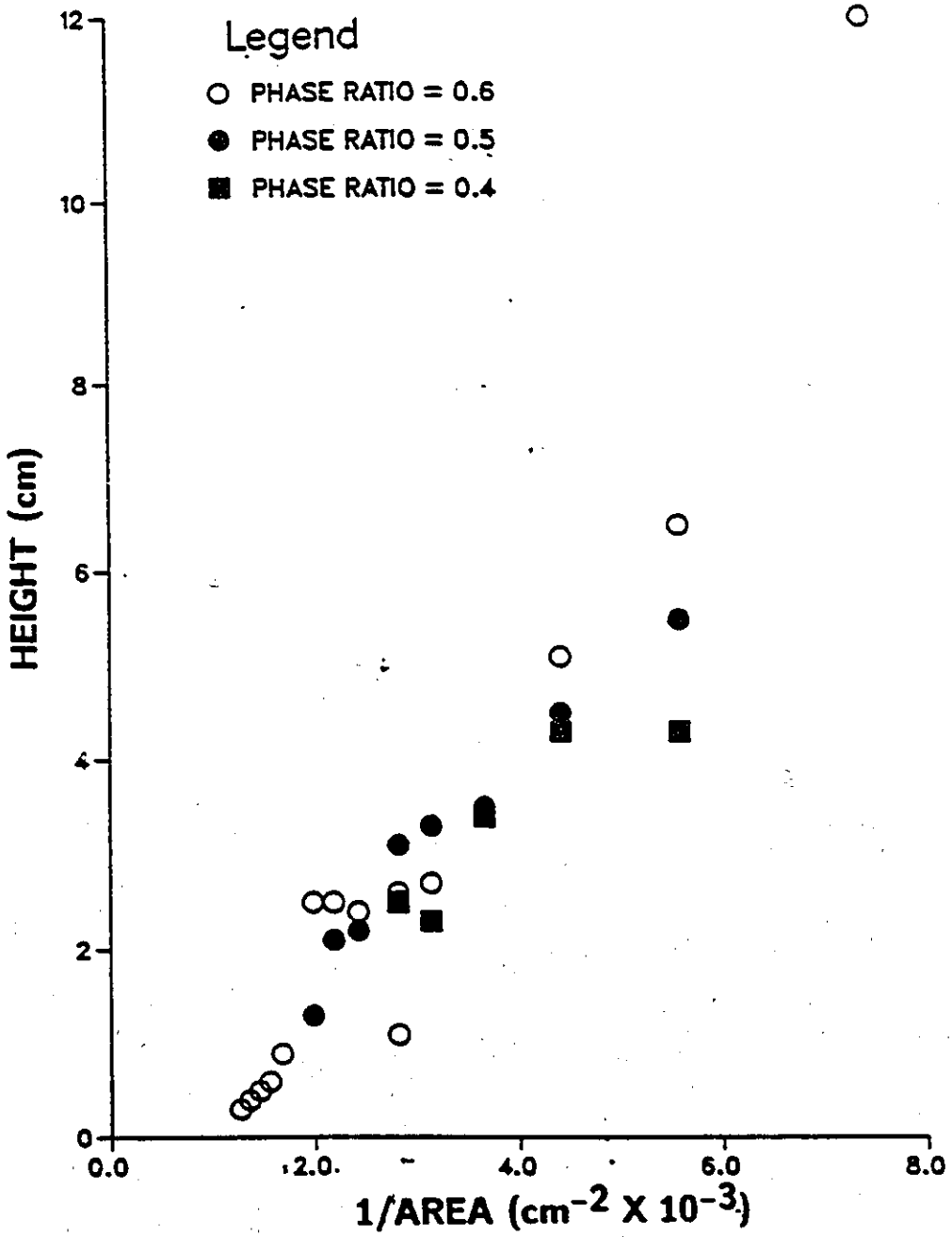

Figure No. 64: Experimental data for the cylindrical mixer. Dispersion band height versus 1/area at Q = 1000 mL/min and RPM = 200.

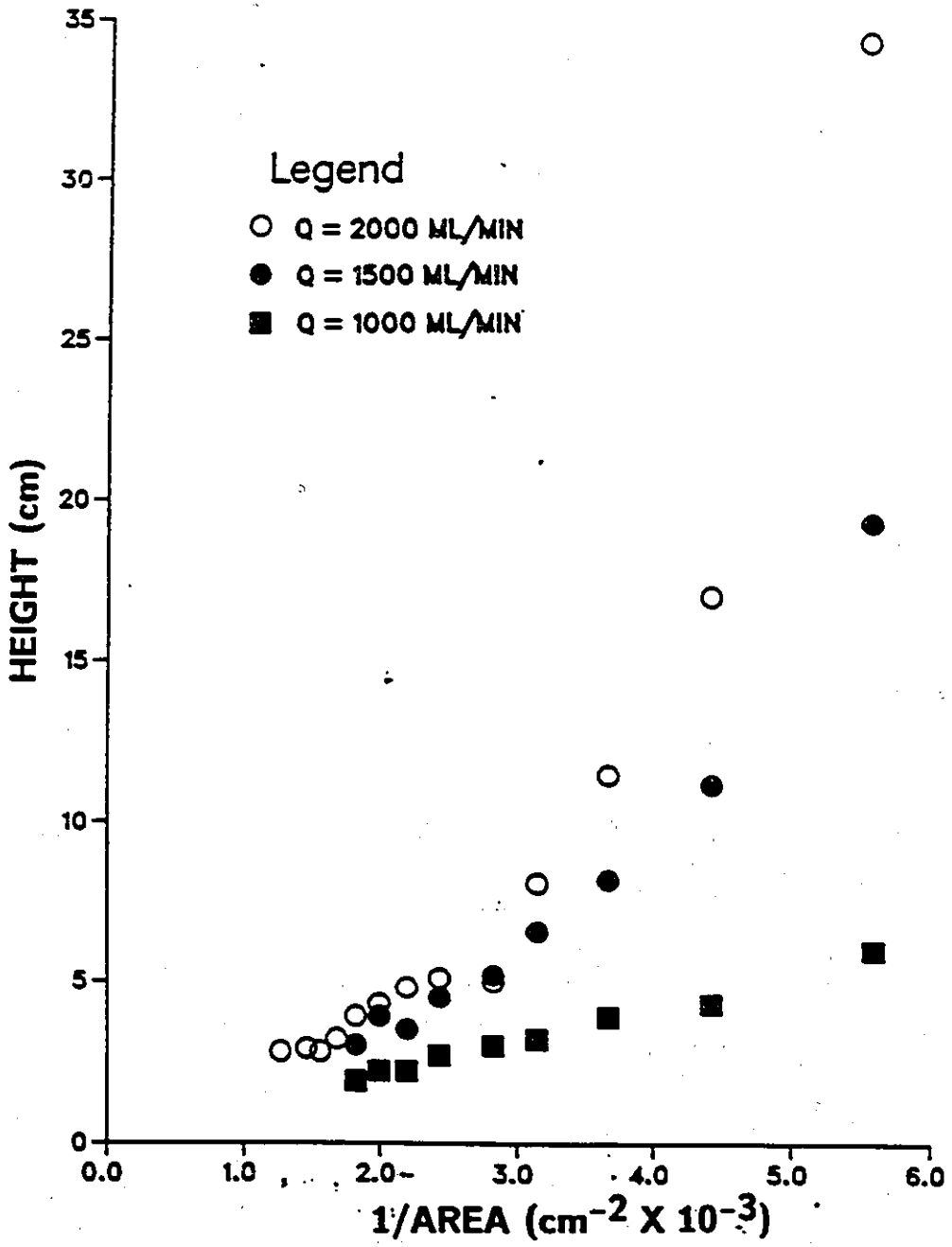

Figure No. 65: Experimental data for the closed mixer. Dispersion band height versus 1/area at RPM = 300 and PR = 0.6.

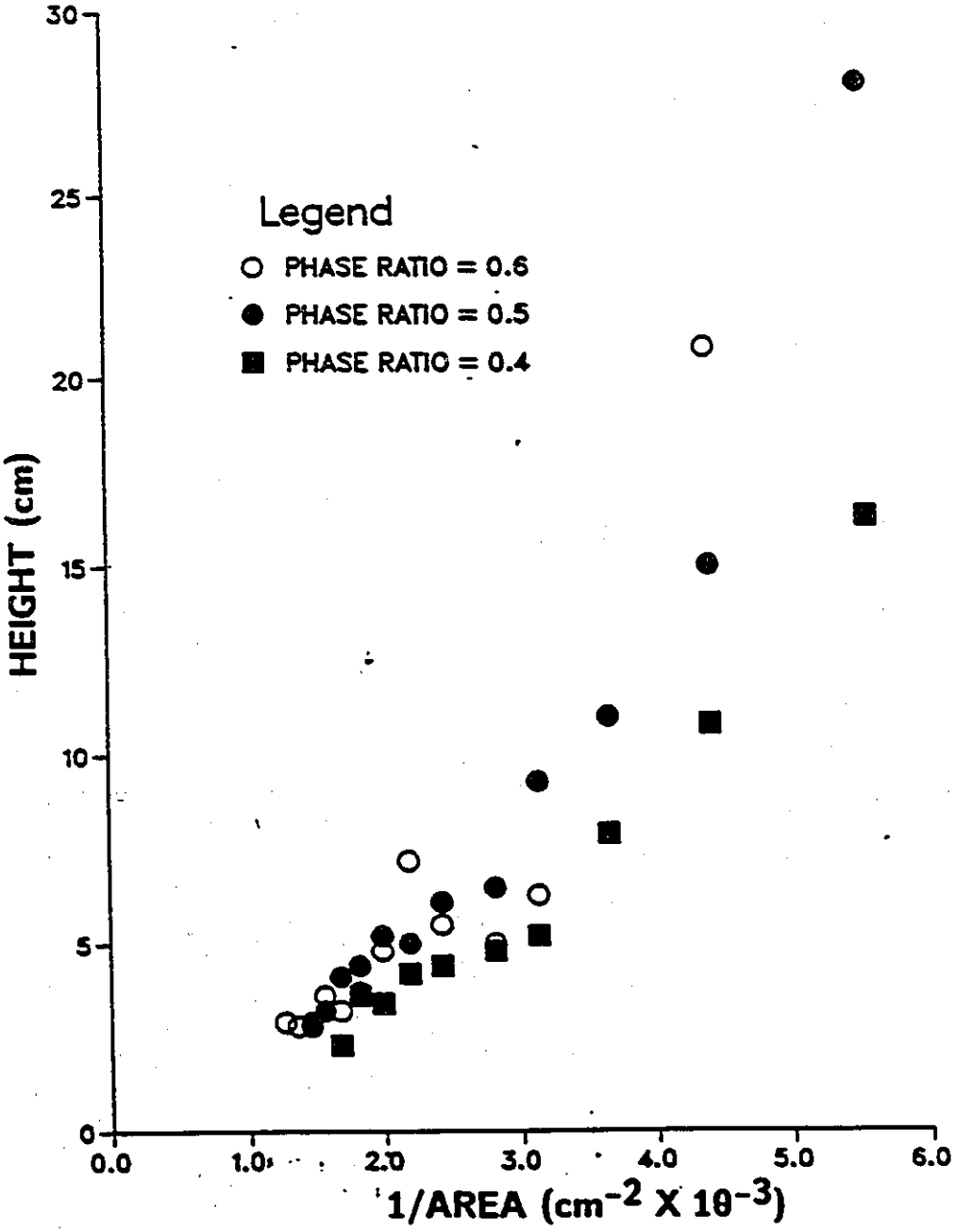

Figure No. 66: Experimental data for the closed mixer. Dispersion band height versus 1/area at Q = 2000 mL/min and RPM = 200.

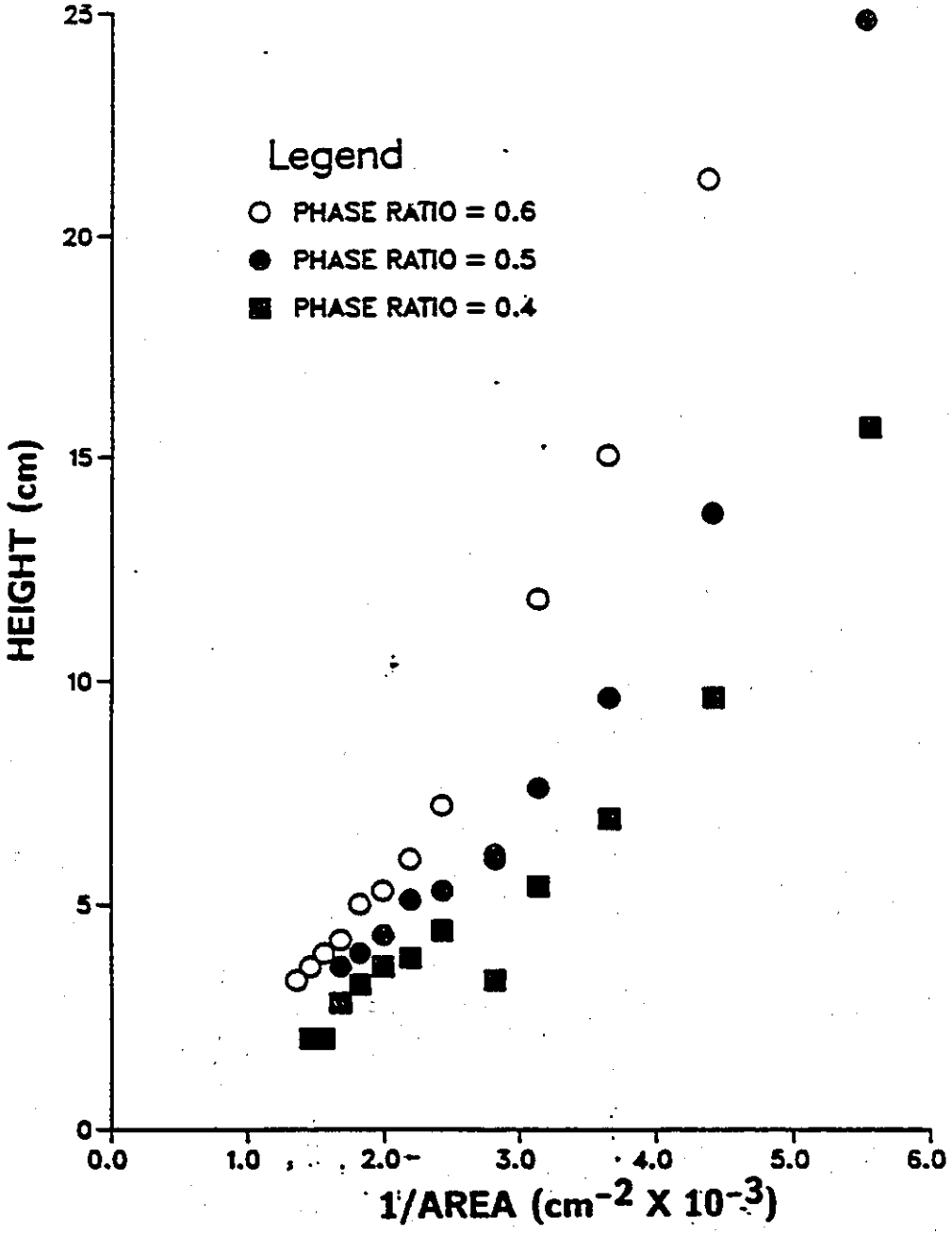

Figure No. 67: Experimental data for the closed mixer. Dispersion band height versus 1/area at Q = 2000 mL/min and RPM = 250.

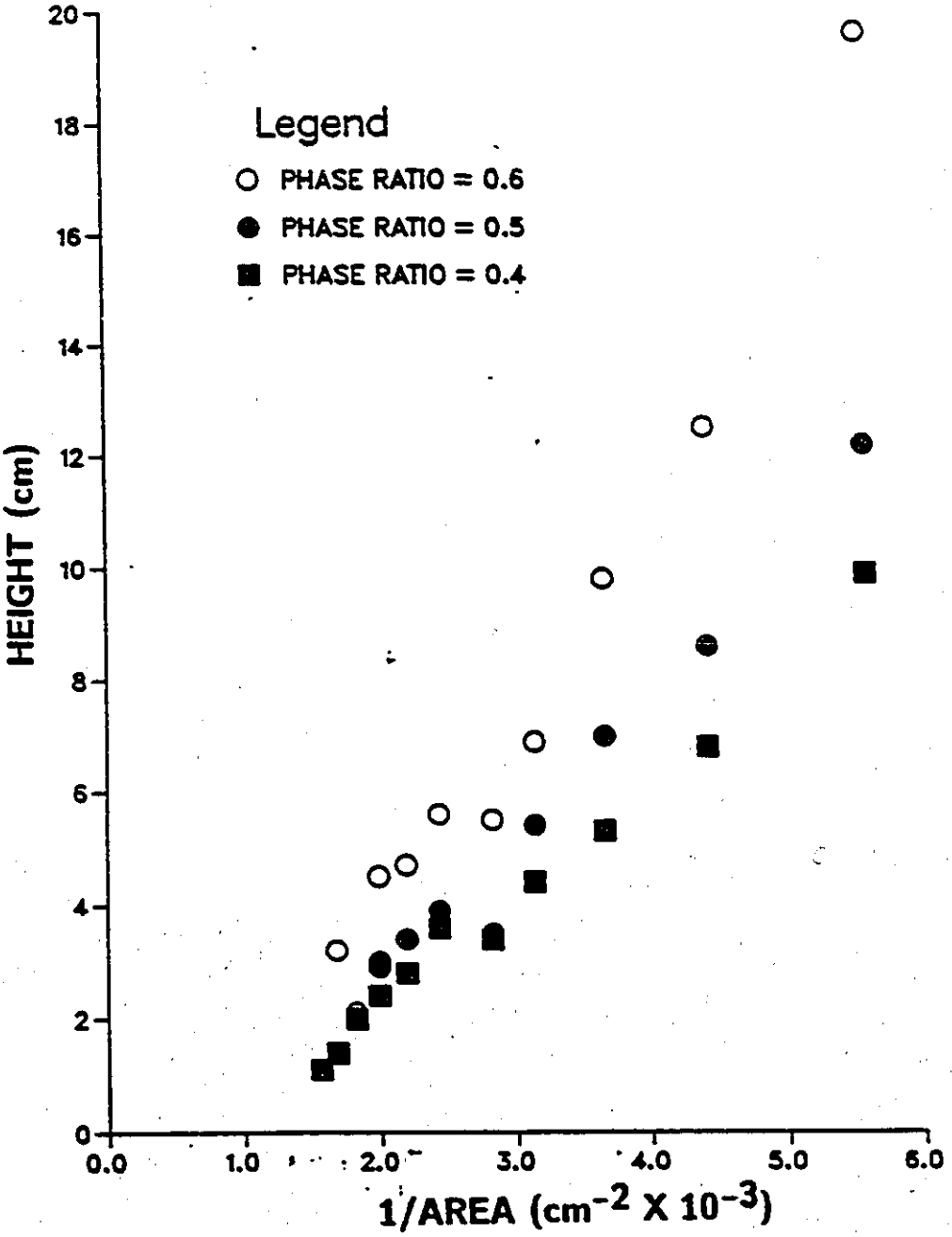

Figure No. 68: Experimental data for the closed mixer. Dispersion band height versus 1/area at Q = 1500 mL/min and RPM = 200.

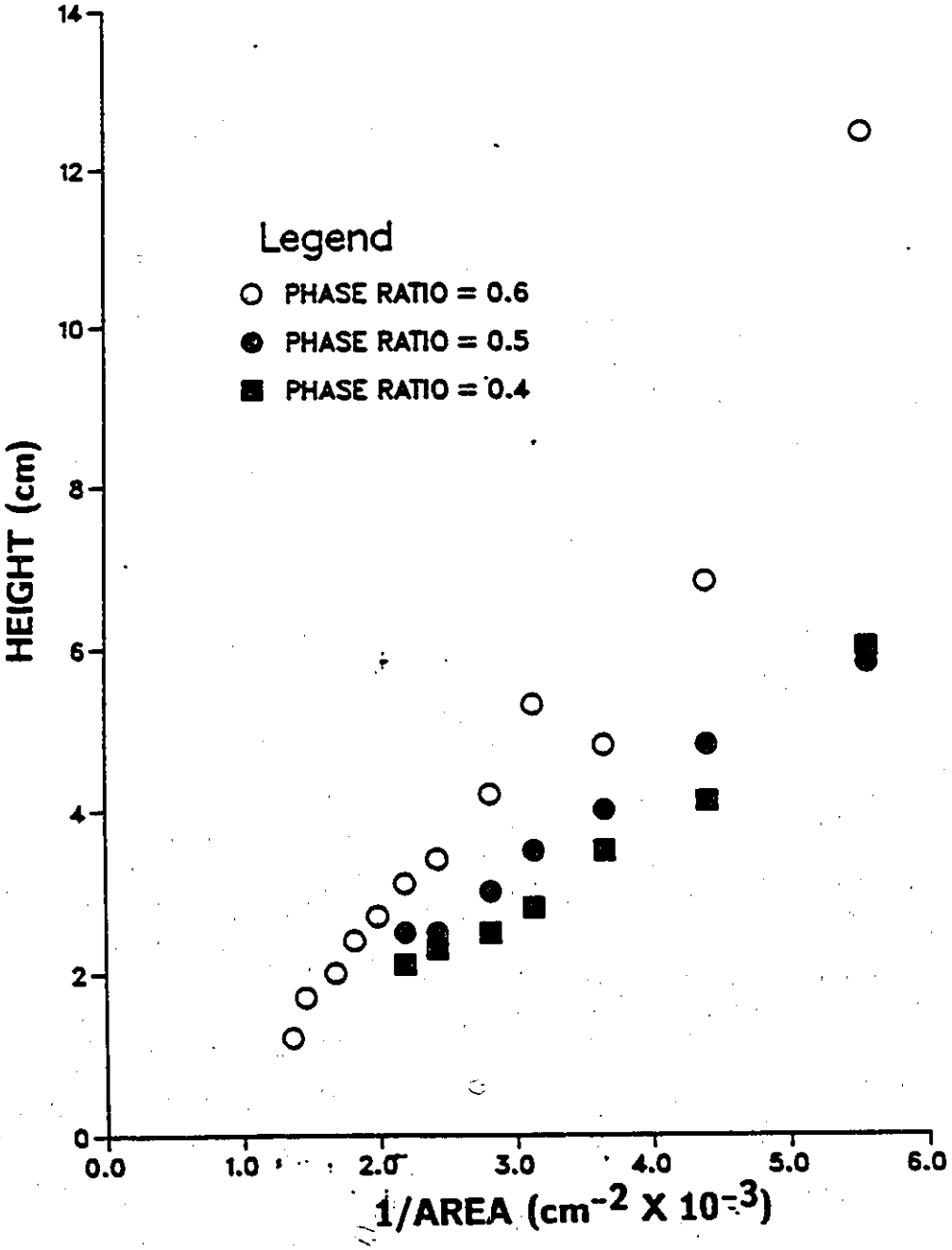

Figure No. 69: Experimental data for the closed mixer. Dispersion band height versus 1/area at Q = 1000 mL/min and RPM = 250.

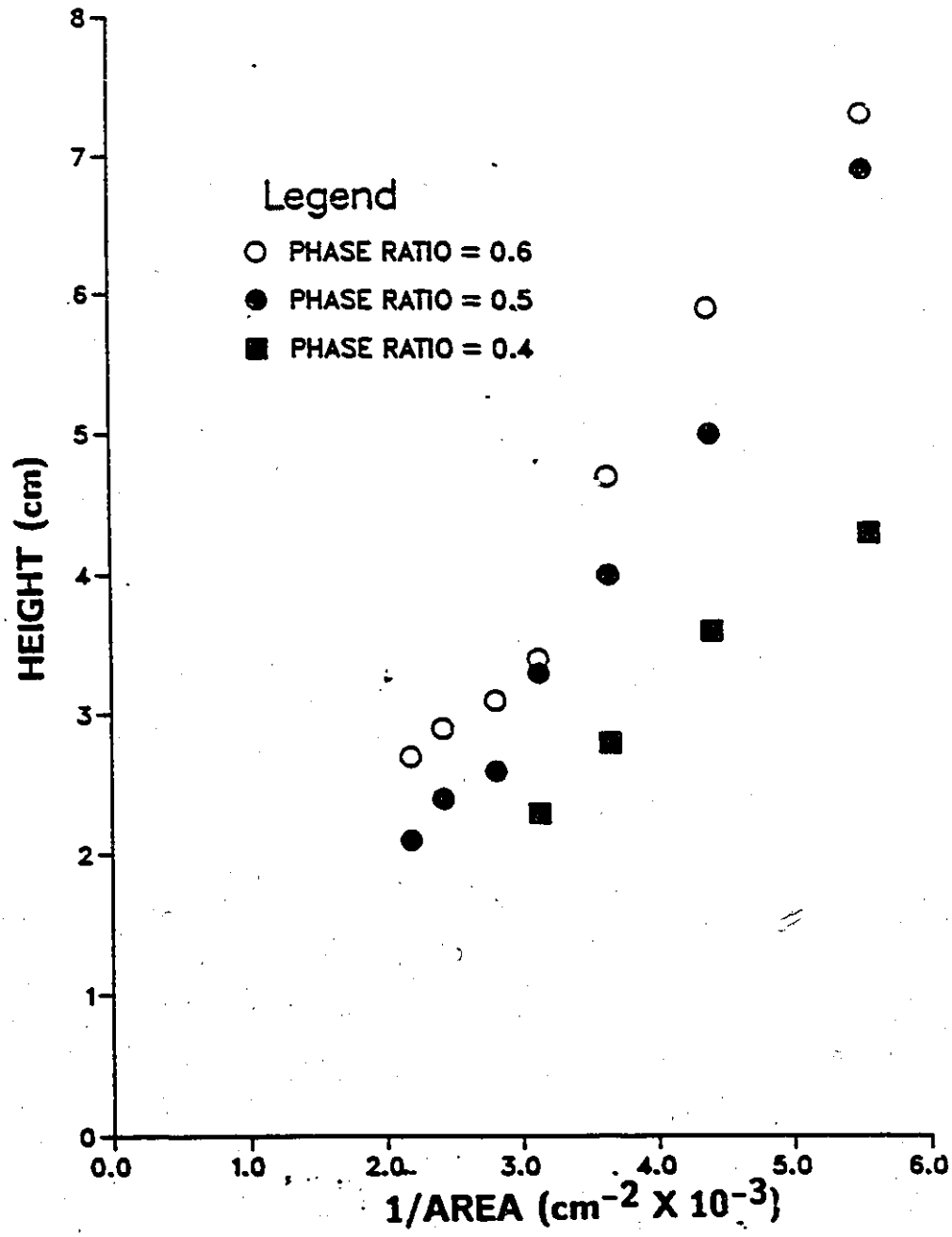

Figure No. 70: Experimental data for the closed mixer. Dispersion band height versus 1/area at Q = 1000 ml/min and RPM = 200.

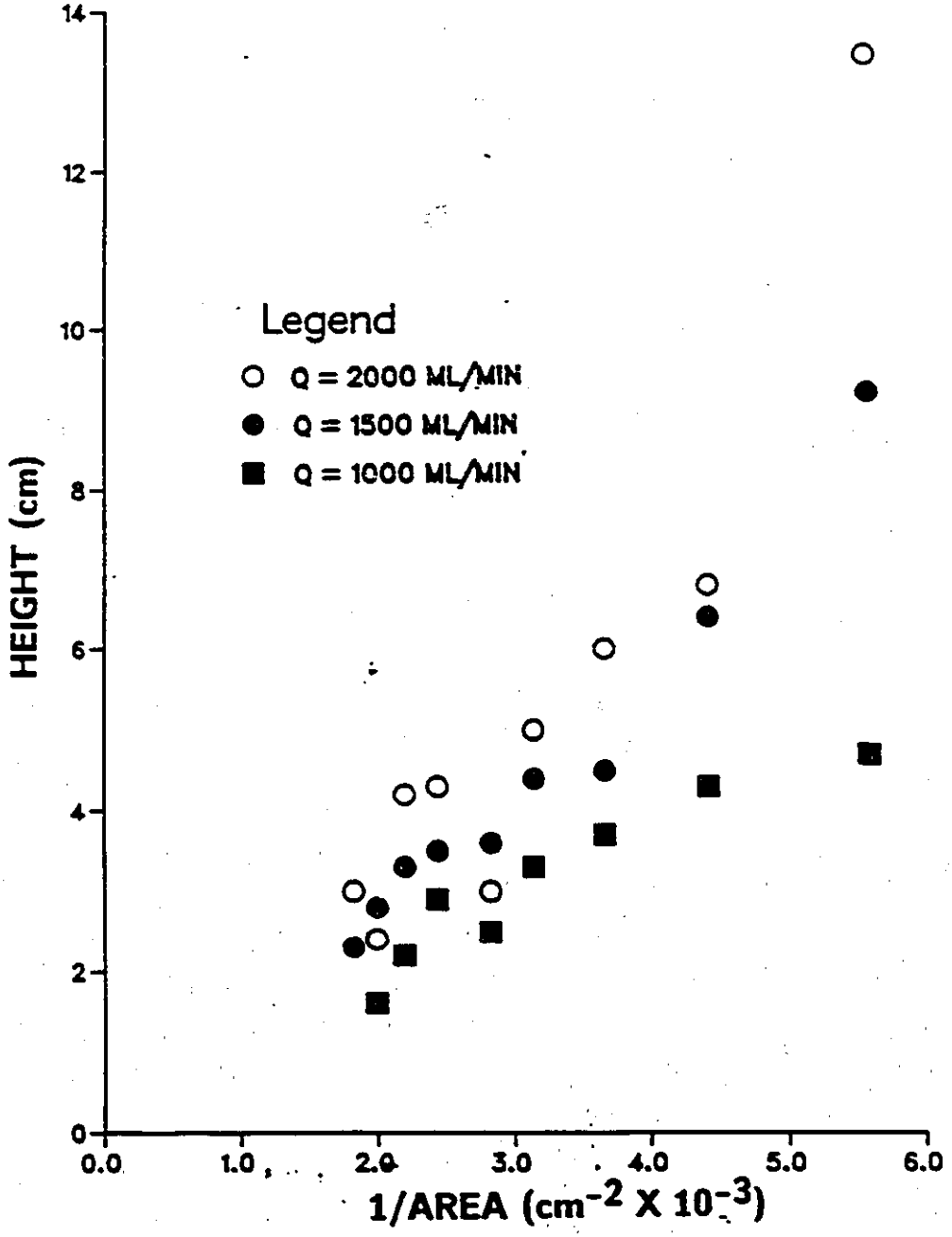

Figure No. 71: Experimental data for the closed mixer. Dispersion band height versus 1/area at RPM = 300 and PR = 0.4.

Appendix C

Transformed Data Plots

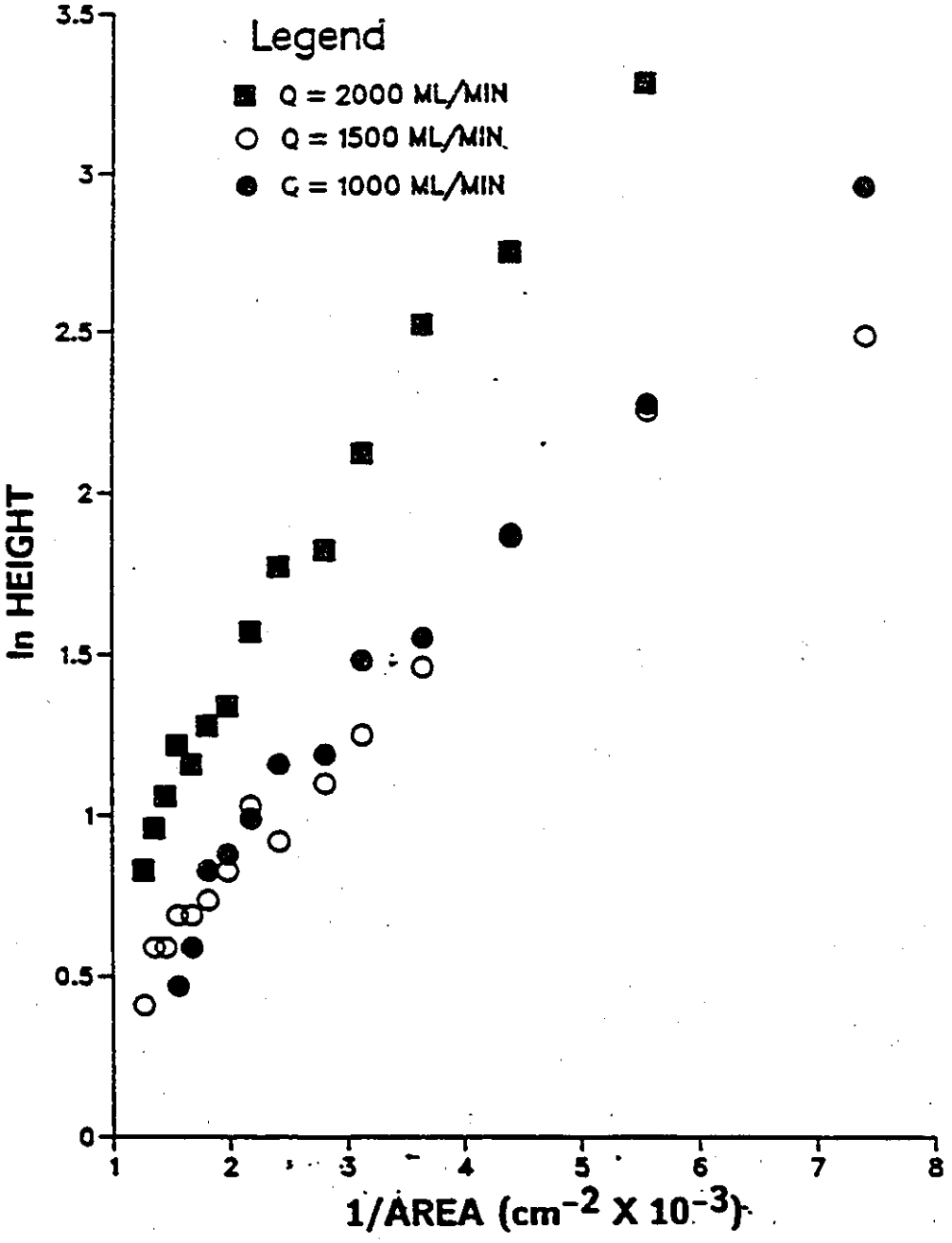

Figure No. 72: ln Height versus 1/area plot for the square mixer data at RPM = 250 and PR = 0.6.

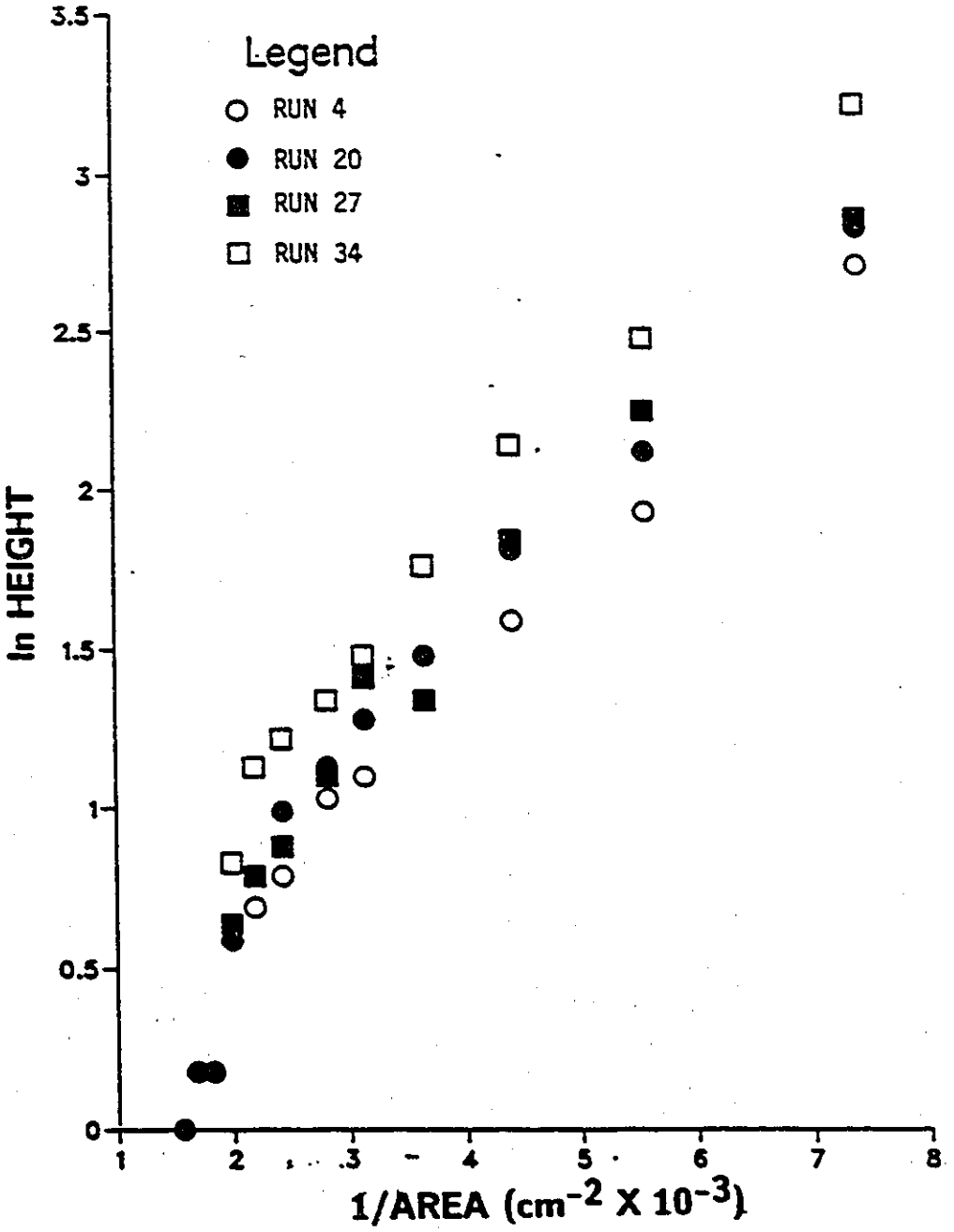

Figure No. 73: lN Height versus l/area plot for the square mixer data at Q = 1500 mL/min, RPM = 200 and PR = 0.5.

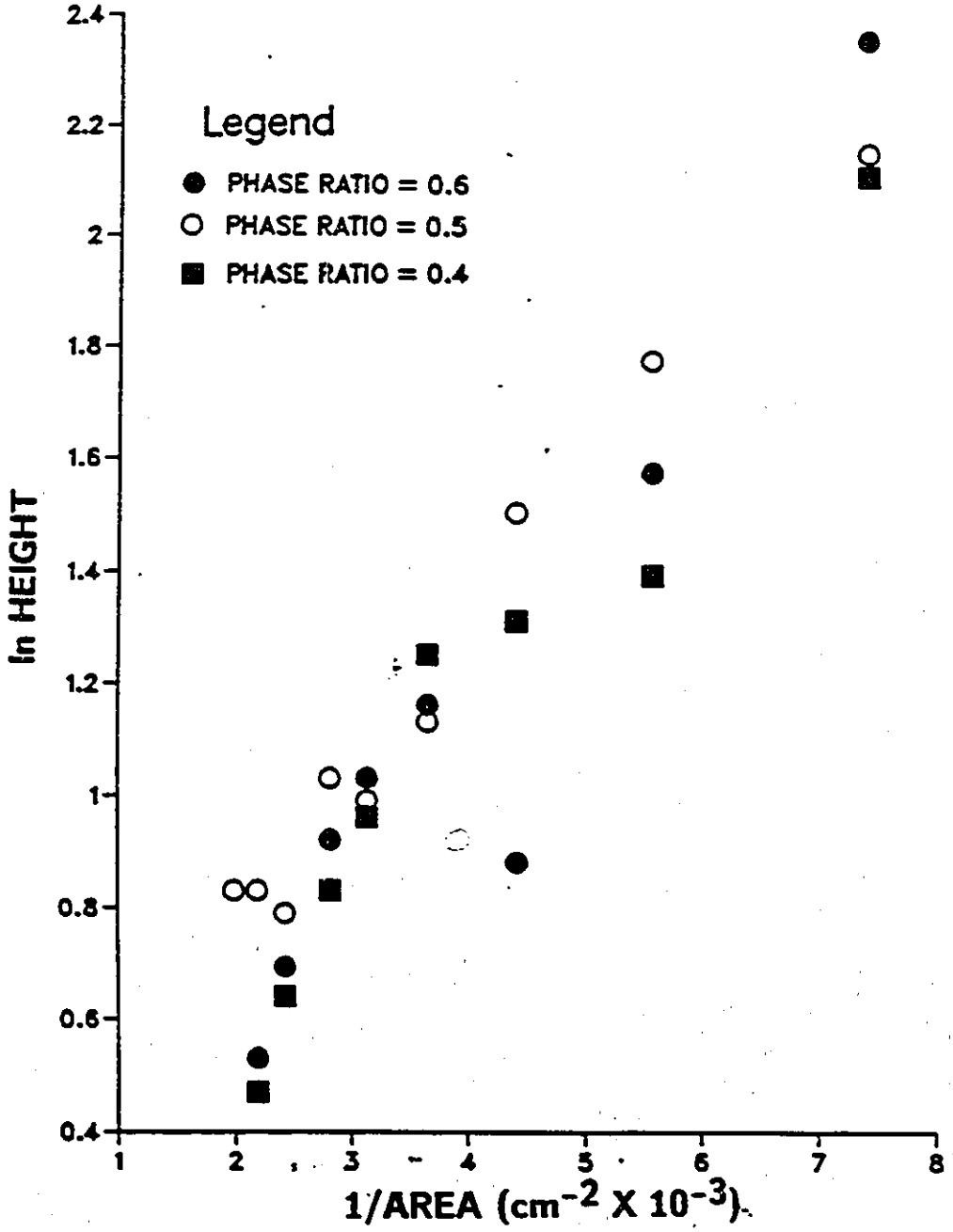

Figure No. 74: in Height versus 1/area plot for the square mixer data at Q = 1000 mL/min and RPM = 200.

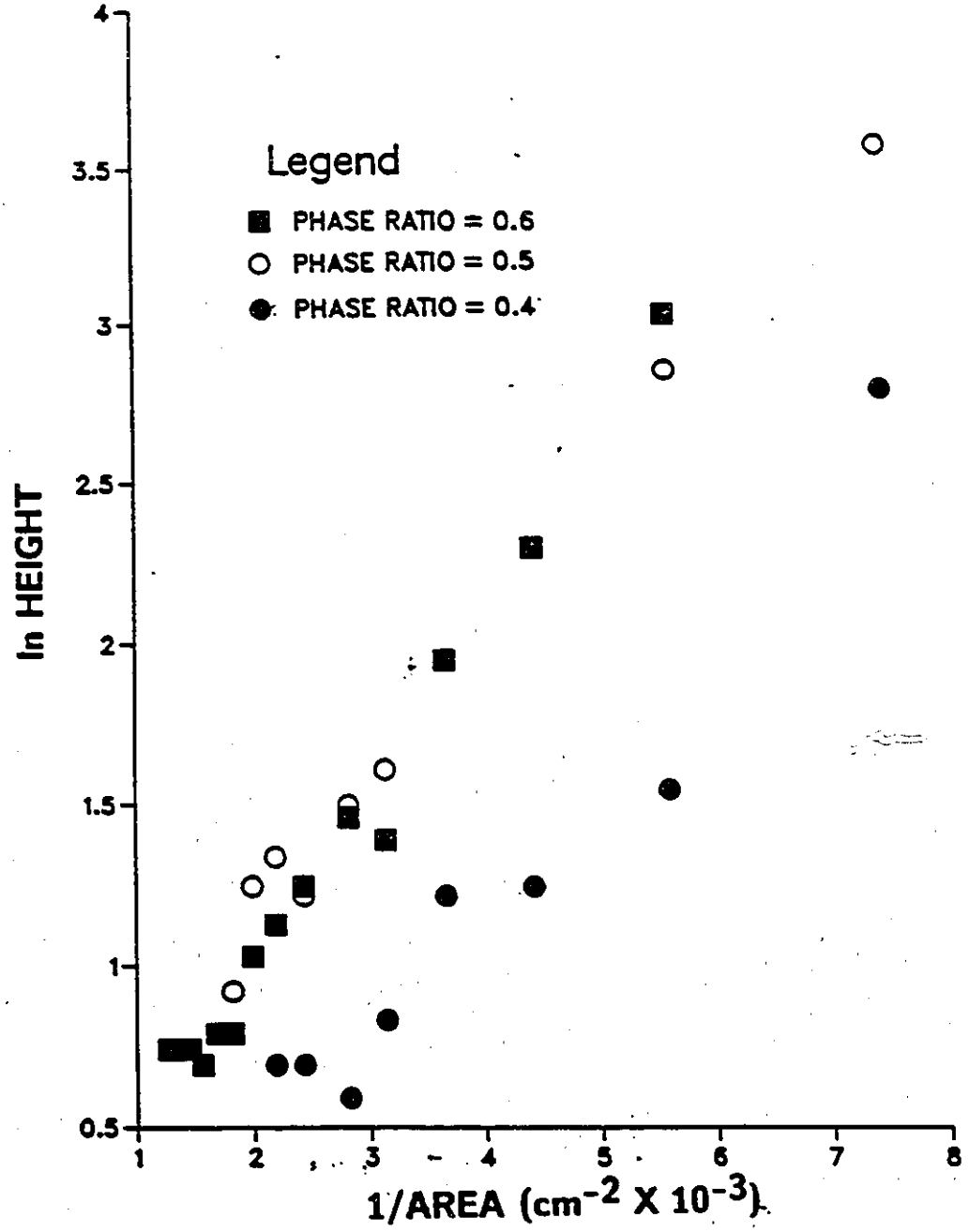

Figure No. 75: ln Height versus 1/area plot for the square mixer data at Q = 2000 mL/min and RPM = 200.

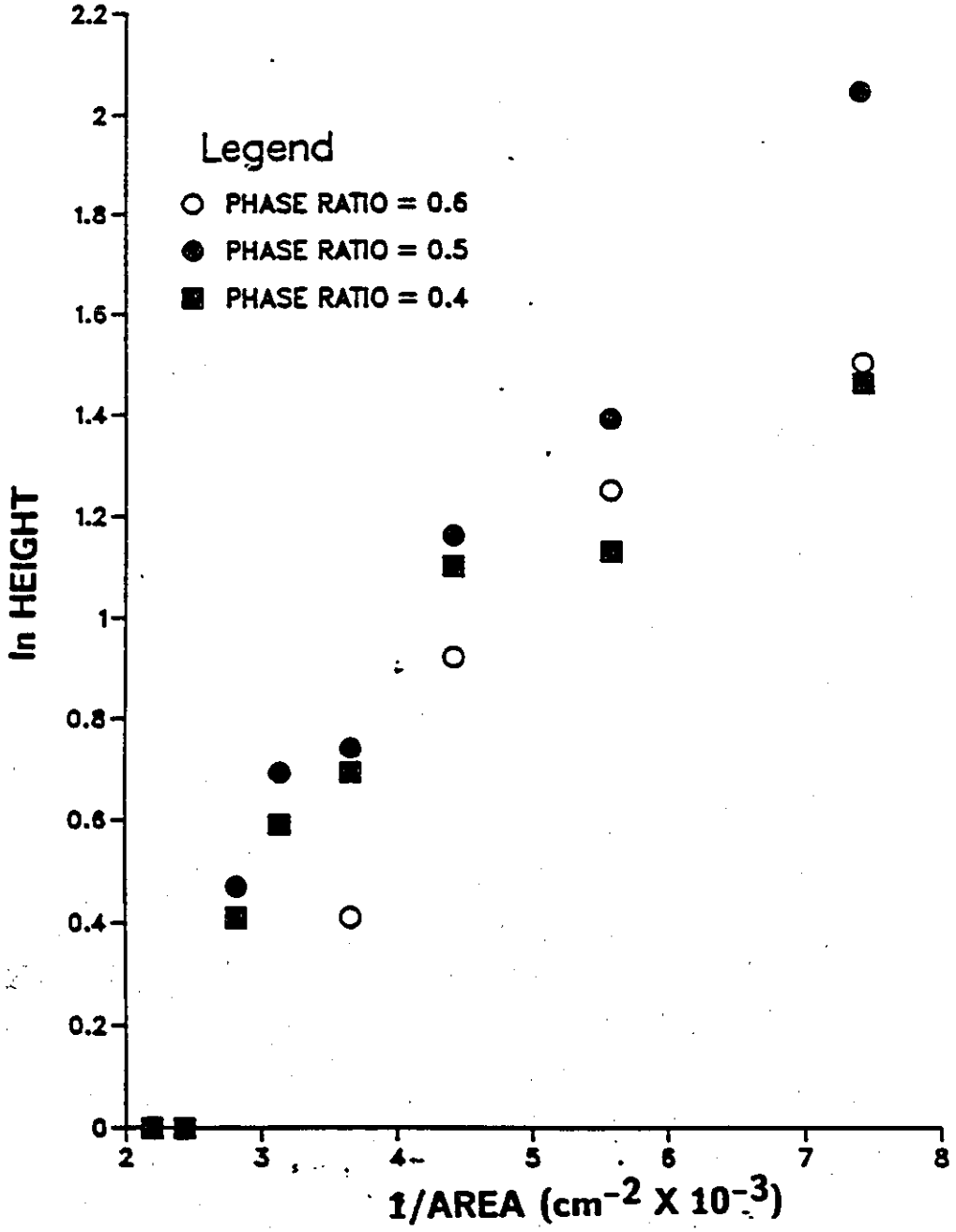

Figure No. 76: ln Height versus 1/area plot for the square mixer data at Q = 1500 mL/min and RPM = 150.

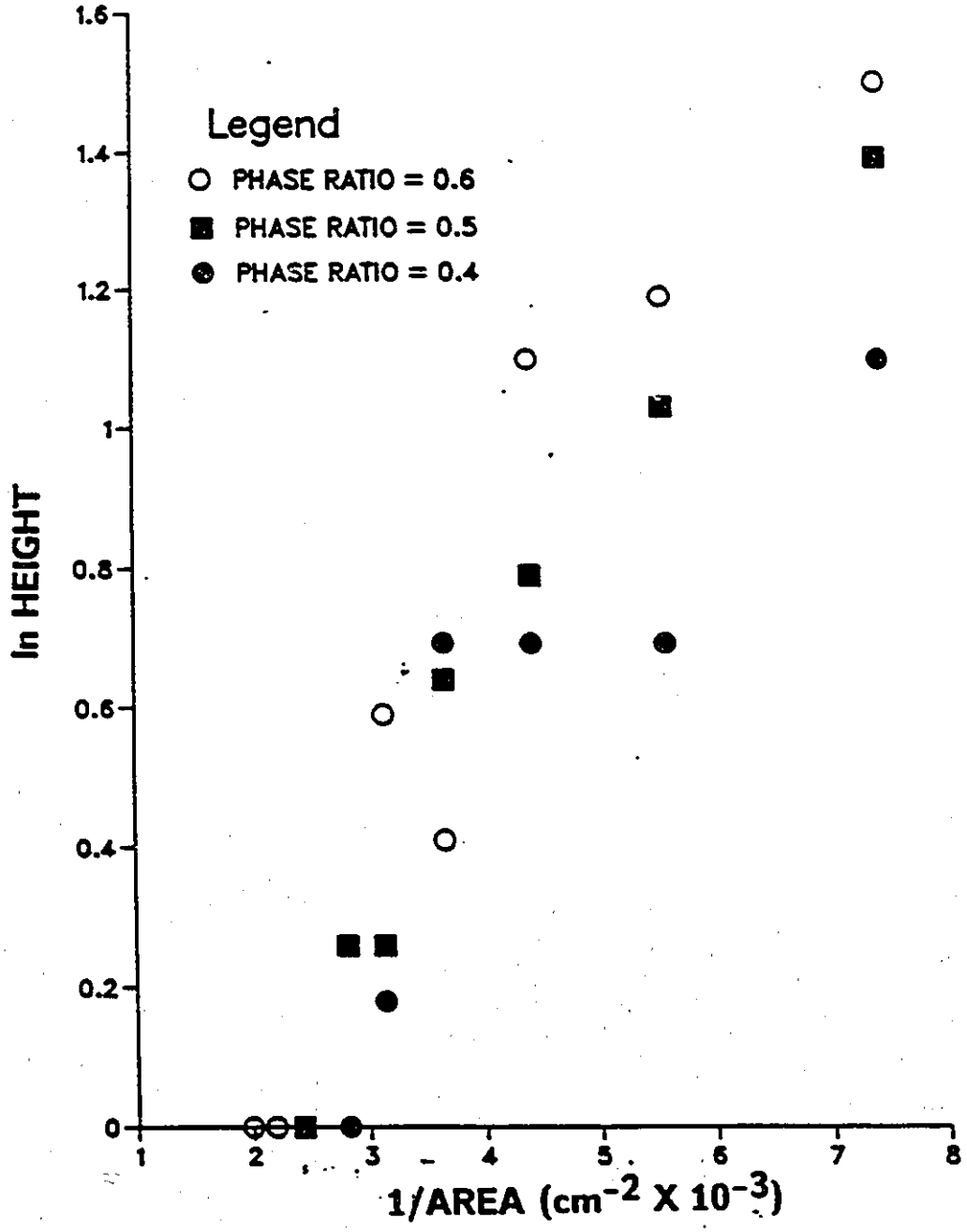

Figure No. 77: ln Height versus 1/area plot for the square mixer data at Q = 1000 mL/min and RPM = 150

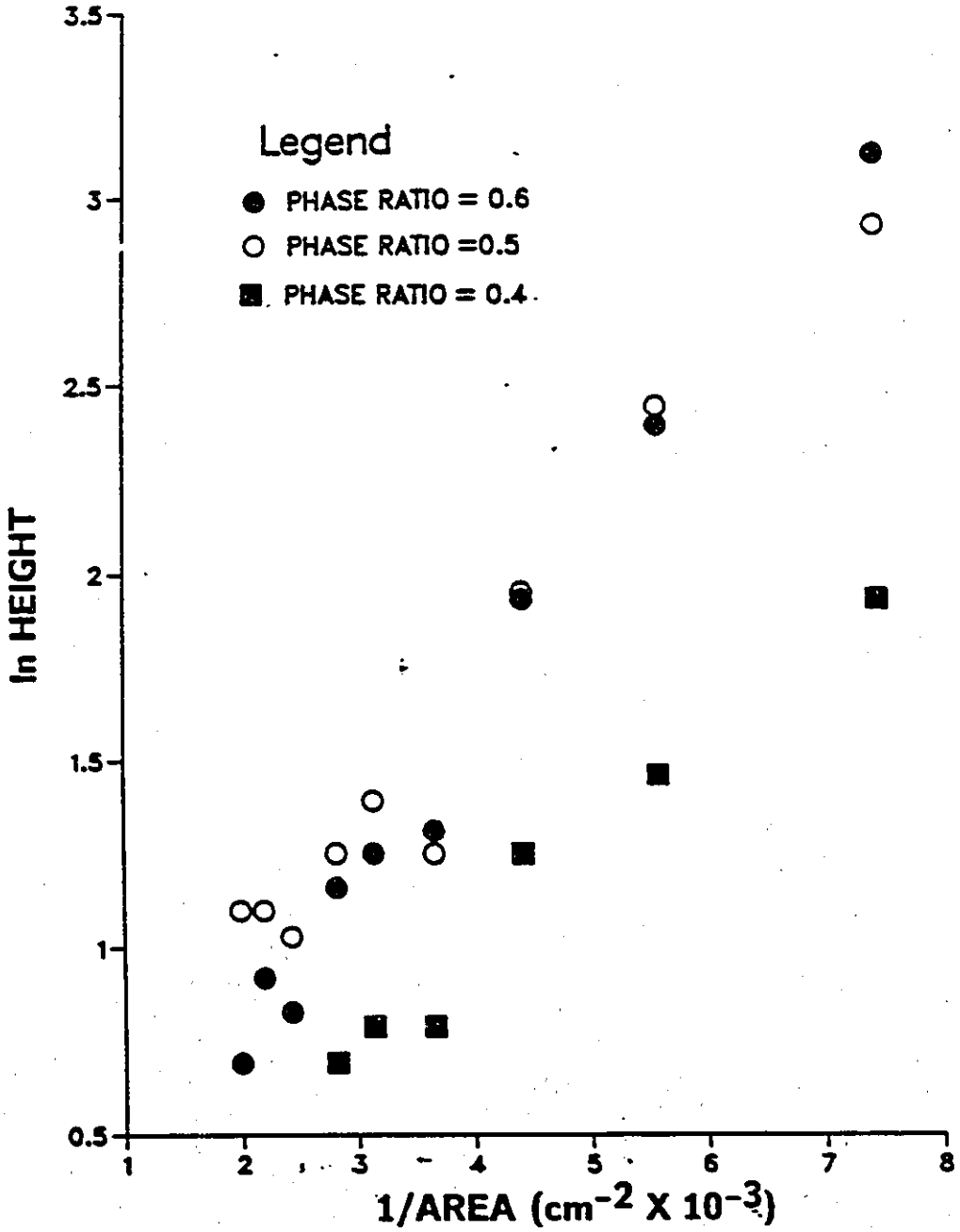

Figure No. 78: ln Height versus 1/area plot for the square mixer data at Q = 2000 mL/min and RPM = 150.

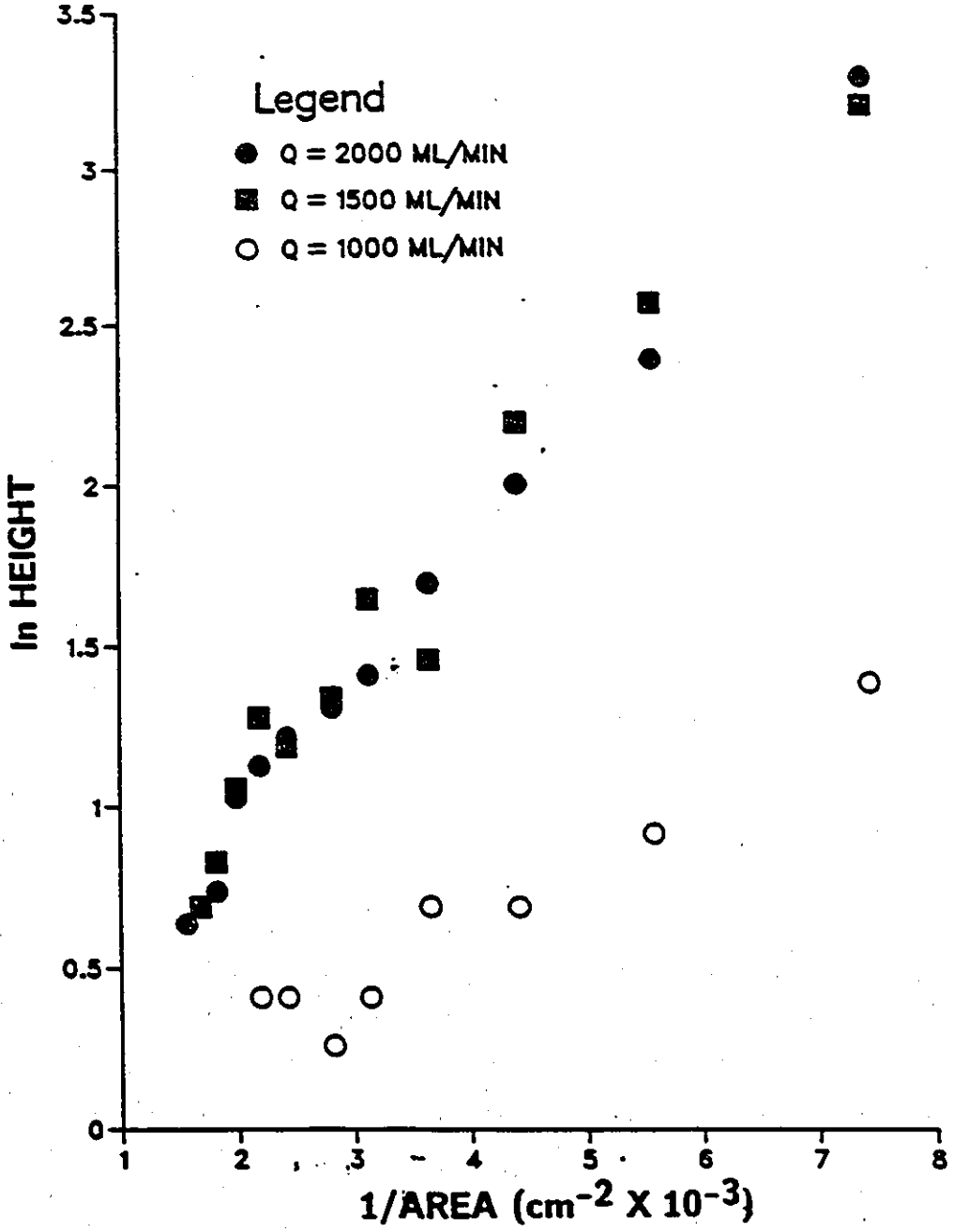

Figure No. 79: ln Height versus 1/area plot for the square mixer data at RPM = 250 and PR = 0.4

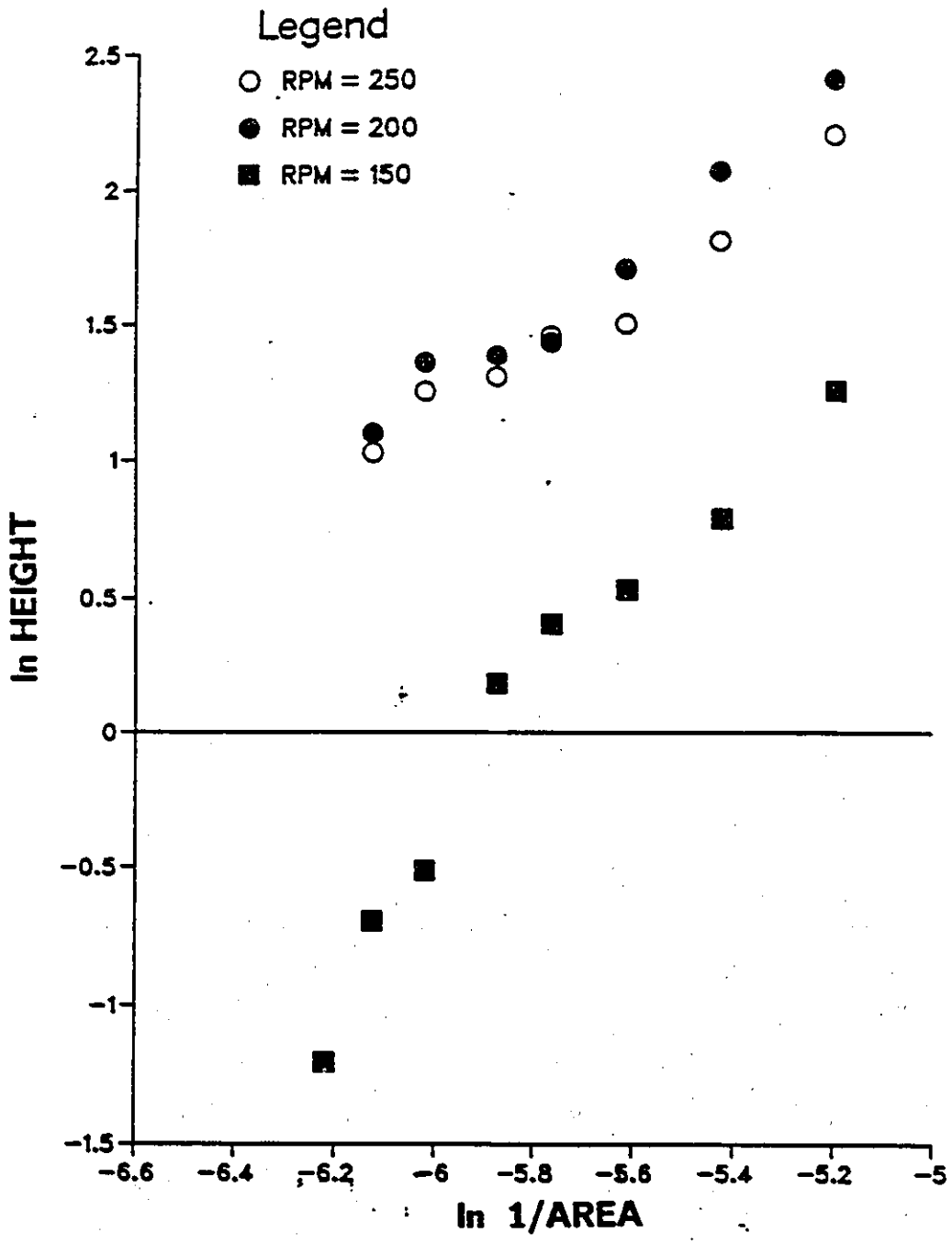

Figure No. 80: ln Height versus ln 1/area plot for the cylindrical mixer data at Q = 1500 mL/min and PR = 0.5

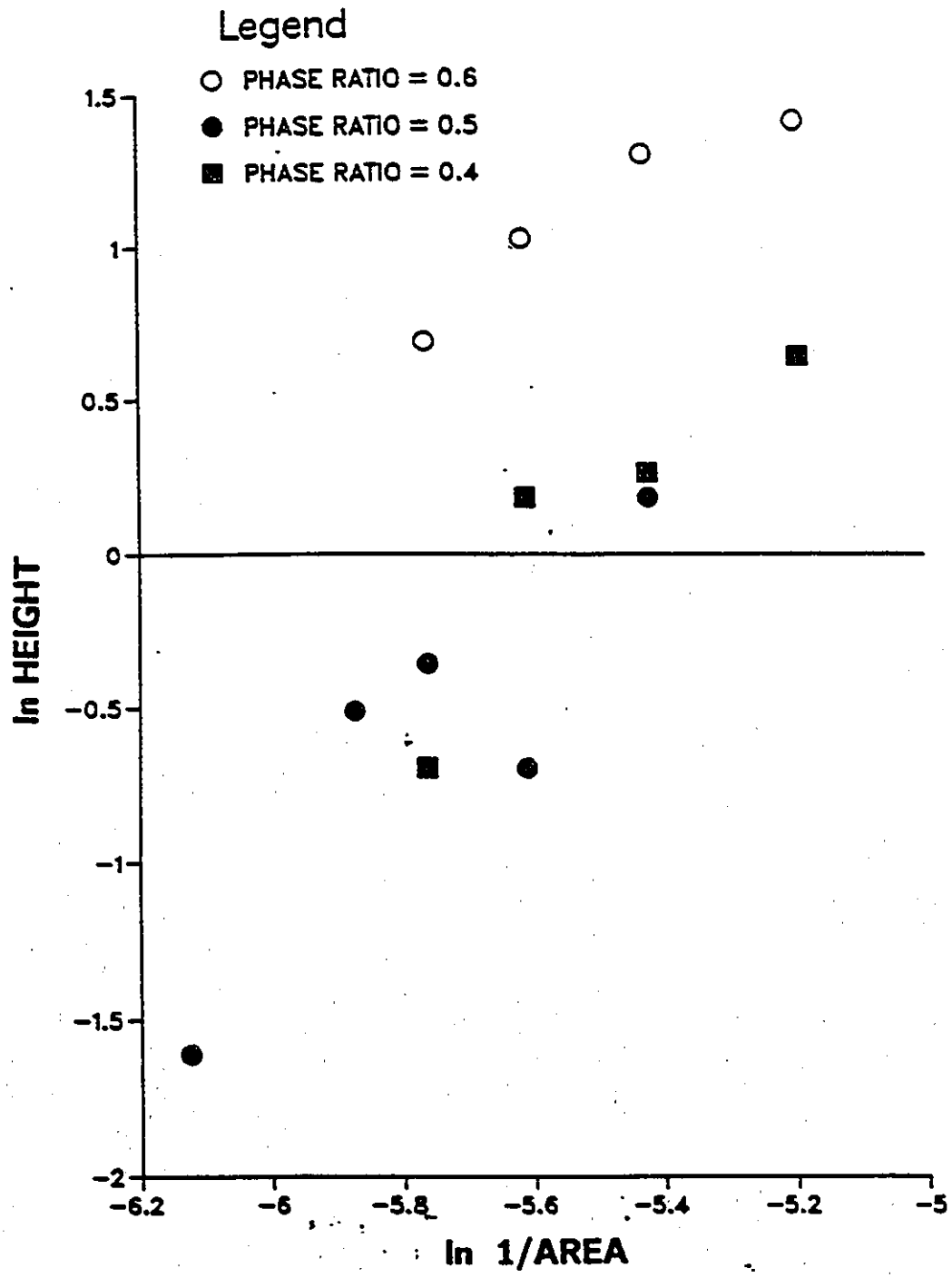

Figure No. 81: ln Height versus ln 1/area plot for the cylindrical mixer data at Q = 1000 mL/min and RPM = 150.

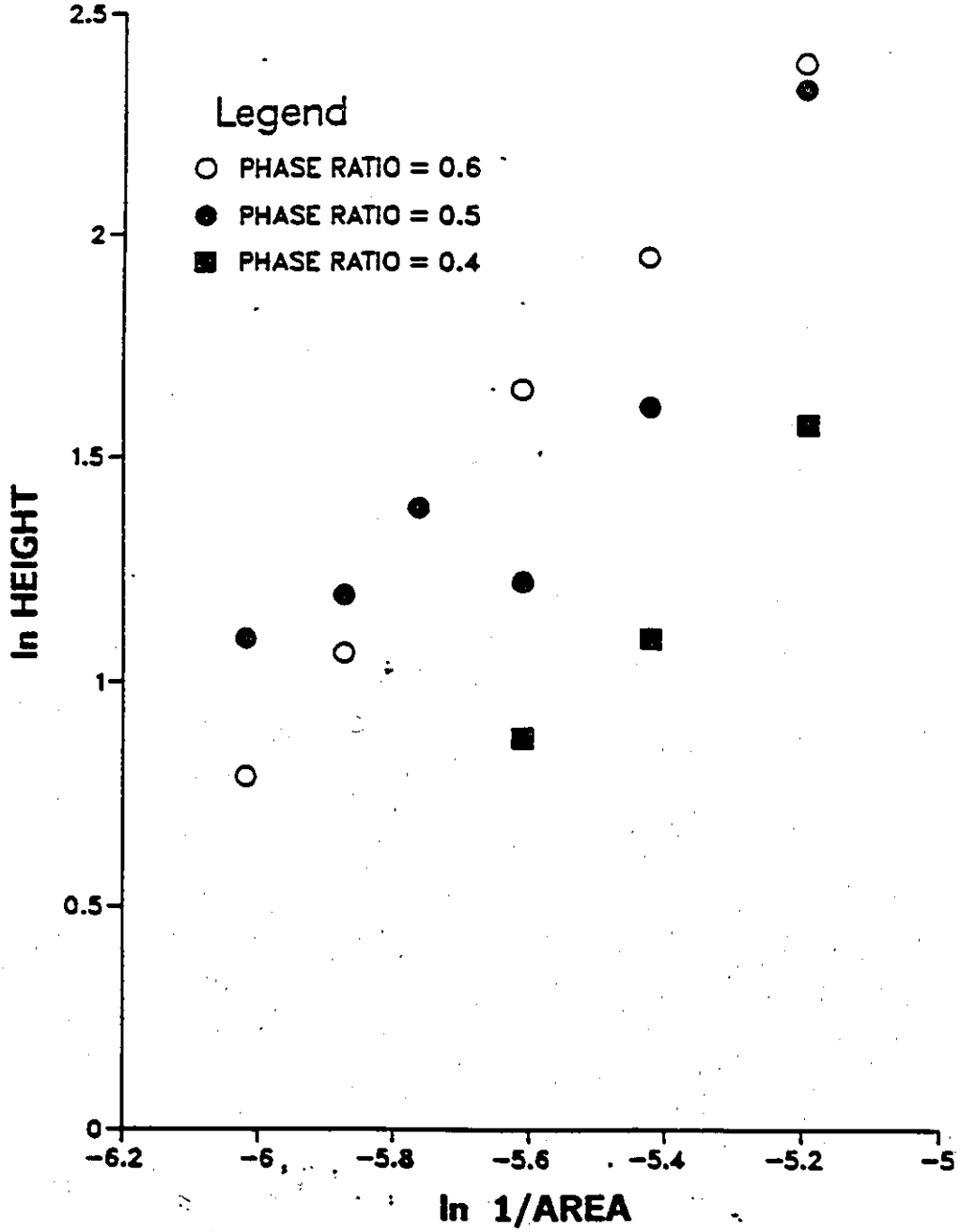

Figure No. 82: ln Height versus ln 1/area plot for the cylindrical mixer data at Q = 2000 mL/min and RPM = 150.

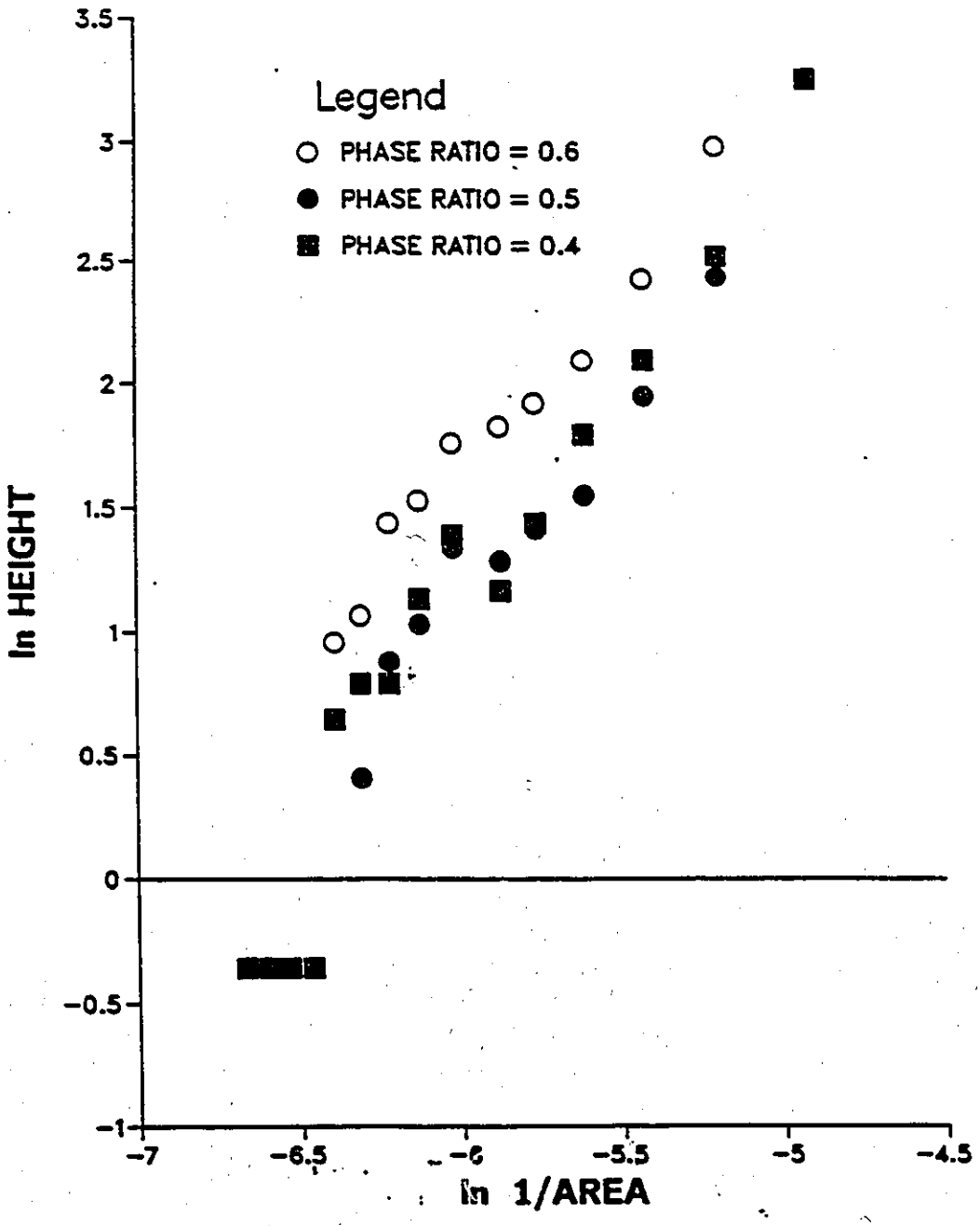

Figure No. 83: ln Height versus ln 1/area plot for the cylindrical mixer data at Q = 2000 mL/min and RPM = 200.

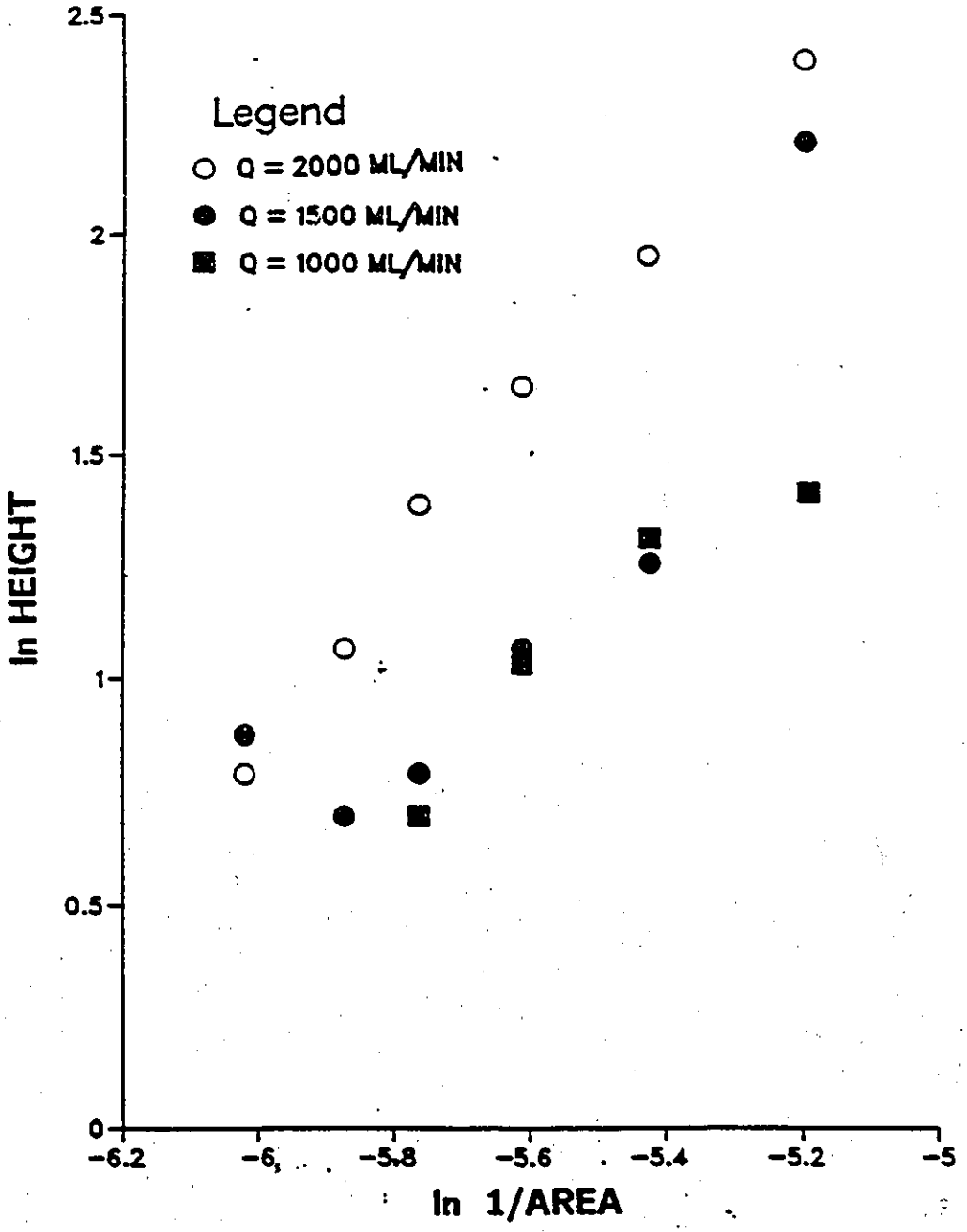

Figure No. 84: ln Height versus ln 1/area plot for the cylindrical mixer data at RPM = 150 and PR = 0.4

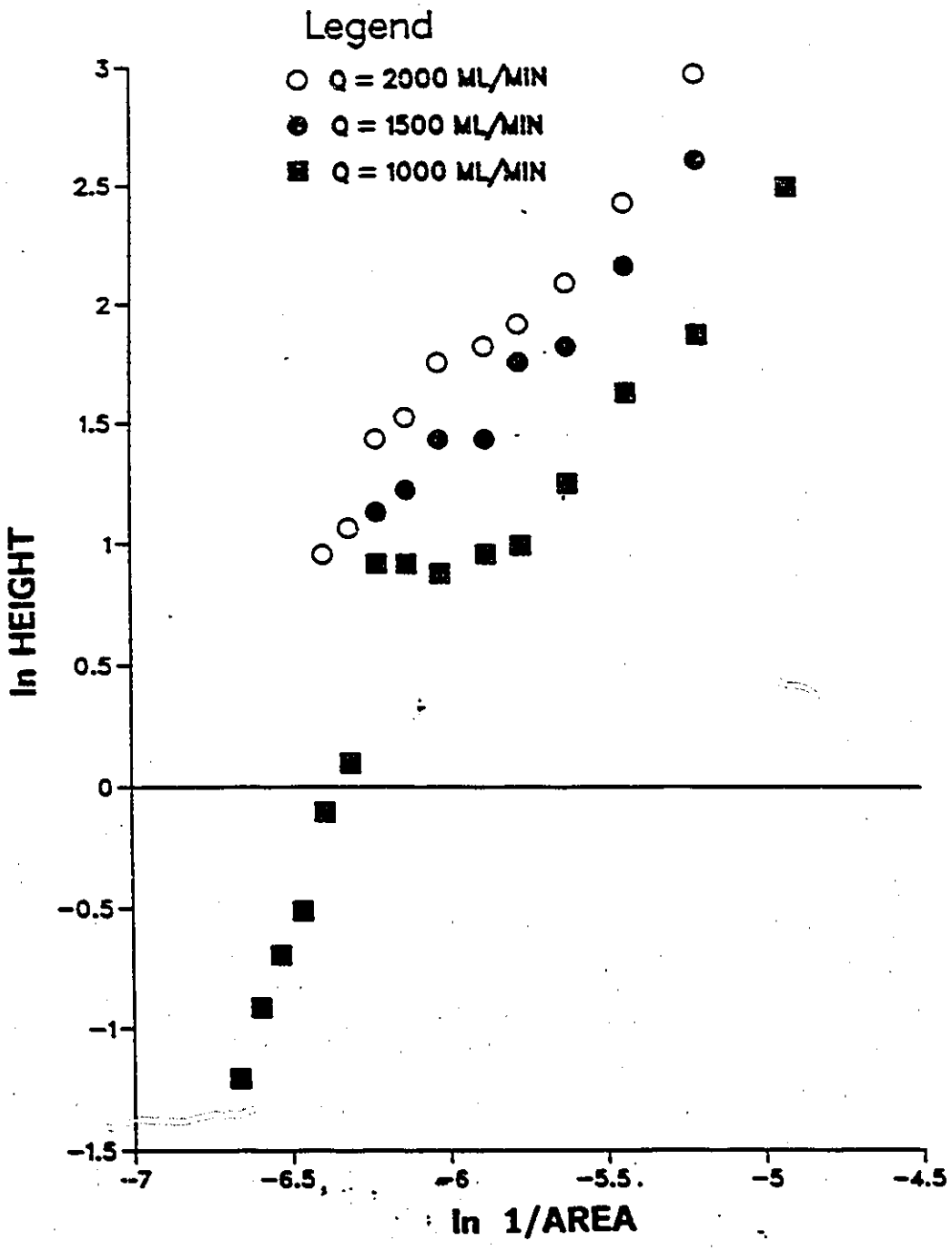

Figure No. 85: ln Height versus ln 1/area plot for the cylindrical mixer data at RPM = 200 and PR = 0.4.

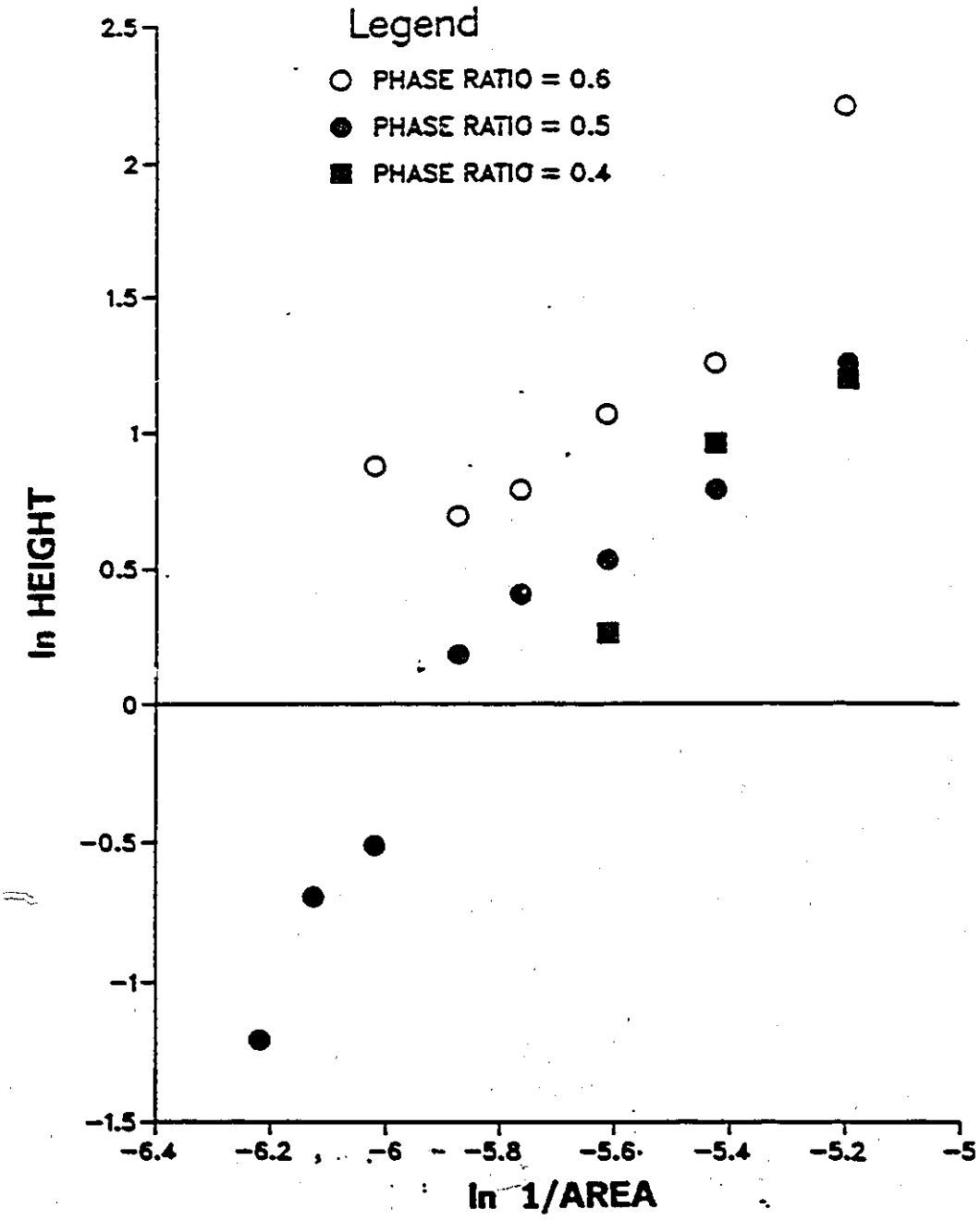

Figure No. 86: ln Height versus ln 1/area plot for the cylindrical mixer data at Q = 1500 mL/min and RPM = 150.

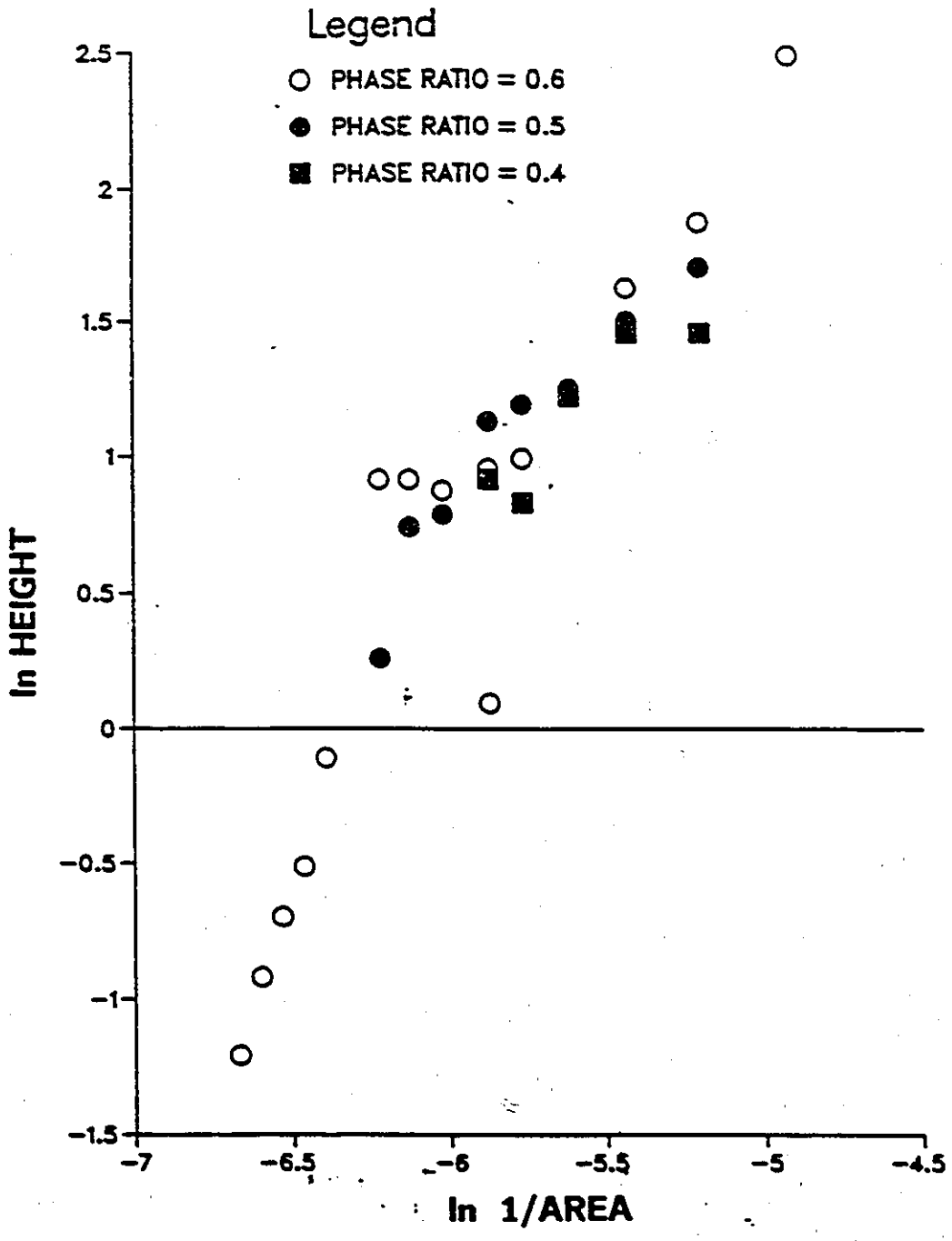

Figure No. 87: ln Height versus ln 1/area plot for the cylindrical mixer data at Q = 1000 mL/min and RPM = 200.

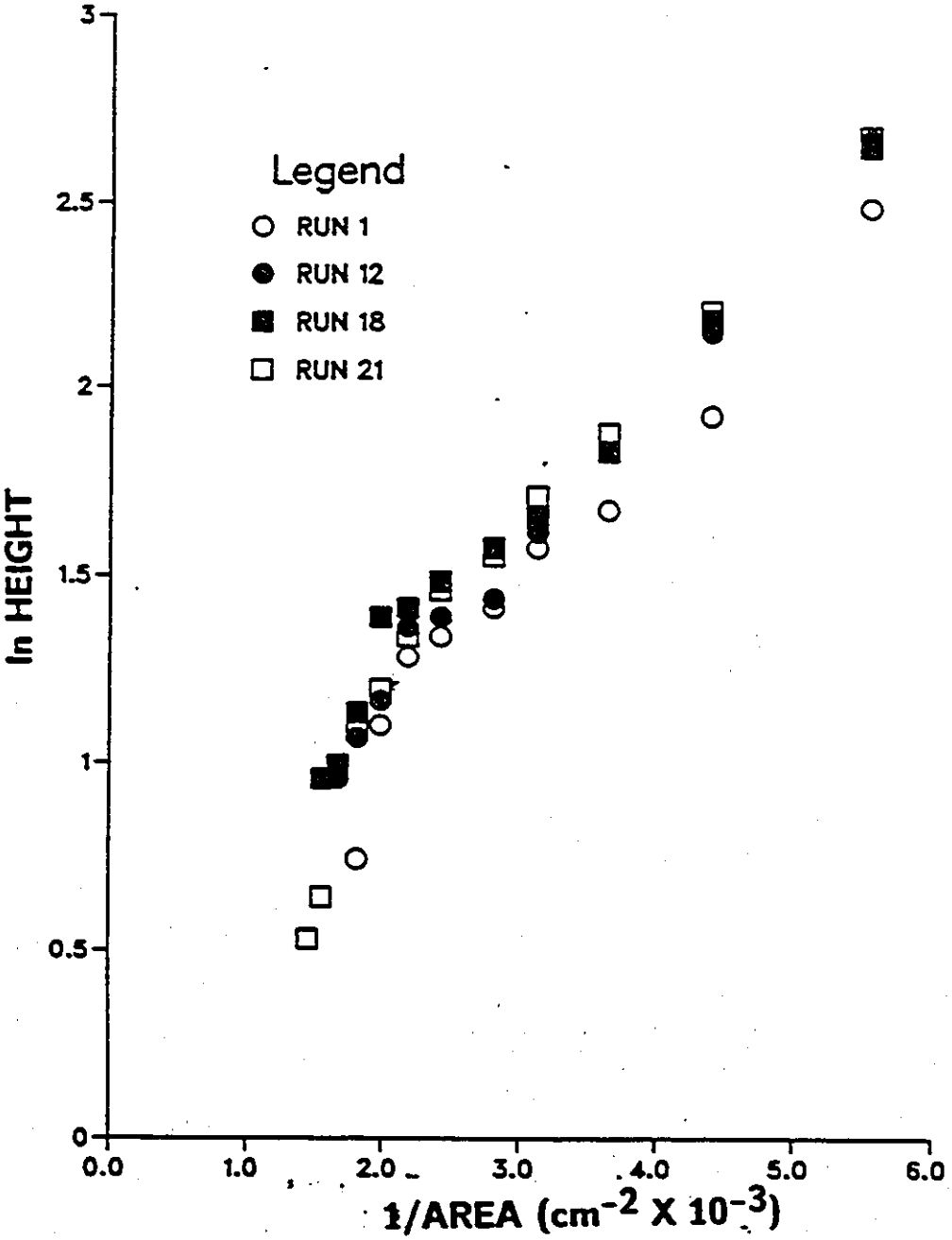

Figur No. 88: ln Height versus 1/area plot for the closed mixer data at Q = 1500 mL/min, RPM = 250 and PR = 0.5.

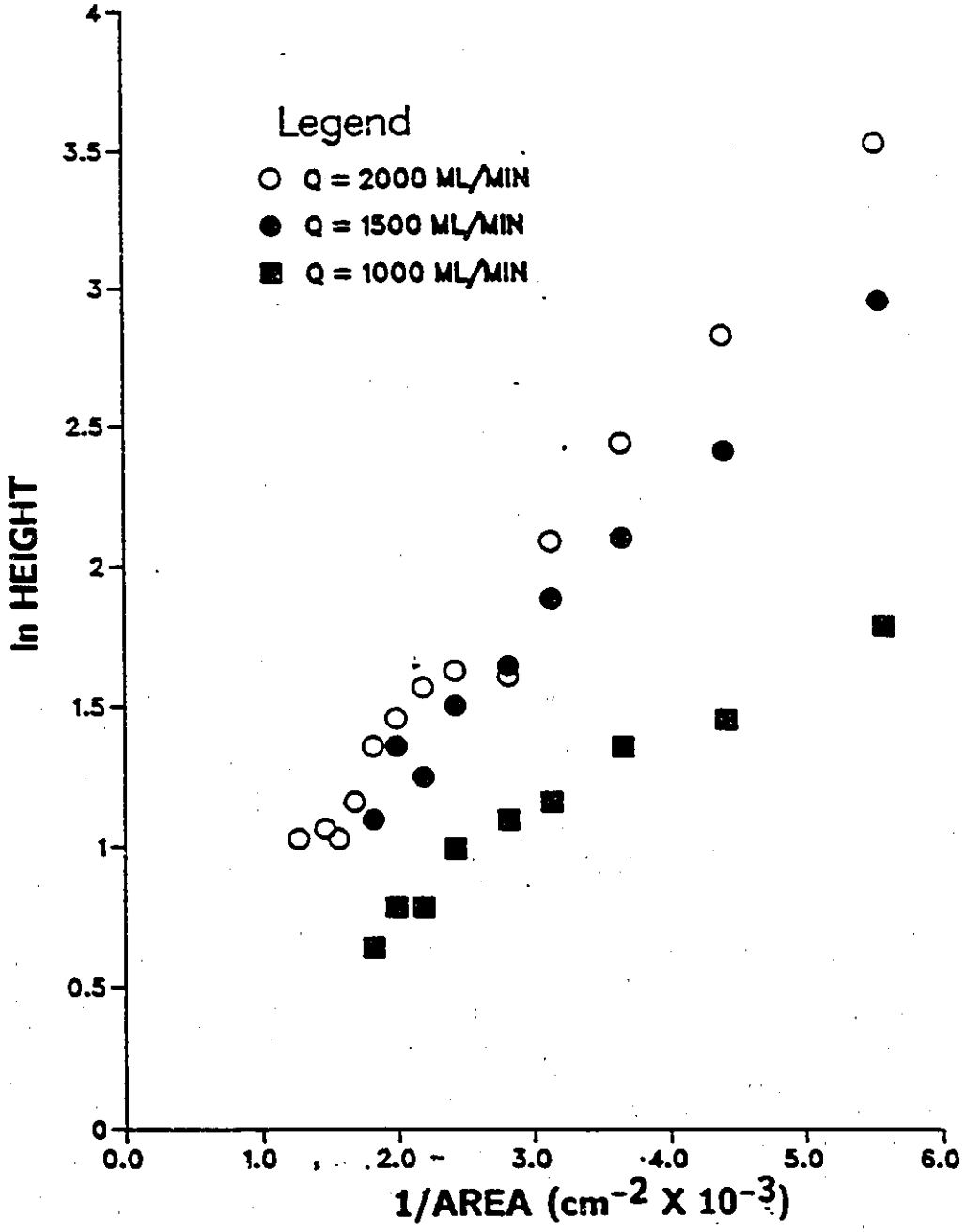

Figure No. 89: ln Height versus 1/area plot for the closed mixer data at RPM = 300 and PR = 0.6.

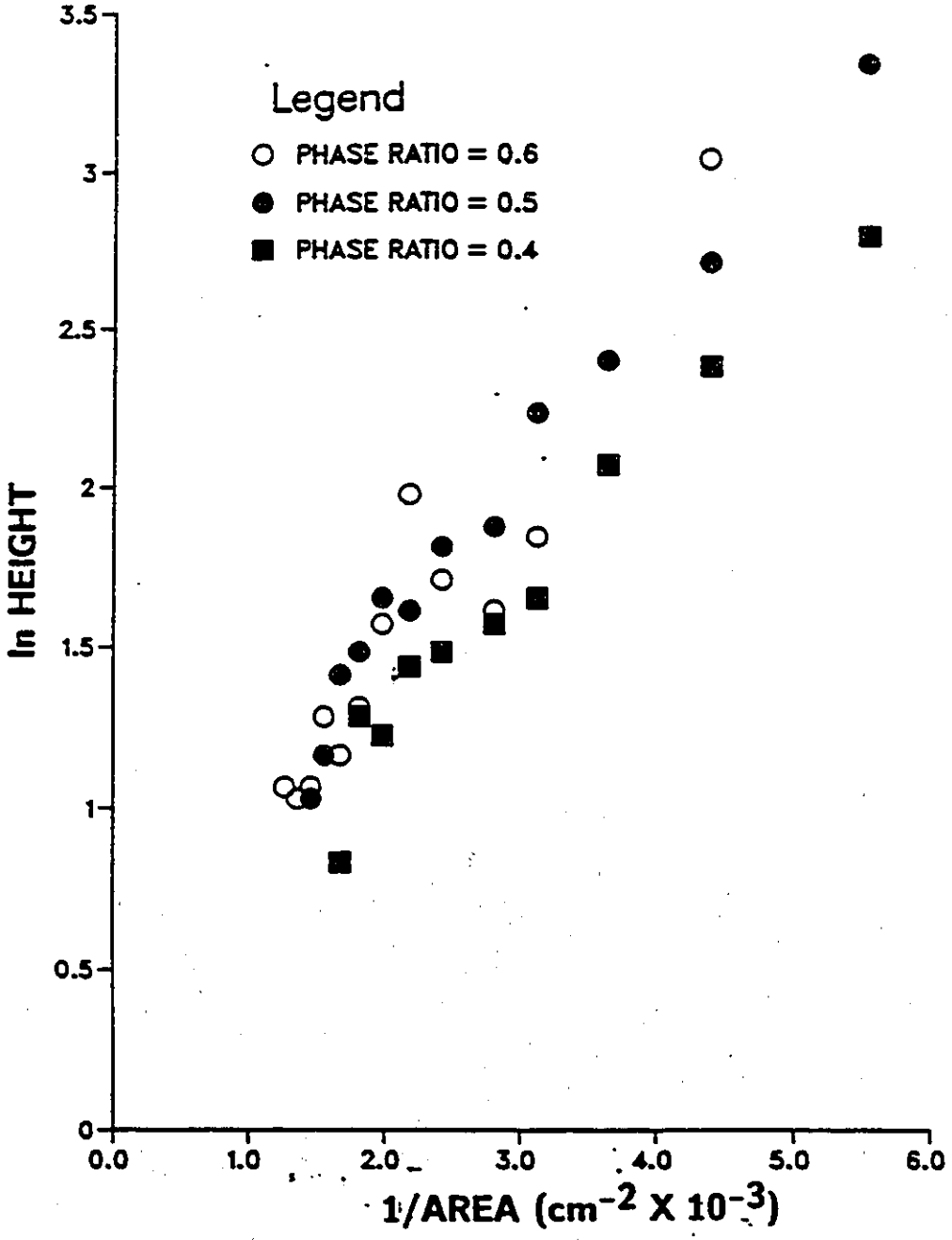

Figure No. 90: ln Height versus 1/area plot for the closed mixer data at Q = 2000 ml/min and RPM = 200.

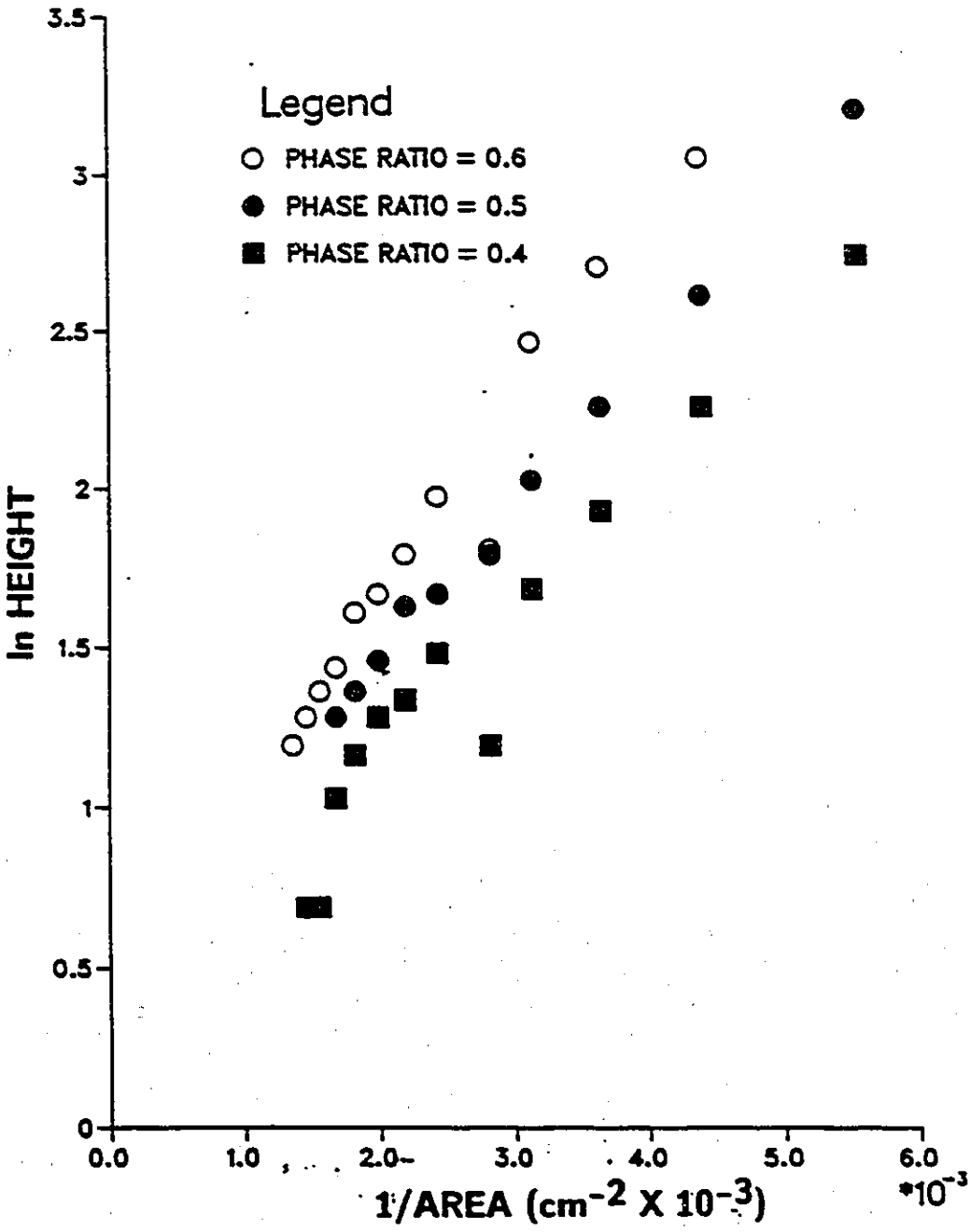

Figure No. 91: ln Height versus 1/area plot for the closed mixer data at Q = 2000 mL/min and RPM = 250.

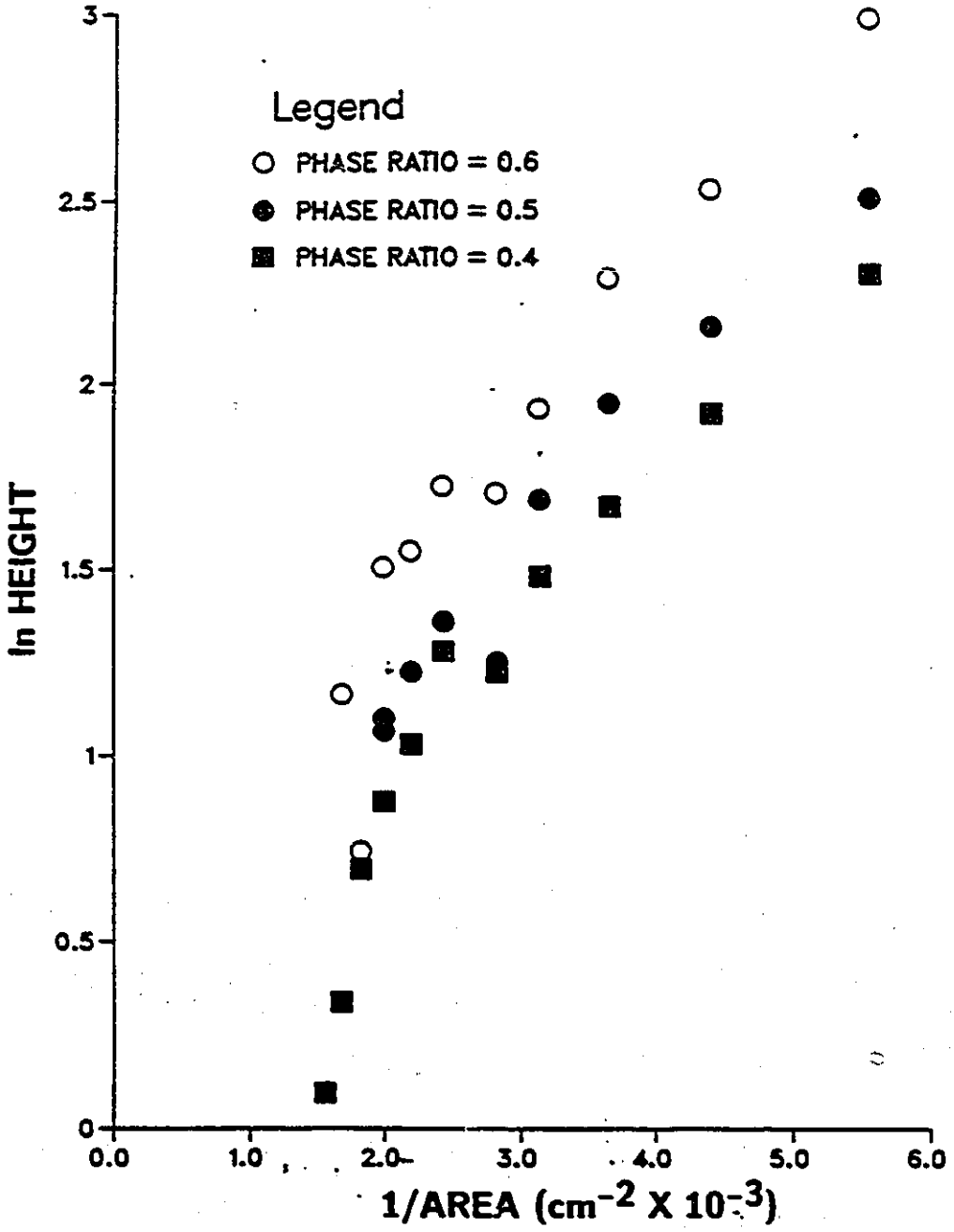

Figure No. 92: ln Height versus 1/area plot for the closed mixer data at Q = 1500 mL/min and RPM = 200

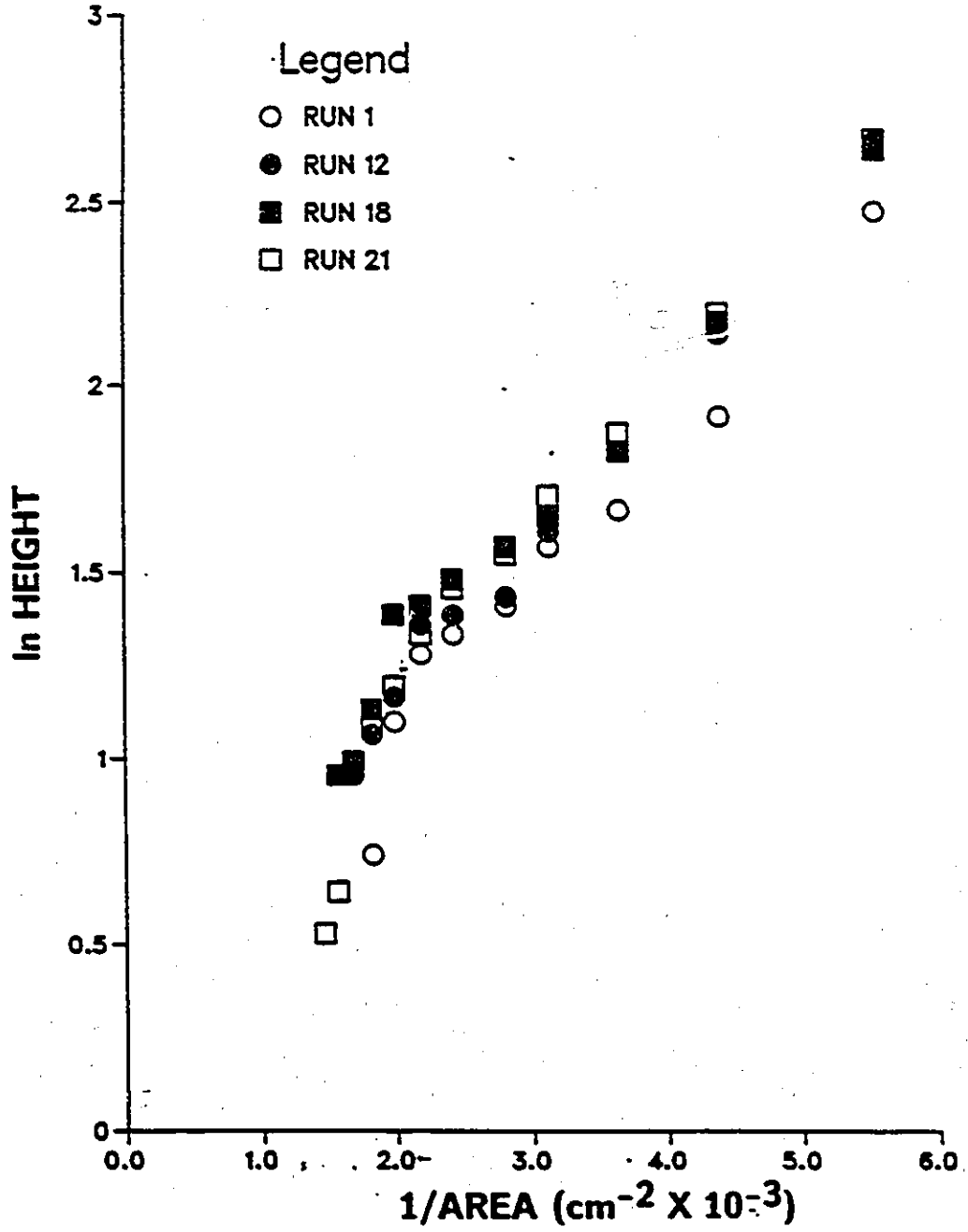

Figure No. 93: ln Height versus 1/area plot for the closed mixer data at Q = 1500 mL/min, RPM = 250 and PR = 0.5

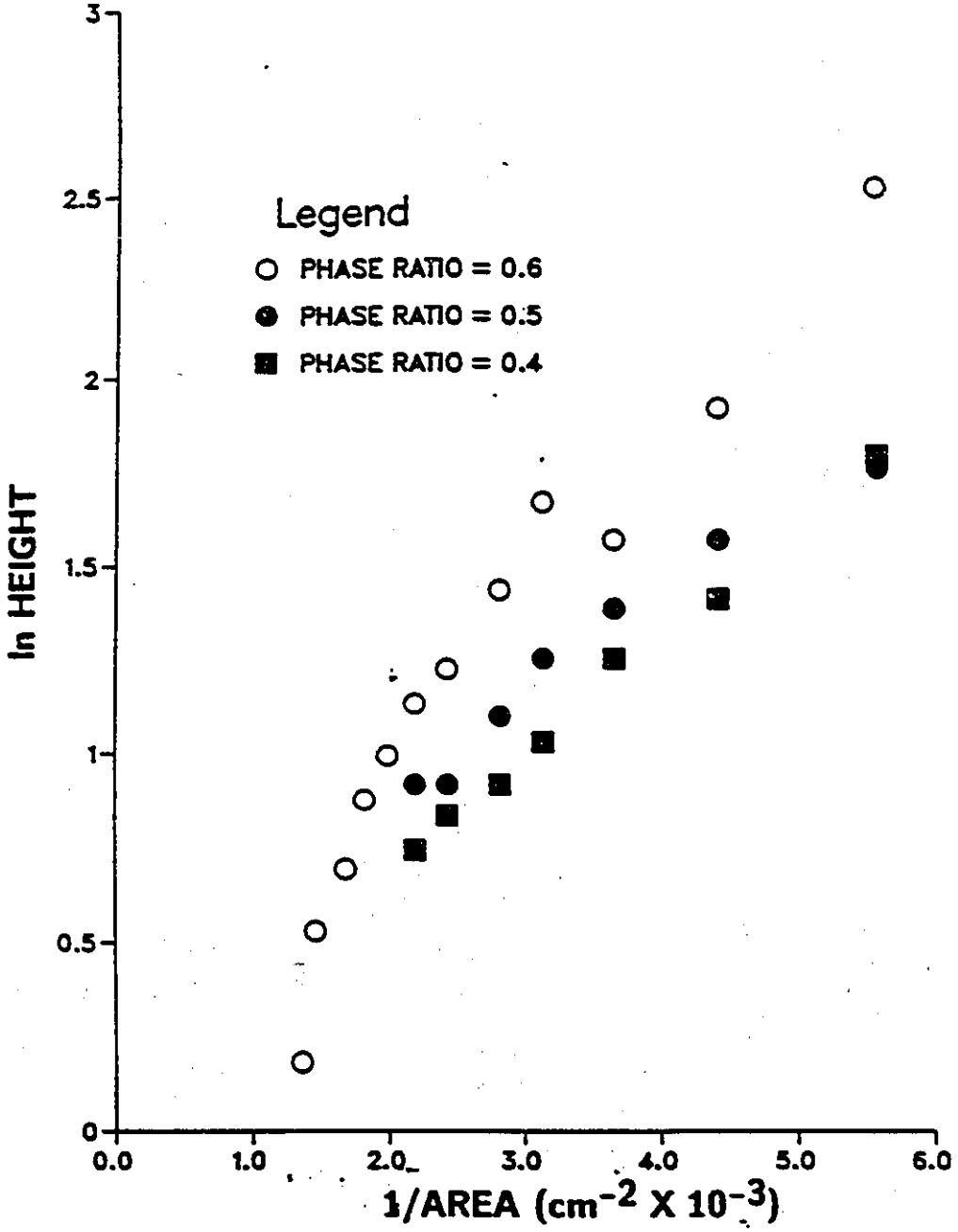

Figure No.94: ln Height versus 1/area plot for the closed mixer data at Q = 1000 mL/min and RPM = 250

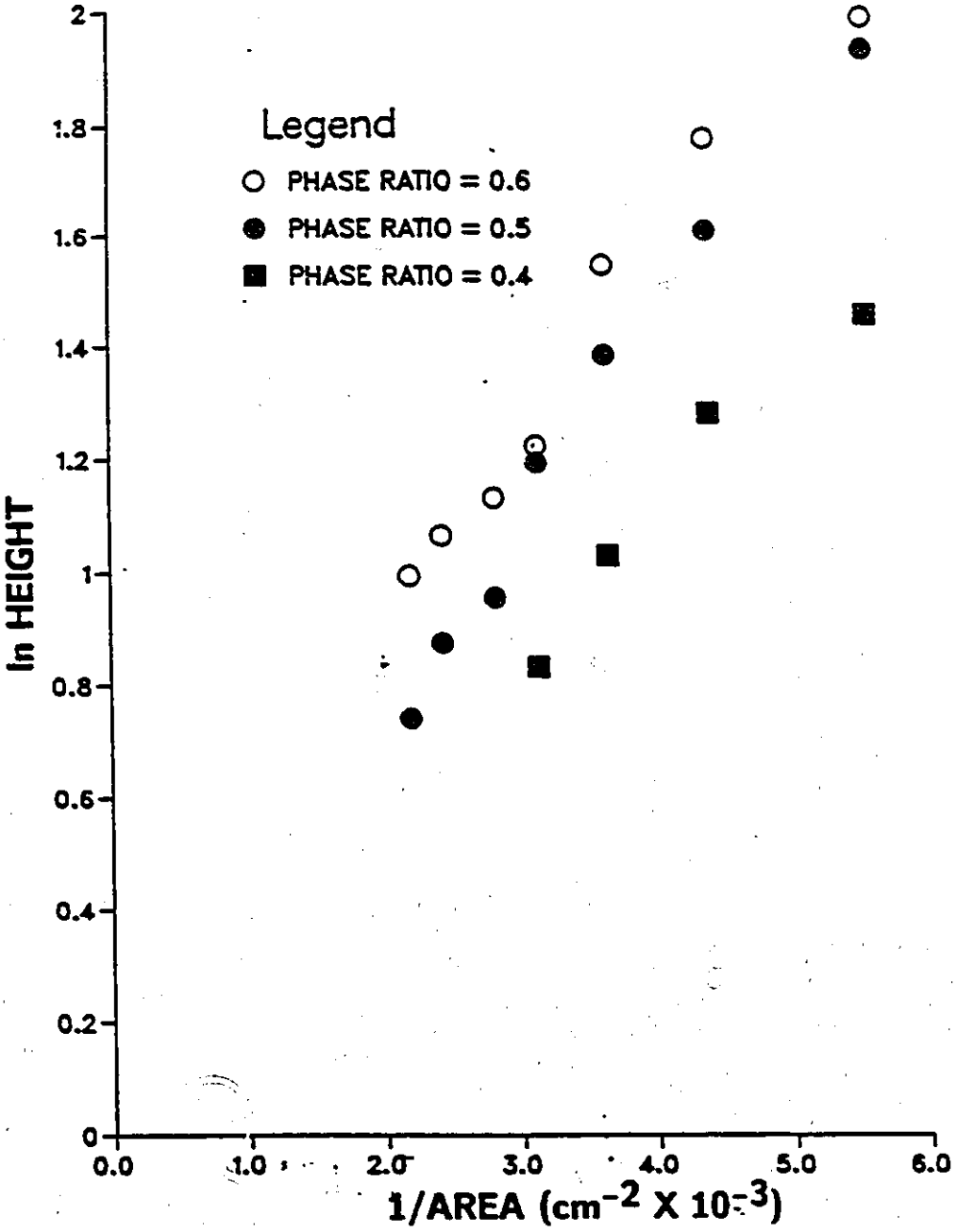

Figure No. 95: ln Height versus 1/area plot for the closed mixer data at Q = 1000 mL/min and RPM = 200

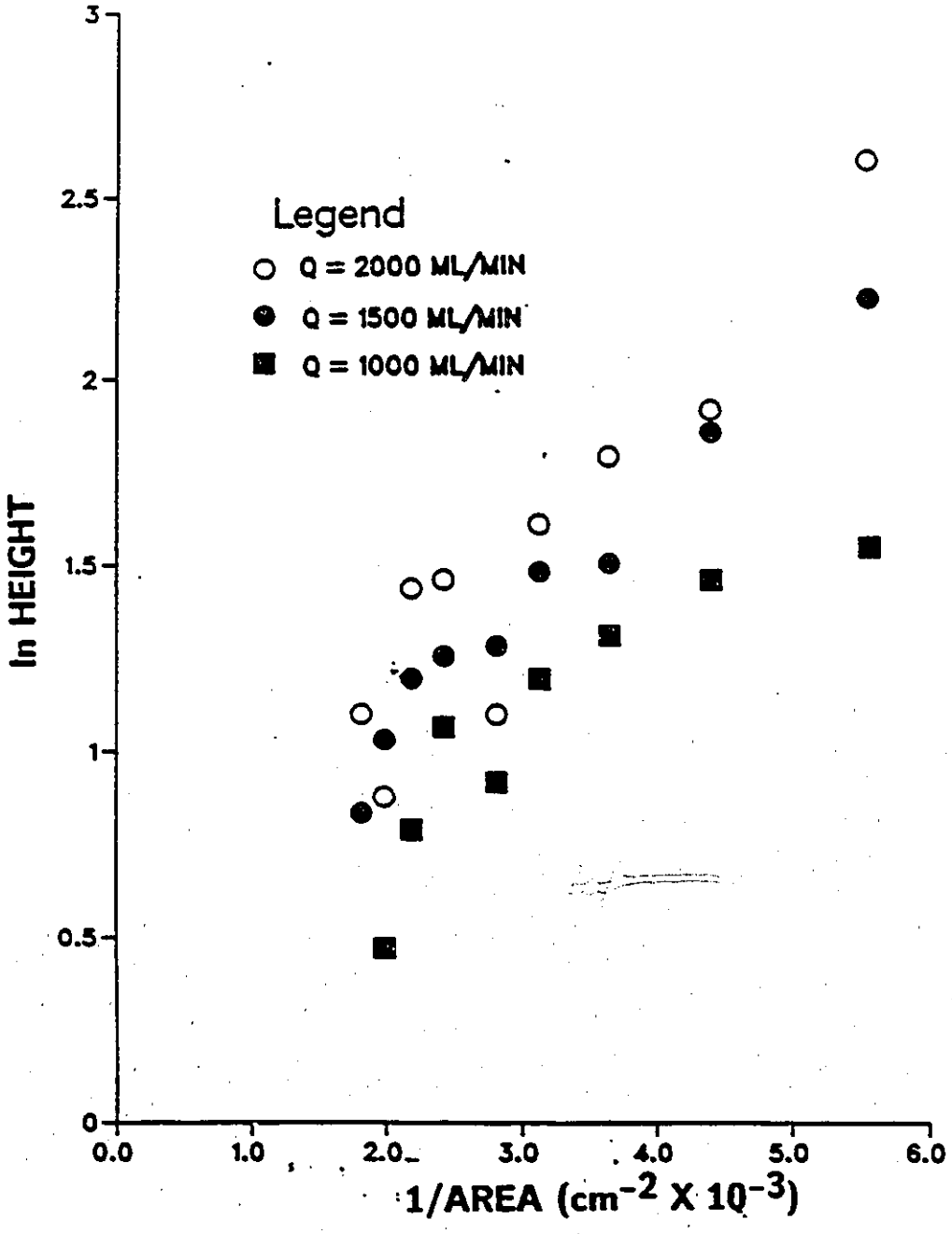

Figure No. 96: ln Height versus 1/area for the closed mixer data at RPM = 300 and PR = 0.4

Appendix D

Physical Data

Pumps	Masterflex peristaltic pumps with 7018 and 7017 heads 400 to 1200 ml/min.	
Rotameters	TRI-FLAT Fischer and Porter Co.	
Settler	Height = 50cm	full width
	Width = 20cm	movable baffle
	Length = 50cm	

Settling areas	A1	134 cm^2
	A2	179
	A3	226
	A4	273
	A5	318
	A6	355
	A7	411
	A8	457

A9	502
A10	549
A11	596
A12	641
A13	687
A14	734
A15	787

Square Mixer	Capacity = 2500 ml, square, open top 13.6 cm X 13.6 cm X 13.6 cm.
Cylindrical Mixer	Capacity = 2500 ml, cylindrical, open top, height 14 cm, Dia. 15 cm
Closed Cylindrical Mixer	Capacity = 2500 ml, cylindrical, closed top, height 14 cm, Dia. 15 cm
Impeller	6 bladed turbine, 5.2 cm O.D. blades 1.7 X 1.4 cm high.
Phase Properties	$\rho_{org} = 0.80$ g/cm^3 $\mu_{org} = 1.6$ cp $\rho_{aq} = 1.07$ g/cm^3 $\mu_{aq} = 1.0$ cp $\gamma = 40$ - 50 dynes/cm